

# Quantum theory of molecular orientations: topological classification, complete entanglement, and fault-tolerant encodings

Victor V. Albert,<sup>1,\*</sup> Eric Kubischta,<sup>1,\*</sup> Mikhail Lemeshko,<sup>2</sup> and Lee R. Liu<sup>3</sup>

<sup>1</sup>*Joint Center for Quantum Information and Computer Science, NIST/University of Maryland, College Park, Maryland, USA*

<sup>2</sup>*Institute of Science and Technology Austria, Klosterneuburg, Austria*

<sup>3</sup>*Department of Physics, University of Colorado, Boulder, Colorado, USA & JILA, NIST/University of Colorado, Boulder, Colorado, USA*

(Dated: January 3, 2025)

We formulate a quantum phase space for molecular rotational and nuclear-spin states. Taking in molecular geometry and nuclear-spin data, we reproduce a molecule’s admissible angular momentum states known from spectroscopy, introduce its angular position states using quantization theory, and develop a generalized Fourier transform converting between the two. We classify molecules into three types — asymmetric, rotationally symmetric, and perrotationally symmetric — with the last type having no macroscopic analogue due to nuclear-spin statistics constraints. We discuss two general features in perrotationally symmetric state spaces that are Hamiltonian-independent and induced solely by symmetry and spin statistics. First, we quantify when and how the state space of a molecular species is completely rotation-spin entangled, meaning that it does not admit any separable states. Second, we identify molecular species whose position states house an internal pseudo-spin or “fiber” degree of freedom, and the fiber’s Berry phase or matrix after adiabatic changes in position yields naturally robust operations, akin to braiding anyonic quasiparticles or realizing fault-tolerant quantum gates. We outline how the fiber can be used as a quantum error-correcting code and discuss scenarios where these features can be experimentally probed.

## I. INTRODUCTION

The quantum-mechanical duality, or conjugacy, between position and momentum [1] has far-reaching consequences in physics, chemistry, and materials science. Conjugate state pairs include states of fixed position and momentum of a continuous-variable system, eigenstates of a qubit’s Pauli- $Z$  and  $X$  matrices, and the Wannier and Bloch functions of an electron. Conjugacy also occurs in angular systems, with the caveat that angular position is continuous but periodic, while angular momentum is unbounded but discrete.

Despite over a century of research, a notion of conjugacy remains underdeveloped for many angular systems. An asymmetry between position and momentum is especially prominent for rotational states of molecules, particularly molecules with symmetries. Molecular orientations, *a.k.a.* angular position states or position states for brevity, have been studied for asymmetric and linear molecules due to their intuitive geometrical picture [2–9], and have been analyzed in local regions of the configuration space, where they are known as pendular states [10–13]. But position states for the *entire* configuration space of *arbitrary* molecules have, to our knowledge, yet to be formulated.

One reason for this is that momentum, not position, plays the dominant role in molecular spectroscopy. Spectroscopic experiments with rotating and vibrating molecular gases provide information about the natural molecular Hamiltonian. This Hamiltonian is nearly diagonal in

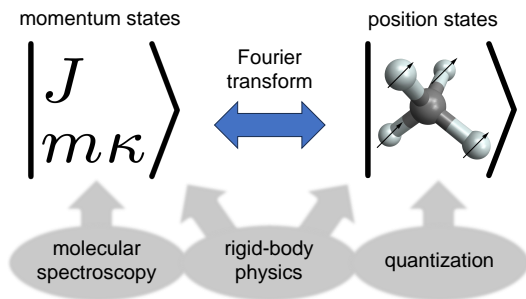


FIG. 1. We use techniques from molecular spectroscopy [14–32] to develop a rigid-body-based [33–38] classification of molecular angular-momentum states. We show that each molecular symmetry species corresponds to a particular quantization [39–42] of the configuration space, yielding angular-position states and a Fourier transform (5).

the momentum-state basis, making it maximally incompatible with position states.

On the other hand, this century has brought forth the ability to cool and trap *individual* molecules [43–74] and to orient molecules using strong electric fields [10–13, 75–78] (see overviews [79–84]). Given this increased level of control, it is both reasonable and necessary to move away from the Hamiltonian-centric approach. For one, the natural Hamiltonian is not particularly useful, and it should be possible to mitigate it or even engineer it away using, e.g., external drives [85–87], creative coupling to ancillae [88, 89], or tools from other platforms [90, 91]. In addition, since the natural Hamiltonian often has more symmetry than the molecule, the molecule’s state space cannot be inferred from that Hamiltonian alone (see Sec. III).

\* Equal contribution.

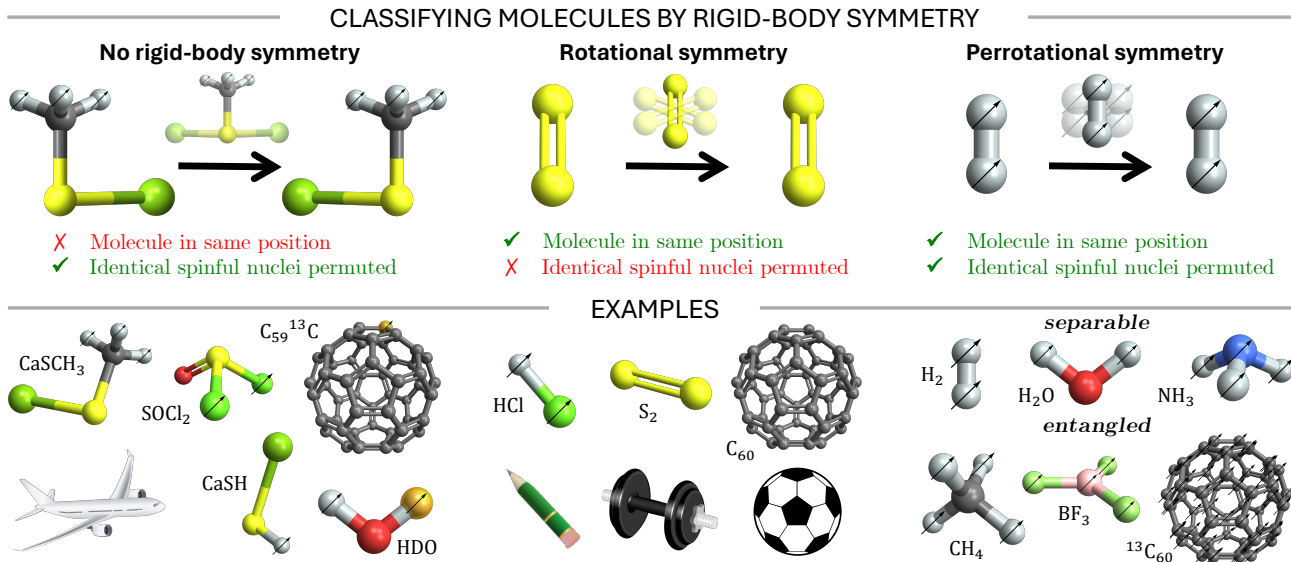


FIG. 2. Molecular rotational states can be characterized by their behavior under orientation-preserving rotations. Orientations, or angular positions, of *asymmetric* molecules are the same as those of any rigid body (e.g., an airplane) whose center of mass is fixed. While every rotation moves an asymmetric molecule to a different position, *rotationally symmetric* molecules remain in the same position under some rotations. Such molecules can have nonzero nuclear spin (marked by “ $\nearrow$ ”), but any rotations that permute identical spinful nuclei must also rotate the rest of the molecule into a different position. Molecule-frame rotations that permute spinful nuclei and *do* leave the rest of the molecule invariant have to produce the molecule’s nuclear-spin statistics. We call any molecule admitting such permutation-rotations a *perrotationally symmetric* molecule. The rotational state space of such molecules has no classical analogue and is the main subject of this work. Perrotationally symmetric molecules with non-commutative symmetries can admit *separable* or *entangled* molecular species, with the latter exhibiting complete rotation-spin entanglement due to a combination of symmetry and nuclear-spin statistics.

Moving toward a more symmetry-centric approach, we determine the admissible angular phase space solely from symmetry and nuclear spin-statistics constraints. We expect this approach to work for all degrees of freedom, but, for this work, assume that orbital, electron-spin, and vibrational degrees of freedom are decoupled and unaffected by symmetry rotations, leaving only the rotational and nuclear-spin degrees of freedom (assuming a fixed center of mass). This rigid-rotor-like approximation [26, Sec. 10.5] captures the leading-order physics of small molecules whose relevant intramolecular interactions are either small on the energy scale of molecular rotations, or can be avoided altogether by working in the vibrational ground state.

We perform a rigid-body-based classification of molecular rotation-spin states (see Fig. 2), adapt spectroscopic recipes for obtaining momentum states, introduce molecular position states via quantization theory, and express each set of states in terms of its conjugate via a generalized Fourier transform (see Fig. 1). Enforcing only the minimal symmetry of the molecule, the resulting phase space can host any Hamiltonian of the same or greater symmetry, failing only for “violent” Hamiltonians that, e.g., break molecules and/or model chemical reactions.

Armed with a birds-eye view of molecular phase space, we proceed to study two of its exotic features. We quantify the nature and strength of symmetry-induced rotation-spin entanglement and identify robust rotation-

induced “topological” operations on position states.

We show that the state spaces of certain molecular species form completely entangled subspaces [92–94] — subspaces that do not admit any separable states with respect to the rotation-spin tensor-product decomposition. Rotation-spin entanglement is well known in the spectroscopy community, but it was never systematically quantified, to our knowledge (see Sec. III). We relate this entanglement to the underlying symmetry-group data and show that it can be quite predominant, with entangled basis states spanning over 98% of the entire state space of certain molecules. Its presence may not seem surprising from the Hamiltonian-centric point of view, as generic molecular eigenstates are highly entangled with respect to the various degrees of freedom. However, complete entanglement is a symmetry-induced property of the *state space*, independent of and unaffected by any symmetric Hamiltonian.

“Topological” operations in the form of Berry phases [95] are present in species as simple as ortho hydrogen (see Sec. VI), and position states of larger molecules admit non-Abelian operations in the form of Berry matrices [96–98]. Such holonomic operations persist even when Gaussian wavepackets are substituted for bona-fide molecular position states (see Sec. XD 3), providing another example of the “holonomy=monodromy” correspondence from condensed-matter physics [99] and quantum information [100]. This suggests a new way to ro-

bustly store and process quantum information, and we show that certain symmetric molecular species provide a similar level of protection against noise as **molecular codes** [§5](#) [101] do for asymmetric molecules (see Sec. XI).

A full-fledged molecular phase space should serve as the backbone for molecular quantum science and technology, akin to the more conventional phase spaces associated with qubit and continuous-variable [102] platforms. This space is primed to be utilized for quantum simulation [103–107], metrology [108–110], ultra-cold chemistry [111, 112], and collision physics [113]. In particular, fiber encodings and their topological operations are relevant to molecular quantum information processing [114–123]. We do not confirm the prevalence of other allegedly fragile quantum effects in large molecules [124] and chemical reactions [125–127], but our noticed features do complement this unique line of thought (see Sec. III).

## II. SUMMARY OF RESULTS

We develop a phase space for molecules whose orbital, electron-spin, and vibrational factors (A) are decoupled from the rotational and nuclear-spin factors and (B) are unaffected by (read: transform trivially under) symmetry rotations. A typical molecule to keep in mind is a rigid one that has been cooled to its ground electronic and vibrational state. Molecules in fixed excited electronic and vibrational states are also allowed, as long as those factors are invariant under symmetry rotations.

### A. Classification of molecular rotational states

We group molecules into three classes, based on their behavior under orientation-preserving, or proper, rotations (see Fig. 2). Asymmetric and rotationally symmetric molecules are analogous to asymmetric and symmetric rigid bodies, respectively. Molecules in the third “perrotationally” symmetric class have no macroscopic analogue because their state space is determined by additional nuclear-spin statistics constraints. Previous treatments do not distinguish the rotational from the perrotational classes, interpreting spinless nuclei as spin-zero particles instead of as classical objects. We build up to our result by first reviewing an established spectroscopic recipe for determining momentum states of all three classes.

**No rigid-body symmetry** Defining the rotational state space of an asymmetric molecule requires two frames: the observer’s *lab frame* and the *molecule frame*, with the latter bolted to and moving with the molecule. Each frame can be rotated, and the two types of lab-based and molecule-based rotations correspond to the two factors of the group  $\text{SO}(3) \times \text{SO}(3)$  of proper rotations acting on the molecule. The basis of fixed-momentum or *rotational* states  $|^J_m, k\rangle$  is labeled by the total angular momentum  $J$  and its projections,  $m$  and  $k$ , onto the  $\mathbf{z}$ -axis

of the lab and molecule frames, respectively.

**Rotational symmetry** For molecules with symmetries, positions that are equivalent under molecule-frame symmetry rotations have to be identified. This identification collapses the molecule frame, restricting the space  $\{|k\rangle\}$  of molecule-frame momenta to a particular subspace. For a *rotationally* symmetric molecule, this admissible state space is the same as that of a rigid body with the same symmetry.

For example, the momentum states of a heteronuclear diatomic (equivalently, a pencil; see Example 8) are  $|^J_m, k=0\rangle$  because only these states are invariant under rotations that form the molecule’s symmetry group,  $C_\infty \cong \text{SO}(2)$ . The state space of  $D_\infty \cong \text{O}(2)$ -symmetric spinless homonuclear diatomics such as disulfur (equivalently, a dumbbell; see Example 9) is further restricted to even  $J$  due to additional invariance under rotations that permute the two nuclei. The state space of rotationally  $C_3 = \mathbb{Z}_3$ -symmetric molecules like cobalt tetracarbonyl hydride (whose cobalt and carbon nuclei have no nuclear spin) admits multiple  $k$ ’s for a given  $J$ ; their admissible state set consists of every  $k \equiv 0$  modulo 3. For other symmetry groups, such as the icosahedral symmetry group of the fullerene (equivalently, a soccer ball; see Example 12), admissible states are superpositions of multiple  $|k\rangle$  states.

In terms of representation theory, restricting to a subspace of symmetric states is equivalent to picking states that transform according to the trivial irreducible representation, or *irrep*, of the symmetry group  $G$ . We label the admissible momentum states of a general rotationally symmetric molecule by  $|^J_{m\kappa}\rangle$ , where  $\kappa$  indexes copies (*a.k.a.* the *multiplicity space*) of the trivial  $G$ -irrep present in the space of  $|k\rangle$  states for each  $J$ .

**Perrotational symmetry** Symmetry rotations acting on *perrotationally* [128–130] symmetric molecules *permute* identical spinful nuclei, correlating rotational states with the nuclear spin. Molecule-frame symmetry rotations gain extra permutation operators to account for effects on the spins, and identification of symmetry-related positions yields a subspace of the *joint* rotation-spin space.

Admissible tensor products of rotational and nuclear-spin states are grouped into molecular *species*. Each species yields the same required Bose or Fermi spin statistics under molecule-based symmetries, but differs from other species in how the *individual* rotational and nuclear-spin factors transform.

For example, consider  $\text{H}_2$  — a perrotationally  $D_\infty$ -symmetric molecule that *cannot* be treated the same way as a dumbbell. Molecule-frame rotations that permute its identical spin-half hydrogen nuclei must result in a spin-statistics phase of  $-1$ . Admissible states are split into two species — para and ortho — with the required phase coming from either the nuclear-spin or the rotational factor (see Sec. VI and Example 16).

Basis states of para hydrogen consist of the same even- $J$  rotational states as a dumbbell, tensored with the anti-symmetric (singlet) nuclear-spin state. States of ortho

hydrogen consist of rotational states of *odd* angular momentum, tensored with symmetric (triplet) nuclear-spin states. The existence of the odd-momentum ortho species shows that perrotationally symmetric molecules (such as hydrogen and deuterium) can occupy momentum states inaccessible to rotationally symmetric molecules with the same symmetry (such as disulfur).

In terms of representation theory, rotational states of para hydrogen transform according to the trivial irrep  $A_1$  of the symmetry group. On the other hand, rotational states of the ortho species transform according to the sign irrep  $A_2$ . Together, products of the rotational and nuclear-spin irreps of each species yield the correct spin-statistics irrep,  $A_1 \otimes A_2 = A_2$  and  $A_2 \otimes A_1 = A_2$ , respectively.

More generally, a species is uniquely determined by the triple of *rotational*, *nuclear-spin*, and *molecular spin-statistics* irreps,

$$\Gamma_{\text{rot}} \otimes \Gamma_{\text{nuc}} \downarrow \Gamma_{\text{mol}}, \quad (1)$$

where “ $\downarrow$ ” means that the tensor-product representation has to be projected into the desired irrep  $\Gamma_{\text{mol}}$ . The projection becomes an equality for scalar irreps ( $\dim \Gamma_{\text{rot}} = \dim \Gamma_{\text{nuc}} = 1$ ), like those of  $\text{H}_2$ , becoming relevant only for irreps of higher dimension. We tabulate all possible irrep triples for all symmetry groups in Table II.

Despite complications due to spin statistics, admissible rotational states of a perrotational species are still indexed by  $J$ ,  $m$ , and  $\kappa$ , but with  $\kappa$  now going over the multiplicity space of  $\Gamma_{\text{rot}}$  for each momentum. This long-known recipe, stemming from nearly a century of rigorous work in spectroscopy [14–32], provides a momentum basis for any molecule.

**Induced representations & quantization** A main result of this work is identifying that momentum states form an *induced representation* [36, 131–136] of the group of lab-based rotations, denoted by  $\text{Ind}_{\Gamma_{\text{rot}}}^G \text{SO}(3)$  or  $\Gamma_{\text{rot}} \uparrow \text{SO}(3)$  when the symmetry group is evident. Induced representations allow us to relate molecular spectroscopy to quantization theory [39–42], revealing that each molecular species is in one-to-one correspondence with a particular quantization of the configuration space of molecular orientations. This relation readily yields molecular position states and the Fourier transform, summarized in Sec. II C.

**Theorem.** *The rotational state space of a  $G$ -symmetric molecular species transforms as an induced representation  $\Gamma_{\text{rot}} \uparrow \text{SO}(3)$  under lab-based rotations, where  $\Gamma_{\text{rot}}$  is an irrep of the symmetry group.*

Molecular species in all three classes are exhaustively classified using induced representations. In the asymmetric case,  $G$  becomes the trivial group. In the rotationally symmetric case, there is only one species, and  $\Gamma_{\text{rot}}$  becomes the trivial irrep. In the perrotationally symmetric case, the combination of symmetry and spin statistics allows for more general irreps  $\Gamma_{\text{rot}}$ , governed by condition (1). For example, the odd- $J$  momentum

states of ortho hydrogen make up the representation  $\text{Ind}_{A_2}^{\text{D}_\infty} \text{SO}(3) = A_2 \uparrow \text{SO}(3)$ . The same classification can be made for molecules confined to move in only two dimensions (see Sec. VI).

Our classification is similar to that of solid-state materials [137] and nematic liquid crystals [138, 139]: all three are based on induced representations and distinguish species with “topologically nontrivial” features. In the case of molecules, induced representations with non-trivial inducing irreps exhibit “topological” behavior under lab-based rotations, and those with vector irreps exhibit complete rotation-spin entanglement.

## B. Complete rotation-spin entanglement

Since admissible states of symmetric molecules form a subspace of the asymmetric molecular state space  $\{|^J_m, k\rangle\}$ , we can decompose the latter into the various induced representations for a given symmetry group.

For abelian  $G$  (i.e., groups with commuting elements), the asymmetric state-space identity operator decomposes as  $\mathbb{1}_{\text{rot}} = \bigoplus_{\Gamma} \Gamma \uparrow \text{SO}(3)$ , where  $\Gamma$  goes over all  $G$ -irreps. Selecting a species projects this space into the  $\Gamma = \Gamma_{\text{rot}}$  sector, which is then tensored with the appropriate nuclear-spin irrep  $\Gamma_{\text{nuc}}$  such that the spin-statistics condition (1) is satisfied. Each such species admits tensor-product states of the form  $|^J_{m\kappa}\rangle_{\text{rot}}|\chi\rangle_{\text{nuc}}$ , where  $\chi \in \{1, 2, \dots, \mathbf{m}_{\text{nuc}}\}$  indexes the multiplicity of the corresponding  $\Gamma_{\text{nuc}}$  irrep up to the statistical weight  $\mathbf{m}_{\text{nuc}}$  [26, 27].

More interesting species occur for *non-Abelian* symmetry groups. Such groups admit both scalar ( $\dim \Gamma = 1$ ) and “vector” irreps ( $\dim \Gamma > 1$ ), with the latter hosting internal degrees of freedom. The asymmetric state-space identity in such cases decomposes as [39–42]

$$\mathbb{1}_{\text{rot}} = \bigoplus_{\Gamma} [\Gamma \uparrow \text{SO}(3)] \otimes \mathbb{1}_{\dim \Gamma}, \quad (2)$$

where the induced representation is present with multiplicity  $\dim \Gamma$  for each irrep  $\Gamma$ . Selecting a species once again projects the above space into the  $\Gamma = \Gamma_{\text{rot}}$  sector.

An analogous selection of the  $\Gamma_{\text{nuc}}$  irrep occurs on the nuclear-spin side, resulting in the bipartite irrep-multiplicity subspace  $\mathbb{1}_{\dim \Gamma_{\text{nuc}}} \otimes \mathbb{1}_{\mathbf{m}_{\text{nuc}}}$ . But since  $\Gamma_{\text{rot}}$  and  $\Gamma_{\text{nuc}}$  may be vector irreps, their internal degrees of freedom have to be *projected*, via Eq. (1), into a subspace transforming according to the spin-statistics irrep  $\Gamma_{\text{mol}}$ . This subspace can be determined using Clebsch-Gordan tables [140, 141] and turns out to always be one-dimensional, defined by a state we denote by  $|\Gamma_{\text{mol}}\rangle$ .

Basis states for a general species can be written as

$$|^J_{m\kappa}\rangle_{\text{rot}}|\Gamma_{\text{mol}}\rangle|\chi\rangle_{\text{nuc}}. \quad (3)$$

The three indices of the first factor belong to the induced representation, the middle factor is supported on the composite rotation-spin space  $\mathbb{1}_{\dim \Gamma_{\text{rot}}} \otimes \mathbb{1}_{\dim \Gamma_{\text{nuc}}}$ , and



the fourth index  $\chi$  indexes the nuclear-spin multiplicity up to the statistical weight.

Exhaustively determining all possible molecular species, we observe that the dimensions of participating irreps always coincide,

$$\dim \Gamma_{\text{rot}} = \dim \Gamma_{\text{nuc}} \equiv \mathfrak{d} \quad (\text{Schmidt rank}), \quad (4)$$

and that the state  $|\Gamma_{\text{mol}}\rangle$  is maximally entangled with respect to the rotation-spin tensor product. Quantitatively, the state has *Schmidt rank*  $\mathfrak{d}$  [142], i.e., it can only be written as a superposition of at least  $\mathfrak{d}$  of any basis states that span the  $\mathfrak{d}^2$ -dimensional composite space  $\mathbb{1}_{\mathfrak{d}} \otimes \mathbb{1}_{\mathfrak{d}}$ . As such, we call molecular species with  $\mathfrak{d} > 1$  *entangled* and denote  $\mathfrak{d} = 1$  species as *separable*.

The state  $|\Gamma_{\text{mol}}\rangle$  “dresses” each basis state in Eq. (3) in a way that is impossible to remove, even by superposition. While basis-state superpositions or changes of basis can certainly yield states of higher entanglement, the Schmidt rank of *any* state of the species cannot go below  $\mathfrak{d}$ . Any entangled species thus forms a *completely entangled subspace* [92–94], i.e., a subspace that does not contain any separable states. This rotation-spin entanglement is enforced by symmetry and spin statistics and cannot be removed without transitioning to another species or breaking the assumptions of the model.

Complete entanglement is quite widespread. Entangled states make up over a third of all basis states from Eq. (3) for a series of dihedrally symmetric chains (see Table III). Tetrahedrally symmetric molecules like methane admit three separable and one entangled species, but the latter occupies over 56% of the entire state space (see Example 23). An extreme case is isotopic  $^{13}\text{C}_{60}$  fullerene: all but one of its species and 98% of its basis states are completely entangled (see Example 24).

### C. Position states

Dual to the momentum states are molecular states that label orientations, or angular positions, of a molecule. Such idealized states are Dirac- $\delta$  orthonormal, just like position states of a harmonic oscillator or a two-dimensional rotor [143]. As with those established systems, normalizable finite-energy approximations of position states have to be considered for applications, and we observe that approximate states’ properties approach those of the ideal states exponentially in their average angular momentum (see Sec. XD 3).

Each position state of an asymmetric molecule is labeled by the proper rotation  $r$  required to orient the lab frame into the molecule frame at that position. For asymmetric molecules, each position is distinct by definition, so all rotations are required to label all possible positions. The states  $|r\rangle$  for  $r \in \text{SO}(3)$  span the induced representation space of  $A \uparrow \text{SO}(3)$  (see theorem above), induced by the trivial irrep  $A$  of the trivial symmetry group.

Rotationally symmetric molecules (and symmetric rigid bodies) are invariant under a subgroup  $G$  of

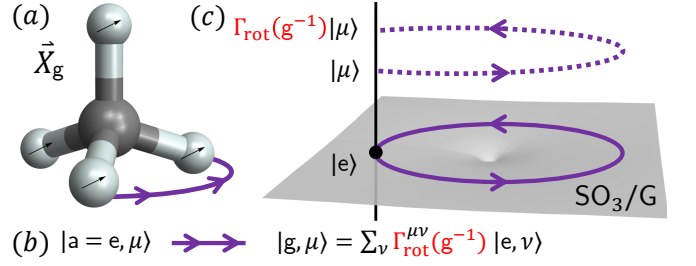


FIG. 3. With the molecular frame collapsed due to identification of positions related by molecule-based symmetries, we are still free to rotate the lab frame. (a) Lab-based rotations,  $\vec{X}_g$  for  $g$  in a molecule’s symmetry group, map the molecule to the same position. For example, a rotation rotates the methane molecule by  $120^\circ$ , with the path traversed by the forward-most nucleus depicted by two arrows. (b) A position state  $|a = e\rangle$  (with  $a$  set to the identity element  $e$  for simplicity) of a perrotationally symmetric molecule carries with it a *fiber* space, spanned by the basis  $\{|\mu\rangle\}$ . Symmetry rotations transform the internal state of fiber via the monodromy matrix  $\Gamma_{\text{rot}}(g^{-1})$ . (c) In a cartoon depiction, the fiber can be thought of as a vertical line at each point  $a$  in the position-state space  $\text{SO}(3)/G$ , with a non-contractible closed path resulting in a monodromy action on the fiber state.

molecule-based rotations and do not require the entire  $\text{SO}(3)$  space to be used as their configuration space. Instead, their position states  $|a\rangle$  correspond to cosets  $aG$  of the symmetry group in  $\text{SO}(3)$ , with coset representatives  $a$  making up the *coset space*  $\text{SO}(3)/G$  [144, 145]. The set  $\{|a\rangle\}$  spans the representation space of  $A \uparrow \text{SO}(3)$ , induced by the trivial irrep of  $G$ .

Perrotationally  $G$ -symmetric molecular position states span the representation space of more general  $\Gamma_{\text{rot}} \uparrow \text{SO}(3)$ . In the context of quantization, induced representations for different  $\Gamma_{\text{rot}}$  correspond to different ways to “quantize” a particle on the coset space. For separable species ( $\dim \Gamma_{\text{rot}} = \mathfrak{d} = 1$ ), positions are still labeled by coset representatives  $a \in \text{SO}(3)/G$ .

For entangled species ( $\mathfrak{d} > 1$ ), coset representatives are *not* sufficient to describe the full state space. Instead, each position carries with it an *internal* degree of freedom in the form of a  $\mathfrak{d}$ -dimensional vector space,  $\{|\mu\rangle, 1 \leq \mu \leq \mathfrak{d}\}$ . From a geometrical perspective, the coset space acts as the base space while the vector space serves as the *fiber* of a fiber bundle [39] [see Fig. 3(c)].

Position states  $|a, \mu\rangle$  can be expressed as superpositions of *many* momentum states  $|^J_{m\kappa}\rangle$ , and visa versa, conforming to the Heisenberg uncertainty principle. Both bases are complete and orthogonal, and the Fourier transform for a general entangled species is

$$|a, \mu\rangle = \sum_{J \downarrow \Gamma_{\text{rot}}} \sum_{|m| \leq J} \sum_{\kappa=1}^{m(J)} H_{m\kappa}^J(a, \mu) |^J_{m\kappa}\rangle \quad (5a)$$

$$|^J_{m\kappa}\rangle = \int_{\text{SO}(3)/G} da \sum_{\mu=1}^{\mathfrak{d}} H_{m\kappa}^{J*}(a, \mu) |a, \mu\rangle, \quad (5b)$$

where the induced harmonic  $H$  is a cousin of the Wigner

$D$ -matrix [146] (see Sec. IX). The shorthand “ $J \downarrow \Gamma_{\text{rot}}$ ” stands for all  $J$  which house at least one copy of  $\Gamma_{\text{rot}}$ , and  $m(J) \geq 1$  labels how many copies there are for that momentum. The above states are tensored with the appropriate  $m_{\text{nuc}}$ -dimensional nuclear-spin factor  $\{|\chi\rangle\}$  from Eq. (3) to yield the correct spin statistics.

#### D. “Topological” holonomy

Lab-based rotations are “passive” in that they rotate the lab frame. However, since molecular position is fully characterized by the molecule’s orientation *relative* to the lab frame, performing lab-based rotations is equivalent to “actively” rotating the molecule about an axis defined in that frame.

Lab-based symmetry rotations rotate each nucleus into a different position *without* permuting any nuclear-spin factors. Acting purely on the rotational factor, lab-based symmetries induce non-trivial species-*dependent* behavior, in contrast to the species-*independent* spin statistics induced by molecule-based perrotations.

A lab-based rotation,  $\bar{X}_g$  for some  $g \in \text{SO}(3)$ , rotates a molecular species from its initial position  $\mathbf{a}$  to a position denoted by  $g\mathbf{a}$ , tracing out a path in the coset space  $\text{SO}(3)/G$ . The fiber  $|\mu\rangle$  is carried along this path, transforming in a way dictated by the species’ inducing irrep  $\Gamma_{\text{rot}}$ . The nuclear factor  $|\chi\rangle$  is also carried along, but transforms trivially and so is omitted from now on.

If  $g$  implements a symmetry of the molecule, then the final and initial positions are identified,  $g\mathbf{a} \cong \mathbf{a}$ , but *only* up to a residual evolution on the fiber (see Fig. 3 for the  $\mathbf{a} = \mathbf{e}$  case). This evolution — a *monodromy* — is the same for the class of paths related to the original path by smooth deformations, depending only on the global, or “topological”, features of the path.

For general closed adiabatic paths in position space, monodromy can be thought of as a robust version of holonomy [96–98] (itself a generalization of the Berry phase [95]). Position-state holonomy does not depend on any local, or geometric, features of the path, yielding an instance of the “holonomy = monodromy” correspondence [99, 100]. With respect to past instantiations of “topological” holonomy (see Sec. III), the surprise here is its presence in “classical” rigid-body position states.

For example, a lab-frame rotation exchanging the positions of the two hydrogens of  $\text{H}_2$  induces a monodromy of  $-1$  for the ortho species, in contrast to the trivial  $+1$  monodromy of the para species. This is easily derived by noting that the former (latter) species hosts only odd-momentum (even-momentum) rotational states; see Sec. VI and Example 39. Each species’ monodromy is independent of the axis of rotation, as long as the rotation exchanges the two nuclear positions. On the other hand, any rotation around the molecule’s principal axis yields the trivial monodromy of  $+1$  for both species.

The monodromies of each species correspond to evaluations of symmetry-group elements in the species’ in-

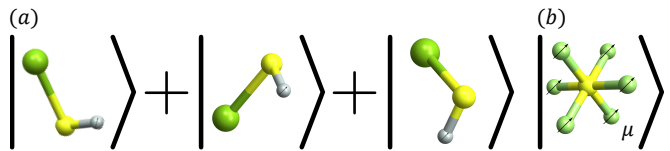


FIG. 4. (a) Molecular code states [101] are superpositions of several position states of an asymmetric molecule, related by rotations in a subgroup  $G$ . (b) Fiber codes  $\{|\mathbf{e}, \mu\rangle\}_{\mu=1}^{\mathfrak{d}}$  (5) encode in a *single* molecular position,  $\mathbf{a} = \mathbf{e}$ , of a perrotationally  $G$ -symmetric entangled species (here, O-symmetric  $\text{SF}_6$ ). The former induces the trivial induced representation,  $\Lambda \uparrow \text{SO}(3)$ , on the asymmetric molecular state space, while the latter forms a non-trivial induced representation,  $\Gamma_{\text{rot}} \uparrow \text{SO}(3)$ , with a fiber degree of freedom of dimension  $\mathfrak{d} = \dim \Gamma_{\text{rot}}$ . Both encodings are comparable in performance against shifts in the molecules’ orientation and kicks in their momenta (see Sec. 4).

ducing irreps. The para-species irrep is trivial, while the ortho-species sign irrep yields the possible  $\pm 1$  monodromy. Which monodromy is induced depends on the homotopy class of the path in position-state space, which in this case is the projective plane,  $\text{SO}(3)/\mathfrak{d}_{\infty} \cong \mathbb{RP}^2$ .

For a species with symmetry group  $G$  and inducing irrep  $\Gamma_{\text{rot}}$ , the possible monodromies correspond to  $\Gamma_{\text{rot}}(g)$  for any  $g \in G$  [see Fig. 3(c)]. This set generates the *monodromy group*, and we determine such groups for all possible species in Table VI.

Separable species, like ortho  $\text{H}_2$ , admit root-of-unity monodromy. The  ${}^2\text{E} \otimes {}^1\text{E} = \text{A}$  separable species of perrotationally  $\text{C}_3$ -symmetric ammonia is the simplest to realize a monodromy that is not  $\pm 1$ . Cyclically permuting the species’ three hydrogen nuclei yields a cube root of unity, as realized by the  ${}^2\text{E}$  irrep of  $\text{C}_3$  (see Example 40). Such a monodromy cannot be directly attributed to Bose/Fermi spin statistics and is instead reminiscent of anyonic statistics [147–151] (themselves stemming from an induced representation [39, 152]).

For entangled species, monodromies are matrices acting on the  $\mathfrak{d}$ -dimensional fibers. These generate *non-Abelian* monodromy groups, akin to those obtained by braiding non-Abelian anyons [99, 153–156] or realizing fault-tolerant quantum gates [100]. There exist several molecular species realizing representations of the dihedral, tetrahedral, octahedral, and icosahedral groups.

The  $\text{E} \otimes \text{E} \downarrow \text{A}_2$  entangled species of dihedrally perrotation-symmetric boron trifluoride admits a two-dimensional fiber (see Example 41). Rotations permuting its three fluorine nuclei realize the two-dimensional irrep  $\text{E}$  of a dihedral group via monodromy.

The four entangled species of icosahedrally perrotation-symmetric  ${}^{13}\text{C}_{60}$  fullerene admit fibers of dimensions  $\mathfrak{d} = 3, 3, 4$ , and  $5$ , respectively. Monodromies of each species realize the 60-element icosahedral group irreps  $\text{T}_1$ ,  $\text{T}_2$ ,  $\text{G}$ , and  $\text{H}$ , respectively (see Example 43).

While our predicted monodromy occurs after an adiabatic path in position-state space, it is not always neces-

sary to initialize a molecule in a fixed position state to obtain the same effect as that arising from a position-state monodromy. In the case of  $\text{H}_2$  confined to two dimensions, *any* ortho or para state will do (see Sec. VI). In three dimensions, one can set the molecule to rotate in the equatorial plane with some fixed angular momentum  $J$ , corresponding to the  $\mathbf{z}$ -axis momentum projection  $m = 0$ . Any rotational state  $|J, m=0\rangle$  yields the same phase of  $-1$  under an equatorial  $\pi$ -rotation (see Example 39).

### E. Fibers as protected encodings

Molecules were postulated to be useful for quantum information processing over 20 years ago [114–123] due to their identical nature and large state space, the latter stemming from their many degrees of freedom. Reference [101] showed that superpositions of *multiple* position states of asymmetric and rotationally  $\text{C}_\infty$ -symmetric molecules form an error-correcting *molecular code*.

On the other hand, the fiber degrees of freedom  $\{|\mu\rangle\}$  of perrotationally G-symmetric entangled species all lie in a *single* molecular orientation,  $\mathbf{a} = \mathbf{e}$  (see Fig. 4). We show in Sec. XI, that, despite not consisting of a superposition, certain fiber encodings have a comparable degree of protection as molecular codes. Moreover, fiber codes, in some cases, allow for a richer set of fault-tolerant gates via monodromy (see previous subsection).

Superposing position states of asymmetric molecules according to the molecular-code prescription [101] induces the same coset structure as that of rotationally symmetric molecules, i.e., the representation  $\mathbf{A} \uparrow \text{SO}(3)$  induced by the trivial irrep of some  $\text{SO}(3)$  subgroup. As such, rotation errors acting on either molecular or fiber code states can be corrected as long those rotations do not implement a non-contractible path in the coset space.

Molecular codes also protect against sufficiently small kicks in an asymmetric molecule’s momentum. Because their code states are superpositions of different position states, momentum kick operators — diagonal in the position-state basis — modulate the code states in a way that can be detected and sometimes corrected.

Fiber codes protect against momentum kicks in a different way. Since a fiber lies within a particular species, any kicks that transition the state out of the given species can be detected. Moreover, shifting the momentum of the molecule *without* transitioning to another species can only be done for certain momenta  $J$ . We identify the species that can only be affected by momentum kicks by  $J \geq J_{\min} > 1$ , meaning that those species are immune to intra-species momentum kicks by  $J_{\min} - 1$ . This restriction narrows down six types of species whose fibers form useful encodings: the  $\text{E}_{i>1}$  irreps of the dihedral, the E and  $\text{T}_2$  irreps of the octahedral, and the  $\text{T}_2$ , G, and H irreps of the icosahedral groups (see Table VI).

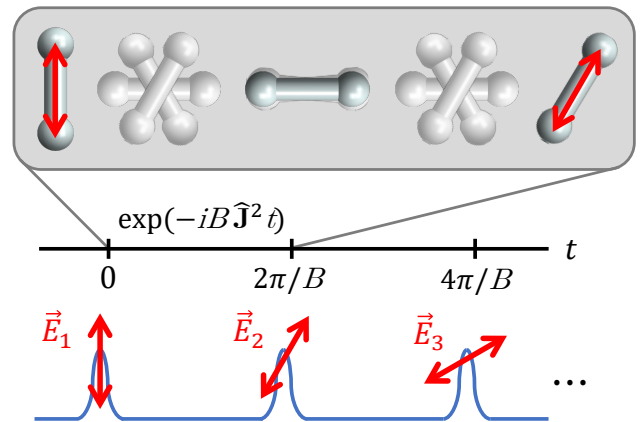


FIG. 5. Sketch of the evolution of a homonuclear diatomic evolving under its intrinsic rigid rotor Hamiltonian,  $B\hat{\mathbf{J}}^2$  with rotational constant  $B$ , while undergoing a stroboscopic reorientation from the  $\mathbf{z}$  to the  $-\mathbf{z}$  axis via a series of ultrafast pulses. The first pulse aligns the molecule along the desired  $\mathbf{z}$ -axis, initializing it in what is a close approximation to the corresponding position state. Subsequent Hamiltonian evolution induces phases,  $\exp(-iBJ(J+1)t)$ , on the molecule’s rotational states  $|J, m\rangle$ , but all phases disappear at times  $t$  that are multiples of the rotational period  $T_{\text{rev}} = 2\pi/B$ . At the rotational period, a second pulse, with slightly rotated polarization relative to the first, is incident on the molecule. Subsequent pulses can be applied at multiples of  $T_{\text{rev}}$ , with each pulse incrementally edging the position state closer to that aligned along the  $-\mathbf{z}$  axis. In the impulsive limit, where the pulse length is much shorter than  $T_{\text{rev}}$ , relative phases are imprinted that cause the molecular wavepacket to rephase at the new, rotated polarization. As long as the tilt between polarizations of successive laser pulses is not too large, a sufficiently discretized set of pulses should incrementally re-orient the molecule from  $\mathbf{z}$  to  $-\mathbf{z}$ .

### F. Experimental signatures

An Abelian position-state monodromy is an overall (undetectable) phase of a molecular species’ position state, but such a phase can be converted into a relative (and thus detectable) phase if the species is in superposition with some reference state. We discuss how to observe both Abelian and non-Abelian monodromy using either superposition via Aharonov-Bohm-type interference or inter-molecular entanglement in a molecular crystal. We mention scenarios where the operation stemming from monodromy can be obtained for molecules initialized in states other than position states. We also conjecture that signatures of complete entanglement should be present in the linear momenta of scattered nuclei upon molecular dissociation.

**Molecular interferometry** One way to convert an Abelian monodromy into a relative phase is to interfere a rotated version of the molecule with a reference, unrotated version of itself. This can be done in a double-slit-type experiment: an incoming molecular species is

split into two “arms” and aligned in some fixed position state, a lab-based rotation is applied to one of the two arms, and the two arms are recombined in order to probe their interference.

Initializing in a separable molecular species  $s$  and nuclear-spin state  $\chi$ , denoting the first (second) arm by an overline (underline), and assuming a lab-based symmetry rotation implementing the transformation  $\mathbf{g}$ , the two arms recombine as

$$|\overline{s}, \overline{\chi}\rangle + \Gamma_{\text{rot}}(\mathbf{g})|\underline{s}, \underline{\chi}\rangle, \quad (6)$$

where  $\Gamma_{\text{rot}}(\mathbf{g})$  is the resulting root-of-unity monodromy.

For the simplest example, we can align a homonuclear diatomic (e.g.  $\text{H}_2$  or  $\text{N}_2$ ) along the  $\mathbf{z}$  axis and re-orient it to the  $-\mathbf{z}$  axis using a  $\pi$ -rotation around any equatorial axis. Upon this rotation, the para (ortho) species yields a positive (negative) monodromy, i.e.,  $\Gamma_{\text{rot}}(\mathbf{g}) = \pm 1$ , respectively. More generally, a  $C_N$ -symmetric molecule can yield an  $N$ th root-of-unity monodromy, but we focus on ortho and para hydrogen from now on for simplicity (see Sec. VI and Example 39). One way to observe a position-state monodromy is to align the molecule in the lab frame and drag the internuclear axis around by an angle of  $\pi$ . However, such adiabatic dragging is difficult to realize in practice due to simultaneous requirements of rotational adiabaticity and high field intensities. We propose to induce lab-frame rotations via a stroboscopic sequence of ultrafast laser pulses [79, 157–160], similar to a quantum kicked-rotor model in which the kick orientation is incremented at each time step (see Fig. 5).

In practice, the two “arms” of the interferometer can represent separated beams in real space that can be obtained via matter-wave diffraction. Alternatively, we propose to realize the interferometer using a coherent superposition of two internal states of the molecule, such as vibrational or metastable electronic states. In this scenario, one state is dark to the re-orienting pulses due to its different rotational constant. We discuss details of and issues with both scenarios in Sec. XII.

**Oriental glasses** Molecules can arrange themselves in crystalline patterns at particular temperatures and pressures, but, the rotational degrees of freedom of each molecule in such patterns are only *partially* restricted. Molecular crystals of hydrogen [161][162, pg. 563], methane [162, pg. 582], and fullerene [163–165] have been synthesized and studied.

As a molecular crystal is cooled, it forms an orientational glass [162], in which each molecule is spontaneously oriented in one of a handful of directions commensurate with the lattice symmetry [166]. The particular orientation depends on neighboring orientations. Thus, molecules are constrained to approximate position states without the application of intense electric fields. Re-orientation may provide a way to probe monodromy, which would be non-Abelian in the case of methane or isotopic fullerene crystals.

**Dissociation** The complete symmetry-induced rotation-spin entanglement within a species cannot be

broken by any operation that maintains the molecular symmetry and keeps the molecule intact. Detecting this entanglement may thus require either a breaking of the molecular symmetry or, more drastically, a breaking (dissociation) of the molecule itself.

Dissociating the molecule should transfer any initial linear and angular momenta into the linear momenta of the individual nuclei. Any inter-nuclear (e.g., singlet or triplet) entanglement may be maintained after dissociation. Similarly, complete rotation-spin entanglement may also leave a mark on the relative motion of the scattered nuclei. If so, the outgoing nuclear state should be species dependent, exhibiting a different entanglement pattern in, say, the entangled E species of dihedrally symmetric boron trifluoride (see Example 20) than in its separable  $A_2^*$  species (see Example 18).

### III. THIS WORK IN CONTEXT

Many of the technical tools we use have been utilized in spectroscopy, but in a different Hamiltonian-centric point of view and often with additional (i.e., electronic and/or vibrational) degrees of freedom.

**Momentum states** Our framework for momentum states is based on what has long been known in the molecular spectroscopy literature [24–32]. There exist several prescriptions to determine admissible states, with each prescription considering slightly different symmetries [24, pg. 54]. These prescriptions, along with a more modern take utilizing Schur-Weyl duality [167, 168], focus mainly on determining the statistical weights  $\mathbf{m}_{\text{nuc}}$  of the nuclear-spin factor. They also tend not to focus on general features, instead working out each molecule in full detail. By exhaustively listing all admissible combinations of irreps satisfying condition (1), we identify two general features — the dimensions of  $\Gamma_{\text{rot}}$  and  $\Gamma_{\text{nuc}}$  are always equal, and the multiplicity of the  $\Gamma_{\text{mol}}$  irrep is always one — and make contact with the theory of induced representations to pave the way for a complete position-momentum phase space.

Induced representations have seen several applications in chemistry. Induced representations of symmetry groups are used in the aforementioned previous work to describe the interplay of symmetry and particular Hamiltonian perturbations [2, 21, 169–175]. Our induced representation is of the *entire* proper-rotation group, acts on the entire admissible state space, and is Hamiltonian-independent.

Entangled species’ states for various symmetric molecules have been studied in pioneering work by Harter, Patterson, and coworkers [2, 21, 171–175], where entangled momentum basis states are referred to as “Pauli states” [173][29, pg. 622]. The explicit form of these states is typically not important for spectroscopic studies because their degeneracy “*cannot be split by any higher-order interactions*” [32, pg. 92]. This may be another reason they have not been investigated further, and we



are not aware of general statements about their complete rotation-spin entanglement.

**Position states** Molecular position states are mentioned at the initial step of prescriptions for finding admissible momentum states in the aforementioned work (e.g., [2, 175]), with a book by Harter [3] explaining position states for asymmetric and linear molecules in a way that is arguably the closest to our symmetry-centric point of view.

Pendular states [10–13] — obtained by orienting the molecule along an axis defined by an electric field — are close approximations to position states. In the strong-field regime, the position-state space is restricted to a local region of states centered at the position of the pendular state. This restriction makes it impossible to notice the topological effects associated with the global position-state space.

Our position states are derived by starting with the Zak basis [101, 176–178] for  $SO(3)$  and entangling Zak basis states with nuclear degrees of freedom according to the prescription stemming from condition (1).

**Symmetric tops** We “mod out” symmetry on the level of the state space, but one can also do so at the Hamiltonian level. The canonical Hamiltonian of a 3D rigid body is defined by the body’s moment-of-inertia matrix  $I$ . Non-linear molecules are classified as asymmetric (generic diagonal  $I$ ), symmetric (doubly degenerate  $I$ ), or spherical ( $I \propto \mathbb{1}$ , the identity) tops [25].

A generic diagonal  $I$  is invariant under rotations forming the dihedral group  $D_2$ , which are represented by diagonal matrices with  $\pm 1$  entries and determinant one [37]. Thus, the coset space  $SO(3)/D_2$  labels distinct rotationally related asymmetric top Hamiltonians; the relevance of the topology of this space has been noted before [179, 180]. Similarly, the coset space  $SO(3)/D_\infty$  labels distinct Hamiltonians of symmetric tops.

The moment-of-inertia Hamiltonian classification is too coarse to determine the position-state space. For example, spherical tops admit only one possible moment-of-inertia Hamiltonian (up to constant pre-factors), but can have various state spaces as determined by their symmetry. Similarly, asymmetric tops need not be asymmetric molecules; e.g., water is an asymmetric top but has the *symmetric* state space  $SO(3)/C_2$ .

**Monodromy in molecules** An Abelian holonomy that is also a monodromy — a “topological” Berry phase — can occur for eigenstates of particular rovibrational Hamiltonians [181–184]. The Hamiltonian degeneracy occurs at a conical intersection (see Example 5), yielding a  $-1$  Berry phase that is independent of the fine-grained details of the state’s path. Non-Abelian holonomy is postulated to occur [185–188], but there is no monodromy because the parameter space is simply connected.

Others have studied monodromy effects [189–195], critical phenomena [196–198], and other topological features [199, 200] of spectra of quantum and semiclassical molecular Hamiltonians, many of which include rotational degrees of freedom.

In contrast to past work, our rotation-spin monodromy effects are intrinsic features of the state space and are independent of any Hamiltonian. They occur for configuration spaces which are coset spaces of  $SO(3)$  — all non-simply-connected except  $SO(3)/C_\infty = S^2$  — and which can yield non-Abelian monodromy.

**Chemical bonding** It is well known that some molecules species, such as ortho hydrogen, do not contain states of zero angular momentum. In other words, a molecule initialized in such a species never stops spinning. Even more surprising is that some molecules, such as boron trifluoride, do not admit *any* species with zero angular momentum (see Example 20). The inability to stop spinning can affect how well a molecular species bonds during a chemical reaction [201]. This idea has been analyzed from a physics perspective for cyclically-symmetric molecules in Ref. [125], and our work can be used to extend their predictions to molecules with arbitrary symmetry.

The work [125] also identified the root-of-unity monodromy (“branch cut”) associated with perrotationally symmetric species with cyclic symmetry. Our work provides a way to realize that and more general monodromy using lab-based symmetry rotations.

**Holonomy calculations** The holonomy of induced-representation spaces is relevant to quantization and gauge theory [39–41, 179, 202–206]. Since discrete symmetry groups were not directly considered, we have to perform explicit holonomy calculations for the spaces of interest (see Sec. X).

We utilize a symmetry of the Berry connection (that generates the holonomy) to prove that the connection is automatically zero for a large set of  $SO(3)$  induced representations. This complements a proof of flatness for  $D_\infty$ -symmetric states, developed in an illuminating paper by Berry and Robbins [207], as well as flatness results for fixed- $J$  “anti-coherent” states [208–210]. Our identified symmetry may be applicable for quantum computation with fixed- $J$  subspaces [211–216].

Position-state connections for the remaining induced representations are either calculated analytically or confirmed by numerics, yielding zero in both cases. Collecting previous examples [42, 155, 217–220] and re-asking the question posed in Ref. [42], we make a conjecture [221] as to the necessary and sufficient criteria for a flat position-state Berry connection on a general induced representation space (see Appx. X E).

## IV. OUTLOOK

Following earlier topological classifications of solid-state band insulators (e.g., [137]) and nematic liquid crystals [138, 139], we classify molecular rotation-spin state spaces, develop a position-momentum duality, quantify their entanglement patterns, and identify a set of robust “topological” features.

**Molecular phase space** Quantum applications in conventional state spaces, such as qubits and harmonic oscillators, hinge on a position-momentum duality. Re-invigorating the duality between rotational position and momentum that has been under-represented in the molecular world, we relate established techniques from molecular spectroscopy [14–32] for finding angular momentum states to those from quantization theory [39–42] for finding angular position states. Our work lays the foundation for using the *entirety* of molecular state space for quantum computing, simulation, and sensing, as well as for finely controlled chemical reactions, frequency conversion, and yet-to-be-discovered future technologies.

In technical terms, we show that the rotation-spin states of a molecular species host an induced representation [36, 131–136] of the group of lab-based rotations, induced by an irreducible representation, or irrep, of the molecule’s symmetry subgroup. While all classical rigid-body state spaces correspond to trivial inducing irreps, spin-statistics restrictions yield non-trivial irreps. Molecular species with such state spaces have no classical analogue and admit two interesting and potentially useful features.

**Complete entanglement** The first feature is that symmetry and spin-statistics force the rotational and nuclear-spin degrees of freedom to *always* be entangled. This entanglement is present in the entire molecular species’ state space, and is *independent* of and *unaffected* by any symmetric Hamiltonian. While the numerical spectroscopy community has long had to deal with this effect, it is worth highlighting that it represents possibly the first instance of symmetry-induced entanglement in a physical system.

We systematically quantify the strength of this entanglement in terms of properties of the molecule’s symmetry group. Molecules straddle the spectrum between the quantum and the classical, and our entanglement classification rigorously determines the degree of “quantumness” of any given molecule. We find that molecules with non-Abelian symmetry groups skew toward the quantum end of this spectrum.

Complete entanglement may seem surprising when interpreted as a fragile resource, but it is, in fact, quite generic in Hamiltonian eigenstates [222] and many-body state space in general [223, 224]. We anticipate that the our symmetry-induced intra-species entanglement will be similar in spirit to fermionic entanglement [225] — a useful resource [226]. The ability to *switch* between species with different entanglement patterns may be relevant to chemical reactions [125] and, more speculatively, may yield quantum processing applications in molecules [124] using, e.g., projective measurements [123]. Our explicit state spaces should help reduce the complexity cost of numerical studies (e.g., those using tensor networks [227]) where inter-species transitions can occur.

**Fibers and their topological operations** The second consequence of our result is that *each* position state of certain molecular species hosts a “hidden”

(cf. [121]) qudit or “fiber” degree of freedom, and that this fiber can be used to store and protect quantum information that is arguably more natural than engineered molecular encodings [101, 122].

Quantifying the robustness of fiber operations using the framework of holonomy (read: Berry phase) [95–98], we reveal that position-state holonomy depends only on global or “topological” properties of paths in position space. The same dependence is observed in the braiding of Abelian and non-Abelian anyons [99, 147–156] and in families of fault-tolerant quantum gates [100]. Such topological holonomy, or *monodromy*, has hitherto been predicted in only engineered and/or exotic systems, while in this case it occurs naturally in the seemingly “classical” position states of molecular species. The simplest monodromy is already present in ortho hydrogen, and we outline ways to observe it in the lab.

**Future directions** We restrict to molecules whose orbital, electronic spin, and vibrational degrees of freedom transform trivially under symmetry rotations. Removing this restriction should yield an expanded classification based on multi-factor generalizations of Eq. (1). This may yield other induced representations not possible in the current framework and generalize interesting ro-vibrational effects [228, 229].

Only proper rotations feature in our rigid-body-based analysis, but improper rotations become important when nuclei are allowed to re-configure themselves via tunneling in ways that are not possible via proper rotations [24–32]. It could be interesting to study chiral molecules that can switch chirality via tunneling (e.g., [121, 168, 230]) or non-rigid molecular dimers, trimers, and other clusters. Our treatment may also be relevant to magnetic rigid-rotor nanoparticles, which feature a similar rotation-spin state space [231–235].

The fiber is well hidden and delocalized across both angular-momentum and nuclear-spin space, and it will be crucial to determine ways to map quantum information to and from this space. It will also be of interest to develop uncertainty relations [236], a Wigner-Weyl-type formalism [237, 238], coherent states [239–244], and extensions of semi-classical methods [175, 245] to general molecular phase spaces. Having laid down a complete molecular phase space, we leave these and other exciting quantum applications to future work.

## ACKNOWLEDGMENTS

V.V.A. acknowledges Jonathan Tennyson, Timur V. Tscherebul, and Sergei N. Yurchenko for advice on placing these results in context, and Brandon R. Brown for advice on scientific writing. We also thank B. Andrei Bernevig, Barry Bradlyn, Chin-wen Chou, Leah G. Dodson, Matthew P. A. Fisher, Gerald T. Fraser, Joseph T. Iosue, Artur F. Izmaylov, William G. Harter, Joseph T. Hodges, Ted Jacobson, Shubham P. Jain, Anton Kapustin, Andrei F. Kazakov, Aleksei Khudorozhkov,

Christiane Koch, Johannes Kofler, Richard Kueng, Dietrich Leibfried, Monika Leibscher, David Long, Svetlana Malinovskaya, Leo Radzihovsky, Nathan Schine, Stafford W. Sheehan, Benjamin Stickler, Ian Teixeira, Christopher David White, and Jun Ye for helpful discussions.

E.K. acknowledges support from NSF QLCI grant OMA-2120757. M.L. acknowledges support by the European Research Council (ERC) Starting Grant No. 801770 (ANGULON). All molecules were drawn in MATHEMATICA 13 [246]. The following public-domain photos from [freemove.org](https://commons.wikimedia.org/wiki/File:Stock_dumbbell.png) were used for Fig. 2: [stock dumbbell](#), [round pencil](#), [plane](#), and [soccer ball](#). Contributions to this work by NIST, an agency of the US government, are not subject to US copyright. Any mention of commercial products does not indicate endorsement by NIST. VVA thanks Ryhor Kandratsenia and Olga Albert for providing daycare support throughout this work.

## V. OUTLINE OF THE REMAINING MANUSCRIPT

The rest of the paper is devoted to technical derivations, but an attempt is made to make said derivations relatable. In addition to providing nearly 50 example demonstrations of the various general ideas with specific molecules, we demonstrate our monodromy result using a simple toy model — the hydrogen molecule confined to rotate in two dimensions — in Sec. VI.

In Sec. VII, we review what is known about the position and momentum state space of an asymmetric molecule and calculate the holonomy of its position states. In Sec. VIII, we formulate the momentum state space of symmetric molecules, proving the induced representation theorem stated above. In Sec. IX, we formulate position states of symmetric molecules and the Fourier transform that converts between position and momentum. In Sec. X, we calculate the holonomy of molecular position states, showing that it depends only on topological features of the position configuration space. In Sec. XI, we quantify the strength of the fiber as a quantum error-correcting code. In Sec. XII, we discuss how to realize the monodromy of homonuclear molecules via various interferometric approaches.

## VI. TOY MODEL: HYDROGEN MOLECULE IN TWO DIMENSIONS

We demonstrate a simple example of the molecules species classification and monodromy effects using diatomic molecules, pinned at their center of mass and confined to rotate in the  $\mathbf{xy}$  plane. All rotations in this section are restricted to be around the  $\mathbf{z}$  axis.

An example of an asymmetric diatomic in two dimensions is HCl. Its state space is that same as that of the planar rotor (*a.k.a.* a particle on a circle) [143]. Rotor momentum states  $|J\rangle$  are labeled by an integer  $J$ ; their

sign determines whether the rotor is spinning clockwise or counterclockwise. The rotor’s momentum operator  $\hat{J}$  satisfies  $\hat{J}|J\rangle = J|J\rangle$ . Rotor position states,

$$|\phi\rangle = \frac{1}{\sqrt{2\pi}} \sum_{J \in \mathbb{Z}} e^{i\phi J} |J\rangle, \quad (7)$$

are labeled an angle  $\phi$ , which determines how the rotor’s orientation deviates from some reference orientation.

On the other hand, the state space of perrotationally symmetric molecules is a subspace of the composite space consisting of a rotational planar-rotor factor and a nuclear-spin factor. The subspace is defined by a constraint on both factors that stems from symmetry and spin statistics.

For example, the two spin-half nuclei of  $\text{H}_2$  are indistinguishable in the molecule’s frame, meaning that the molecule is symmetric under molecule-based rotations by  $\pi$ . A  $\pi$ -rotation in the molecule’s frame rotates the molecule while also exchanging nuclei. This operation corresponds to a *perrotation*,

$$\widehat{X}_\pi = e^{i\pi \hat{J}} \otimes \text{SWAP} \quad (\text{molecule-based rotation}), \quad (8)$$

where the operator on the first factor acts on the rotational state space, and the operator on the second nuclear-spin factor performs a swap of the two spins.

The joint rotation-spin constraint is

$$\widehat{X}_\pi \psi_{\text{mol}}(\phi_1, \phi_2, s_1, s_2) = \psi_{\text{mol}}(\phi_2, \phi_1, s_2, s_1) \quad (9a)$$

$$= -\psi_{\text{mol}}(\phi_1, \phi_2, s_1, s_2), \quad (9b)$$

for any admissible wavefunction  $\psi_{\text{mol}}$  of the two nuclear positions  $\phi_{1,2}$  and spin-functions  $s_{1,2}$ . The minus sign, stemming from the spin statistics of the two fermionic hydrogen nuclei, can come from the rotational or the nuclear-spin factor, resulting in two molecular *species* — para and “ortho” hydrogen.

Basis states of the para species consist of tensor products of rotor states with *even* angular momentum and the unique anti-symmetric nuclear-spin *singlet* state,  $|\uparrow\downarrow\rangle - |\downarrow\uparrow\rangle$ . Basis states of the ortho species consist of tensor products of states with *odd* angular momentum and any nuclear-spin state in the span of the three symmetric *triplet* states,  $|\uparrow\uparrow\rangle$ ,  $|\downarrow\downarrow\rangle$ , and  $|\uparrow\downarrow\rangle + |\downarrow\uparrow\rangle$ . The required spin-statistics phase comes from the nuclear-spin (rotational) factor for the para (ortho) species.

The two species’ spaces can also be defined using rotor position states  $|\phi\rangle$  (7). If one of the nuclei is at position  $\phi_1 = \phi$ , we automatically know the position of the other nucleus,  $\phi_2 = \phi + \pi$  modulo  $2\pi$ , so position states of this dumbbell-like molecule are labeled by a single angle. The  $\pi$ -perrotation symmetry implies that states  $|\phi\rangle$  have to be identified with their antipodes,  $|\phi + \pi\rangle$ . Identification is done by superposing the two states for each angle  $\phi \in [0, \pi)$ . There are two ways to do so — using either a  $+1$  or a  $-1$  relative phase — corresponding to the position states of the para and ortho species, respectively.

Omitting the accompanying nuclear-spin factors for brevity, admissible rotational states can be expressed in two different ways for each species,

$$\begin{aligned} |\psi_{\text{para}}\rangle &= \sum_{J \text{ even}} c_J^{\text{para}} |J\rangle = \int_0^\pi d\phi c^{\text{para}}(\phi) (|\phi\rangle + |\phi + \pi\rangle) \\ |\psi_{\text{ortho}}\rangle &= \sum_{J \text{ odd}} c_J^{\text{ortho}} |J\rangle = \int_0^\pi d\phi c^{\text{ortho}}(\phi) (|\phi\rangle - |\phi + \pi\rangle), \end{aligned} \quad (10)$$

for some momentum-state coefficients  $c_J$  and position-state functions  $c(\phi)$ .

Monodromy occurs when we examine how the two species' states transform under “passive” lab-based symmetry rotations. Such rotations occur in the lab frame, there is no permutation action on the spins. The  $\pi$ -rotation,

$$\vec{X}_\pi = e^{i\pi\hat{J}} \otimes \mathbb{1} \quad (\text{lab-based rotation}), \quad (11)$$

rotates each nucleus to a position that coincides with the initial position of the other nucleus.

Lab-based rotations should, in some physical settings, be generated by the *total* angular momentum,  $\hat{J} + \hat{s}_1 + \hat{s}_2$ , where  $\hat{s}_{1,2}$  are momentum generators for the two spins. These produce extra transversal operations that re-orient the individual nuclei to a new frame, but they cannot produce perrotational permutation factors like the SWAP operation in Eq. (8). We ignore such effects in this work for simplicity, noting that they may have to be taken into account in an experimental setting.

The hydrogen molecule is symmetric under the lab-based rotation from Eq. (11), but the two species transform in different ways:

$$\vec{X}_\pi |\psi_{\text{para}}\rangle = +|\psi_{\text{para}}\rangle \quad (12a)$$

$$\vec{X}_\pi |\psi_{\text{ortho}}\rangle = -|\psi_{\text{ortho}}\rangle. \quad (12b)$$

This can be shown either by noting that the two species are spanned by momentum states of different parity, or by directly shifting each position state by  $\pi$  in Eq. (10). In the case that the molecule is initialized in a position state, the different signs correspond to the monodromy of each species after an adiabatic path from  $\phi$  to  $\phi + \pi$  in position-state space.

The above two species can also be obtained by restricting the theorem from Sec. II to two dimensions. The symmetry group of  $\text{H}_2$  is  $\text{C}_2 = \mathbb{Z}_2$ , a subgroup of  $\text{C}_\infty \cong \text{SO}(2)$ , the two-dimensional proper-rotation group. The symmetry group has two irreps, the trivial irrep A and the sign irrep B. The even momentum states of the para species house the induced representation  $A \uparrow \text{SO}(2)$  of the group of lab-based rotations, while the odd-momentum ortho species correspond to  $B \uparrow \text{SO}(2)$ .

More generally, a  $\text{C}_N = \mathbb{Z}_N$ -symmetric molecule confined to a plane admits one or more of the induced representations  $\Gamma_{\text{rot}} \uparrow \text{SO}(2)$ , where  $\Gamma_{\text{rot}}$  is some root-of-unity irrep of  $\text{C}_N$ . Each representation corresponds to a particular way to quantize a particle on a circle. The planar

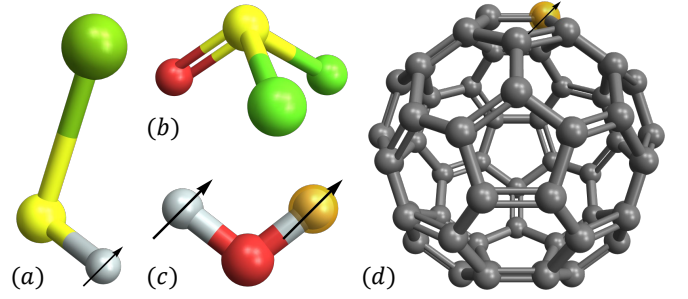


FIG. 6. Examples of asymmetric molecules (a) CaSH, (b)  $\text{SOCl}_2$ , (c) HDO, and (d)  $\text{C}_{59}^{13}\text{C}$  from Examples 1-4. Any proper rotation maps each molecule into a different position.

rotor from Eq. (7) corresponds to  $A \uparrow \text{SO}(2)$  — the representation induced by the sole irrep of the trivial group.

The rest of the manuscript addresses the extra complexities of molecules that are free to rotate in *three dimensions*. In that case, the rotational factors,  $e^{i\pi\hat{J}}$ , on the right-hand side of Eqs. (8) and (11) no longer coincide. So while the full rotation group of an asymmetric molecule is  $\text{SO}(2)$  in two dimensions, it is  $\text{SO}(3) \times \text{SO}(3)$  in three dimensions because lab- and molecule-based rotations correspond to independent operations even for rigid bodies with no spin.

## VII. ASYMMETRIC MOLECULES

A molecule is said to be symmetric under a coordinate transformation when the transformation maps the molecule to the same position that the molecule was in before the transformation was applied. For example, the  $\text{HCl}$  molecule, when aligned along some axis, is symmetric under rotations around that axis by any angle. These rotations are examples of the symmetry transformations or *symmetries* of such a molecule.

Symmetries include rotations that reorient the molecule while keeping the origin of its coordinate frame fixed, or reflections through either planes defined in the frame or the origin itself. In our symmetry-centric perspective aiming to reveal the *angular* Hilbert space available for particular symmetries (as opposed to the Hamiltonian-centric perspective that focuses on spectra and dynamics of concrete molecules), we consider only symmetries that can be applied to a rigid molecule by an observer. All admissible symmetries therefore lie in  $\text{SO}(3)$ , the group of orientation-preserving or *proper* rotations in three dimensions.

We say that a molecule is *asymmetric* if it admits no symmetries other than the identity; see Fig. 6 for examples. In other words, any nontrivial proper rotation maps the molecule to a position that is different from the molecule's initial position. From now on, the most abundant nuclear-spin isotope is assumed for each nucleus when no specific isotope is given.



**Example 1** (calcium hydrosulfide). Since we consider only proper-rotation symmetries, an asymmetric molecule can still be symmetric under *improper* rotations such as reflections through planes. An example of this is the CaSH molecule from Fig. 6(a). It is not linear [247] and is symmetric under reflection through the plane defined by its three atoms. However, it is not symmetric under any proper rotations, so it is considered an asymmetric molecule for our purposes.

**Example 2** (methanamine). The  $\text{CH}_3\text{NH}_2$  molecule also has reflection symmetry, but no proper rotation leaves the molecule invariant. While a proper rotation by  $2\pi/3$  around the axis defined by the CN bond *does* cyclically permute the three hydrogen nuclei attached to the carbon, this rotation simultaneously rotates the bent  $\text{NH}_2$  end into a different position. The final position state of the molecule as a whole is thus different from the initial state under such a rotation. In fact, there are *no* proper rotations that permute any subset of nuclei while leaving the rest of the molecule invariant, making this molecule asymmetric.

**Example 3** (semi water). While water is symmetric under a proper rotation, substituting one of its identical hydrogen nuclei with deuterium yields semi-heavy water, HDO [see Fig. 6(c)], which is asymmetric. Substituting a different spinful isotope for the oxygen in water does not change its symmetry because the oxygen atom is not permuted with another oxygen by any symmetry transformation.

**Example 4** ( $\text{C}_{59}^{13}\text{C}$  doped fullerene). Perhaps the most drastic example of the symmetry breaking [175] happens when one of the carbons in  $\text{C}_{60}$  fullerene is substituted with carbon-13 [see Fig. 6(d)]. Since the carbon-13 is in a different place after any of the original symmetry rotations, the initial icosahedral symmetry of the molecule, which constitutes 60 different proper rotations, breaks down to no symmetry at all.

### A. Asymmetric position states

When applied to a fixed reference position, each rotation  $r \in \text{SO}(3)$  maps the molecule to a position distinct from the reference; otherwise, the molecule would be symmetric. We assume there are no other possible transformations that the molecule can undergo, so proper rotations  $r \in \text{SO}(3)$  can be used as labels for the distinct position states  $|r\rangle$  of an asymmetric molecule [24, Appx. 2][3, Ch. 5]. These position states are identical to those of any asymmetric rigid body, e.g., an airplane [38].

Molecular position states are “orthonormal” in the same sense as the position states of a free particle, satisfying

$$\langle r|r'\rangle = \delta^{\text{SO}(3)}(r, r'), \quad (13)$$

where the Dirac  $\delta$ -function is infinite for rotations  $r = r'$  and zero otherwise. This relation makes the position

states not normalizable —  $\langle r|r\rangle$  is technically infinite — but approximate normalizable position states exist which are localized at  $r$  and which qualitatively have the same features (see Sec. XD 4). We focus on the idealized non-normalizable case since normalization is not relevant to most of our analysis.

Position states are also complete, yielding a decomposition of the identity,  $\mathbb{1}_{\text{rot}}$ , on the rotational state space of an asymmetric molecule,

$$\mathbb{1}_{\text{rot}} = \int_{\text{SO}(3)} dr |r\rangle\langle r|, \quad (14)$$

where  $dr$  is the Haar measure on  $\text{SO}(3)$  with  $\int dr = 8\pi^2$ .

The molecule’s reference position, denoted by  $|r = e\rangle$  with  $e$  the identity rotation, defines a *lab frame* of reference. Meanwhile, the orientation of the molecule relative to that lab frame defines a *molecule frame* (a.k.a. the Eckhart frame [20, 248, 249]), which is “bolted” to the molecule and not allowed to rotate without the molecule rotating in the same way.

The rotation  $r$  labeling the molecule’s position characterizes the orientation of the molecule frame relative to the lab frame. Each frame can be re-oriented, and both types of re-orientations can be interpreted as rotations performed on the molecule (see Fig. 7).

Re-orienting the molecule frame corresponds to a rotation performed on the molecule around an axis defined in the molecule frame. Such *molecule-based rotations*, denoted by  $\widehat{X}_g$  for any  $g \in \text{SO}(3)$ , act by post-multiplying the rotation matrix labeling the molecular position,

$$\widehat{X}_g|r\rangle = |rg^{-1}\rangle. \quad (15a)$$

Re-orienting the lab frame is done by *lab-based rotations*, denoted by  $\overleftarrow{X}_g$ . These act by pre-multiplication,

$$\overleftarrow{X}_g|r\rangle = |gr\rangle. \quad (15b)$$

Since the only piece of information encoded in molecular position is the *relative* orientation of the molecule w.r.t. the lab frame, we can fix the lab frame in place and think of lab-based rotations as “active” rotations of the molecule around an axis defined in the lab frame.

When the molecule is initially in its reference position  $|r = e\rangle$ , a lab-based rotation  $g$  maps the molecule to the same position as does the molecule-based rotation  $g^{-1}$ . This equivalence corresponds to

$$\overleftarrow{X}_g|e\rangle = \widehat{X}_{g^{-1}}|e\rangle \equiv |g\rangle, \quad (16)$$

where it is necessary to take the inverse of  $g$  since the two types of rotations change the relative orientation between the two frames in opposite ways.

In general, lab- and molecule-based rotations map an initial position  $r$  to two *different* positions,  $gr \neq rg$ , because the group  $\text{SO}(3)$  is *non-Abelian*. Since their actions on position states are not equivalent, the two types of rotations correspond to distinct and independent operators

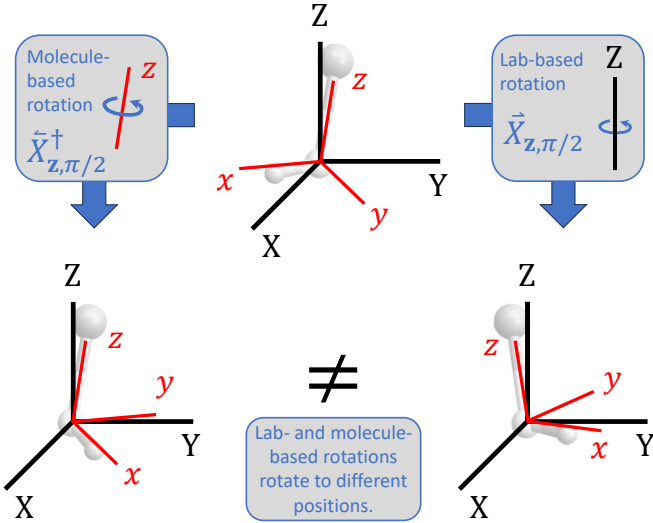


FIG. 7. Position of an asymmetric molecule is characterized by the relative orientation of the molecule frame ( $xyz$  axes) w.r.t. the lab frame ( $XYZ$  axes). Each frame can be re-oriented independently, yielding two types of rotations. Molecule-based and lab-based rotations rotate around axes defined in the molecule and lab frames, respectively (cf. [38, Fig. 3.9]). The resulting position state after the two types of rotations is generally *not* the same [see Eq. (15)], and the full group of asymmetric rigid-body rotations,  $\text{SO}(3) \times \text{SO}(3)$ , consists of products of the two rotation types.

on the rotational state space. The full group of asymmetric rigid-body rotations is  $\text{SO}(3) \times \text{SO}(3)$ , realized by products of the lab- and molecule-based rotations.

It is not possible to use one type of rotation to induce the effect of the other in a *state-independent* way. To see this, let  $\mathbf{r}$  be the initial molecular position. Applying a lab-based rotation  $\mathbf{g}$  yields the final position  $\mathbf{g}\mathbf{r}$ . Alternatively, one can apply a molecule-based rotation  $\mathbf{h}$  that yields the same final position,  $\mathbf{g}\mathbf{r} = \mathbf{h}\mathbf{r}$ , by solving for  $\mathbf{h}$ . However, the solution,  $\mathbf{h} = \mathbf{r}^{-1}\mathbf{g}^{-1}\mathbf{r}$ , depends on the initial state because proper rotations do not commute.

The lab frame and its corresponding  $\text{SO}(3)$  factor break down when the molecule is placed in an environment that is less symmetric than free space because symmetry-related positions are no longer distinguishable; this occurs, e.g., when the molecule is placed in a crystal lattice [3, pg. 372]. The molecule frame and its corresponding  $\text{SO}(3)$  factor break down when the molecule itself is symmetric under some proper rotations. Maintaining a perfectly symmetric *external* environment, we demonstrate, in subsequent sections, several features imposed by a molecule's *internal* symmetry.

## B. Asymmetric rotational states

Lab- and molecule-based rotations are each generated by their own angular momentum operators, with each set yielding a basis for a copy of the Lie algebra of  $\text{SO}(3)$ .

Due to the equivalence from Eq. (16), these two sets are coupled in the sense that they share the same total integer angular momentum  $J \geq 0$ .

A molecule can admit different values of the total momentum's projection onto the lab- and molecule-frame axes. As a consequence of the Peter-Weyl theorem [135, 136, 250], the identity on the rotational state space,  $\mathbb{1}_{\text{rot}}$  from Eq. (14), can alternatively be decomposed into a direct sum indexed by the total momentum  $J$ ,

$$\mathbb{1}_{\text{rot}} = \bigoplus_{J \geq 0} \mathbb{1}_{2J+1} \otimes \mathbb{1}_{2J+1}, \quad (17)$$

with blocks of dimension  $(2J+1)^2$  that further split into two tensor factors spanned by states of quantized values of the momentum components into the lab- and molecule-frame axes, respectively. Above,  $\mathbb{1}_d$  for natural number  $d$  denotes the  $d$ -dimensional identity matrix.

The choice of basis for the two  $\mathbb{1}_{2J+1}$  factors in Eq. (17) is arbitrary, but both are typically expressed in terms of *rotational states*  $|^J_m, k\rangle$ , where  $m$  and  $k$  denote the  $\mathbf{z}$ -axis projection of the momentum into the respective frames. We relegate  $m$  to a subscript because we will mostly focus on  $k$ . The decomposition (17) becomes

$$\mathbb{1}_{\text{rot}} = \sum_{J \geq 0} \sum_{|m| \leq J} \sum_{|k| \leq J} |^J_m, k\rangle \langle ^J_m, k|. \quad (18)$$

Lab-based (molecule-based) rotations act only on the first (second) factor in Eq. (17), decomposing in terms of rotational states as [3][101, footnote 145]

$$\vec{X}_{\mathbf{g}} = \bigoplus_{J \geq 0} D^J(\mathbf{g}) \otimes \mathbb{1}_{2J+1} \quad (19a)$$

$$\overleftarrow{X}_{\mathbf{g}} = \bigoplus_{J \geq 0} \mathbb{1}_{2J+1} \otimes D^{J*}(\mathbf{g}), \quad (19b)$$

where  $D^J$  is a matrix representing  $\text{SO}(3)$  rotations.

Rotational states  $|^J_m, k\rangle$  can be expressed as superpositions of position states  $|\mathbf{r}\rangle$ , and visa versa,

$$|^J_m, k\rangle = \sqrt{\frac{2J+1}{8\pi^2}} \int_{\text{SO}(3)} d\mathbf{r} D^{J*}_{mk}(\mathbf{r}) |\mathbf{r}\rangle \quad (20a)$$

$$|\mathbf{r}\rangle = \sum_{J \geq 0} \sqrt{\frac{2J+1}{8\pi^2}} \sum_{|m|, |k| \leq J} D^J_{mk}(\mathbf{r}) |^J_m, k\rangle. \quad (20b)$$

The overlap between elements of these Fourier-dual angular position and momentum states,

$$\langle ^J_m, k | \mathbf{r} \rangle = \sqrt{\frac{2J+1}{8\pi^2}} D^J_{mk}(\mathbf{r}) = \sqrt{\frac{2J+1}{8\pi^2}} \langle m | D^J(\mathbf{r}) | k \rangle, \quad (21)$$

is proportional to a Wigner  $D$ -matrix element, i.e., a matrix element of the rotation matrix  $D^J$  in the  $\mathbf{z}$ -axis momentum component eigenbasis [146, Ch. 4][251].

The breaking down of the molecule frame due to symmetry results in restricting the molecule-frame momentum space  $\{|k\rangle\}$  to particular subspaces. We perform these restrictions in Sec. VIII, obtaining sets of momentum and position states for symmetric molecules.

### C. Incorporating nuclear spin

Asymmetric molecules have no symmetries, meaning that any rotations that permute nuclei will necessarily map the molecule to a distinct orientation (see Example 2). There are thus no restrictions on the state space due to spin statistics, so the nuclei are not required to be in any particular (e.g., single or triplet) state. We denote the identity on the state space of any nuclear spins as  $\mathbb{1}_{\text{nuc}}$ .

The combined rotational-nuclear space for an asymmetric molecule is a tensor product of the rotational and nuclear-spin spaces,

$$\mathbb{1}_{\text{mol}} = \mathbb{1}_{\text{rot}} \otimes \mathbb{1}_{\text{nuc}} \quad (22a)$$

$$= \int_{\text{SO}(3)} dr |r\rangle\langle r| \otimes \mathbb{1}_{\text{nuc}} , \quad (22b)$$

$$= \sum_{J \geq 0} \sum_{|m| \leq J} \sum_{|k| \leq J} |J_m, k\rangle\langle J_m, k| \otimes \mathbb{1}_{\text{nuc}} , \quad (22c)$$

where we plug in the two position-state and rotational-state decompositions of the rotational factor from Eqs. (14) and (18), respectively. If the nuclear spin of each atom participating in a given molecule is zero, then the  $\mathbb{1}_{\text{nuc}}$  factor is dropped, and only the rotational factor remains.

Given a basis  $|\chi\rangle$  for the nuclear-spin factor  $\mathbb{1}_{\text{nuc}}$ , a basis for the entire state space of an asymmetric molecule consists of states

$$|J_m, k\rangle_{\text{rot}} \otimes |\chi\rangle_{\text{nuc}} , \quad (23)$$

where we have explicitly split each basis state into a factor coming from the rotational space and a factor coming from the nuclear-spin space. Each of these states is rotation-spin *separable*, i.e., is in tensor-product form with respect to the rotation-spin factorization. Rotation-spin non-separable or *entangled* states can then be expressed as superpositions of more than one of these states.

While there exist separable states in the state space of asymmetric molecules, the combination of symmetry and spin-statistics can make it impossible for separable states to exist at all in state spaces of symmetric molecular species. In later sections, we show that, after imposing symmetry and spin-statistics constraints, rotation-spin basis states are dressed by the nuclear spin in a way that makes *each* basis state entangled [see Eq. (57)]. Since such states form an orthonormal basis, superposing them can only increase their degree of entanglement and thus cannot yield a separable state.

The nuclei carry angular momentum  $S$  in the form of nuclear spin, which can be defined with respect to the molecule frame ( $\vec{S}$ ) or the lab frame ( $\vec{S}$ ) [232, Table I]. When incorporating spin in certain physical settings, lab-based and molecule-based rotations are extended to rotate both the rotational degrees of freedom and the nuclear spins. In other words, while the original rotations in

Eq. (19),  $\vec{X}_{\text{g}}$  and  $\vec{X}_{\text{g}}$ , are generated by rotational angular momenta,  $\vec{J}$  and  $\vec{J}$ , composite rotations are generated by the total angular momenta,  $\vec{J} + \vec{S}$  and  $\vec{J} + \vec{S}$ , in the lab and molecule frames, respectively. The extra nuclear-spin terms induce tensor-product rotations of the form  $U^{\otimes M}$  acting on any subset of  $M$  identical spins, where  $U$  is an  $\text{SU}(2)$  rotation representing  $\text{g}$ . These operations are distinct from the nuclear-spin permutations highlighted in this work (due to Schur-Weyl duality [167, 252]) and so are neglected from now on for simplicity, with the caveat that they may have to be accounted for in an experimental setting.

### D. Holonomy of asymmetric position states

We are interested in what happens when a molecule is initialized in a particular position state  $|r(0)\rangle$  and then adiabatically traverses a *closed path* —  $\{r(t), t \in [0, 1]\}$  with  $r(1)$  identified with  $r(0)$  — in its position space. This path can, for example, be induced by applying lab-based rotations  $\vec{X}_{r(t)}$ , which rotate the molecule to a different position state according to Eq. (15b).

The full molecular position state in Eq. (22b) includes a nuclear-spin factor. This factor tags along and is unaffected during the position-state path. As such, we omit the nuclear states below for simplicity.

Upon traversing a closed path in its position-state space  $\text{SO}(3)$ , the molecular state undergoes a *holonomy* [96, 98, 253],

$$|r(0)\rangle \rightarrow U_{\text{hol}} |r(0)\rangle . \quad (24)$$

The holonomy operator is, in this case, a scalar whose argument is called the geometric or *Berry phase* [95]. Note that a Hamiltonian is not required for determining the holonomy, which can be determined solely from the set of states and their parameter space.

The holonomy is invariant under changes in phase convention of the “instantaneous” states,  $|r(t)\rangle \rightarrow e^{i\varphi(t)} |r(t)\rangle$ , and different phase conventions (sometimes called “gauges”) and path parameterizations provide different ways to calculate the same holonomy.

We parameterize closed paths by the same set of coordinates for all points except, potentially, the last point  $r(t=1)$ . To account for cases when the last point requires a different set of coordinates, we express the holonomy as a product of two terms [99, Eq. (1.2)],

$$U_{\text{hol}} = U_{\text{mono}} \exp \left( - \int_{r(0)}^{r(1)} dr A(r) \right) . \quad (25)$$

The second term on the right-hand side of Eq. (25) is an integral of the *Berry connection*,

$$A(r) = i \langle r | \partial r \rangle / \langle r | r \rangle , \quad (26)$$

defined for all points  $r = r(t)$  in the path but the last one (i.e., for  $t < 1$ ), and with the partial derivative being with

respect to  $t$ . This connection depends on “local” features of the parameter space, such as the curvature. We will show that  $A(r(t)) = 0$  for all  $0 \leq t < 1$ , which means the connection is *locally flat*.

The first term on the right-hand side of Eq. (25) — the *monodromy*  $U_{\text{mono}}$  — can occur when  $r(1)$  is labeled with a *different* set of coordinates than  $r(0)$ . In order to resolve the labeling mismatch, the final state  $|r(1)\rangle$  has to be re-expressed in terms of the initial state  $|r(0)\rangle$ . A non-trivial  $U_{\text{mono}}$  is precisely the transformation relating the two states in the case when they are not equal; this happens when  $r(t)$  parameterizes a non-contractible path. As such, the monodromy piece depends on “global” or “topological” features of the parameter space.

The celebrated Aharonov-Bohm phase [254, 255] is due to a monodromy [256], and so is the  $\pi$ -phase due to circling a conical intersection [182]. In such Hamiltonian-based cases, a non-simply-connected parameter space is induced by the structure of the eigenstates.

**Example 5** (conical intersection toy model). Consider evolving a family of two-level system states [257],

$$|\phi\rangle = \begin{pmatrix} \sin \phi/2 \\ -\cos \phi/2 \end{pmatrix} \quad \text{for} \quad 0 \leq \phi < 2\pi, \quad (27)$$

along the path  $\phi(t) = 2\pi t$ . The Berry connection is locally flat for this case,  $\langle \phi | \partial \phi \rangle = 0$ , a fact that we can immediately observe because all states in the path are real-valued [96]. However, the state at the end point,  $\phi(1) = 2\pi$ , still has to be re-expressed in terms of that at the initial point,  $\phi(0) = 0$ , in order to conform to the chosen parameterization. The two states differ by a phase,  $|\phi = 2\pi\rangle = -|\phi = 0\rangle$ , and re-expressing reveals a monodromy of  $-1$ . This simple example holds more generally for any  $2 \times 2$  symmetric matrix [258].

We now show that the Berry connection in Eq. (26) is locally flat for asymmetric molecular position states  $|r\rangle$ . Plugging in the expression in terms of rotational states in Eq. (20b), using  $D_{mk}^{J*}(r) = D_{km}^J(r^{-1})$ , and re-expressing the result as a trace of a product within the angular momentum space yields

$$\langle r | \partial r \rangle = \sum_{J \geq 0} \sum_{|m|, |k| \leq J} \frac{2J+1}{8\pi^2} D_{mk}^{J*}(r) \partial D_{mk}^J(r) \quad (28a)$$

$$= \sum_{J \geq 0} \frac{2J+1}{8\pi^2} \text{tr} \left( D^J(r^{-1}) \partial D^J(r) \right). \quad (28b)$$

The quantity inside the trace is a representation the molecule’s angular velocity matrix relative to the molecule frame,  $r^{-1} \partial r$  [38, Prop. 3.9]. Angular velocity is valued in the tangent space of the space  $\text{SO}(3)$  of position-state labels, otherwise known as the  $\text{SO}(3)$  or angular momentum Lie algebra [146]. This Lie algebra is generated by the angular momentum operators, all of which are traceless. Therefore, the angular velocity matrix is also traceless,  $\text{tr}(D^J(r^{-1}) \partial D^J(r)) = 0$  for all  $J$ . Since the numerator  $\langle r | \partial r \rangle$  is zero and the denominator  $\langle r | r \rangle$  is positive, the connection (26) is zero.

symmetry	examples		irreps
	rotational	perrotational	
$C_1$	CaSH	none	A
$C_{2N}$	SO <sub>2</sub>	H <sub>2</sub> O	A, B, ${}^1E_{i \leq N-1}$ , ${}^2E_{i \leq N-1}$
$C_{2N+1}$	HCo(CO) <sub>4</sub>	CaOCH <sub>3</sub>	A, ${}^1E_{i \leq N}$ , ${}^2E_{i \leq N}$
$C_\infty$	HCl	none	A, $0 \neq \lambda \in \mathbb{Z}$
$D_2$	C <sub>2</sub> S <sub>4</sub>	C <sub>2</sub> H <sub>4</sub>	A, B <sub>1</sub> , B <sub>2</sub> , B <sub>3</sub>
$D_{2N}$	S <sub>8</sub>	XeF <sub>4</sub>	A <sub>1</sub> , B <sub>1</sub> , A <sub>2</sub> , B <sub>2</sub> , $E_{i \leq N-1}$
$D_{2N+1}$	SO <sub>3</sub>	BF <sub>3</sub>	A <sub>1</sub> , A <sub>2</sub> , $E_{i \leq N}$
$D_\infty$	S <sub>2</sub>	H <sub>2</sub>	A <sub>1</sub> , A <sub>2</sub> , $0 < \lambda \in \mathbb{Z}$
T	XeO <sub>4</sub>	CH <sub>4</sub>	A, ${}^1E$ , ${}^2E$ , T
O	Mo(CO) <sub>6</sub>	SF <sub>6</sub>	A <sub>1</sub> , A <sub>2</sub> , E, T <sub>1</sub> , T <sub>2</sub>
I	C <sub>60</sub>	C <sub>20</sub> H <sub>20</sub>	A, T <sub>1</sub> , T <sub>2</sub> , G, H

TABLE I. List of rigid-body symmetry groups, i.e., the possible subgroups of  $\text{SO}(3)$ : the cyclic ( $C_M = \mathbb{Z}_M$  for  $M \geq 1$ ), dihedral ( $D_M$  for  $M \geq 2$ ), continuous ( $C_\infty \cong \text{SO}(2)$ ,  $D_\infty \cong \text{O}(2)$ ), and exceptional (T, O, I) groups. An example of a rotationally and perrotationally symmetric molecule is provided when possible. Asymmetric molecules can be thought of as rotationally symmetric molecules whose symmetry group is the trivial group  $C_1$ . As such, symmetry alone is not sufficient to determine whether a molecule is rotationally or perrotationally symmetric: one needs to also know about the spin of any identical nuclei that are permutable via a symmetry rotation. The last column lists group irreps, labeled by Mulliken symbols [140, 141] (see also [259, 260]). We use complex (instead of real) irreps because we do not consider time-reversal symmetry.

Since the space  $\text{SO}(3)$  is not simply connected [250], there could be a nontrivial monodromy piece. However,  $U_{\text{mono}}$  turns out to be the identity for this particular case. For example, if the original coordinates parameterizing position states are Euler angles  $(\alpha, \beta, \gamma)$  with  $0 \leq \alpha < 2\pi$  (*excluding*  $\pi$ ), but the path is parameterized by  $(2\pi t, 0, 0)$  (*including*  $\pi$ ), then the final point  $(2\pi, 0, 0)$  has to be mapped back into the initial point  $(0, 0, 0)$ . The states corresponding to the two points are proportional (up to the monodromy) and, in this case, are exactly equal,

$$|r = (2\pi, 0, 0)\rangle = |r = (0, 0, 0)\rangle, \quad (29)$$

yielding a  $U_{\text{mono}}$  of identity. We prove the general case using tools from the symmetric molecule formulation (see Example 37).

Together, the above results show that there is no holonomy for closed loops in the position state space of an asymmetric molecule and, by extension, any asymmetric rigid body. This should not be surprising since other “classical” states of fixed position do not have Berry phases either, such as position states of a free particle on a line or a planar rotor. We will see in Sec. X that this is no longer the case for position states of many symmetric molecules with non-zero nuclear spin.



## VIII. SYMMETRIC ROTATIONAL STATES

In this work, we define a symmetric molecule as one whose position is invariant under a set of proper-rotation symmetry operations. This set forms the molecule’s

*rigid-body symmetry group*,  $G \subset \text{SO}(3)$ ,

a subgroup of the group  $\text{SO}(3)$  of proper (i.e, orientation-preserving) rotations. This symmetry group is a subgroup of the *full* symmetry group of the “static molecular model” [24, Eq. (2.21)] which can include reflections, improper rotations, and parity symmetry. Since we concern ourselves only with symmetry transformations that are realizable by rigid-body rotations, we consider only  $G$  and refer to it as simply “the symmetry group” throughout the text.

Subgroups of  $\text{SO}(3)$  can be discrete, meaning that they have a finite set of elements, or continuous, meaning that some of their elements are parameterized by a continuous variable (see Table I).

The two continuous symmetry groups are isomorphic to the group of planar rotations,  $C_\infty \cong \text{SO}(2)$ , and the group of planar rotations and reflections,  $D_\infty \cong \text{O}(2)$ . The  $\text{HCl}$  molecule, along with any heteronuclear diatomic, is invariant under rotations by any angle around its principal axis, meaning that its symmetry group is  $C_\infty$ . The  $\text{H}_2$  molecule, along with any homonuclear diatomic, is invariant under those same rotations and also  $\pi$ -rotations around axes perpendicular to its principal axis, all of which exchange its two constituent atoms; its symmetry group is  $D_\infty$ .

The possible discrete symmetry groups include the trivial group  $C_1$  (corresponding to no symmetry at all), the cyclic groups  $C_N$ , and the dihedral groups  $D_N$  (both for  $N \geq 2$ ). All asymmetric molecules, studied in Sec. VII, have the trivial symmetry group. The  $C_N$  group can be thought of as a discretized version of  $C_\infty$ , where rotations are only by multiples of  $2\pi/N$ . Examples of  $C_3$ -symmetric molecule is ammonia ( $\text{NH}_3$ ), whose atoms *do not* lie in a plane. The  $D_N$  group is a similarly discretized version of  $D_\infty$ . Boron trifluoride ( $\text{BF}_3$ ) or sulphur trioxide ( $\text{SO}_3$ ), whose four atoms *do* lie in a plane, both have  $D_3$  symmetry.

Rounding out the list of symmetry groups are the three “exceptional” subgroups — the tetrahedral  $T$ , octahedral  $O$ , and icosahedral  $I$  group. Methane is a canonical example of tetrahedral symmetry — the symmetry group of a tetrahedron. Examples of octahedral and icosahedral symmetry include sulfur hexafluoride ( $\text{SF}_6$ ) and fullerene ( $\text{C}_{60}$ ), respectively. To reiterate, a (rigid-body) symmetry group consists of only proper rotations collected from the full symmetry group of a molecule, which is  $O_h$  and  $I_h$ , respectively, in the latter two cases.

There are cases where symmetry rotations permute identical nuclei, *and* those nuclei have non-zero nuclear spin. A simple example is water, which admits a proper rotation that exchanges the two hydrogen atoms while

leaving the oxygen atom intact. In such cases, in addition to restricting the state space to only  $G$ -symmetric states, we also have to take into account any Bose or Fermi spin statistics realized by the nuclei.

We split symmetric molecules into two categories, depending on whether or not symmetries permute identical spinful nuclei. If all identical nuclei that are permuted under symmetry rotations have zero nuclear spin, then we call the molecule *rotationally symmetric*. Identical nuclei in rotationally symmetric molecules can be treated as points, and such molecules are special cases of symmetric rigid bodies. While technically correct, ascribing the invariance of such molecules to the statistics of any “spin-zero nuclei” is as necessary as attaching a zero spin to the end of a dumbbell.

If any of the identical permuted nuclei have non-zero nuclear spin, then we call the molecule *perrotationally symmetric*. Nuclei in perrotationally symmetric molecules have a non-trivial nuclear-spin space whose factors are permuted by molecule-based symmetry rotations, requiring a treatment deviating from that of symmetric rigid bodies.

For example, dihydrogen  $\text{H}_2$  is  $D_\infty$ -symmetric, but its two atoms have spin one-half nuclei. A molecule-based rotation that exchanges the identical nuclei in  $\text{H}_2$  results in a  $-1$  Fermi spin-statistics factor, making the molecule perrotationally symmetric. On the other hand, disulfur  $\text{S}_2$  is also  $D_\infty$ -symmetric, but has spinless nuclei. There is no spin-statistics factor to worry about, so  $\text{S}_2$  is rotationally symmetric and can be treated in the same way as a dumbbell.

A similar distinction is observed between rotationally  $D_3$ -symmetric sulfur trioxide ( $\text{SO}_3$ ) and perrotationally  $D_3$ -symmetric boron trifluoride ( $\text{BF}_3$ ), and between rotationally  $T$ -symmetric xenon tetroxide ( $\text{XeO}_4$ ) and perrotationally  $T$ -symmetric methane ( $\text{CH}_4$ ). More examples are provided in Table I. To reiterate, shape and symmetry are not enough to determine whether a molecule is rotationally or perrotationally symmetric; one needs to also know about the spin of any identical nuclei.

### A. Rotationally symmetric molecules

We now consider cases where molecule-based symmetry-group rotations *do not* permute identical spinful nuclei, meaning that the rotational state space of such symmetric molecules is identical to that of a rigid body with the same symmetry.

Rotationally  $G$ -symmetric molecular states span a subspace of the asymmetric molecular state space, defined by  $\mathbb{1}_{\text{mol}}$  (22) and spanned by the basis in Eq. (23). This subspace is defined by the restriction that

$$\widehat{X}_{\mathbf{g}}|\psi_{\text{mol}}\rangle = |\psi_{\text{mol}}\rangle, \quad \forall \mathbf{g} \in G, \quad (30)$$

for any state  $|\psi_{\text{mol}}\rangle$  of the symmetric molecule and any molecule-based rotation  $\widehat{X}$ .

In representation-theoretic terms, Eq. (30) implies that the molecule transforms under the trivial irreducible representation, or irrep, of  $G$ . In this irrep, denoted by  $A$  (and sometimes by  $A_1$ ), all elements  $g$  are mapped into one, i.e.,  $A(g) = 1$ . We need to keep only states in the decomposition of  $\mathbb{1}_{\text{mol}}$  (22) that transform as this irrep. We can determine this space by evaluating molecule-based rotations at elements of the symmetry group, decomposing the result into all the irreps of  $G$ , and keeping only copies of the trivial irrep.

Restricting  $g$  to rotations in the symmetry group, each  $D$ -matrix for a given  $J$ , while forming an irreducible representation of  $SO(3)$ , forms a *reducible* representation of  $G$ . This representation is unitarily equivalent to a block matrix whose blocks are labeled by any  $G$ -irreps  $\Gamma$  that are present in the  $D$ -matrix. Each block is characterized by two numbers, the dimension,  $\dim \Gamma$ , of the irrep and the number of copies of the irrep — the frequency or *multiplicity*  $\text{mlt}_J \Gamma$  — present in the block. The irrep dimension is  $J$ -independent, while the multiplicity can depend on the angular momentum.

We can “distribute out” the irrep and unitarily transform each block into tensor-product form, with the first factor housing the irrep, and the second factor housing the multiplicity space. This yields the *isotypic decomposition* (a.k.a. canonical decomposition) [136, 252],

$$D^{J*}(g) \cong \bigoplus_{\Gamma \uparrow J} \Gamma(g) \otimes \mathbb{1}_{\text{mlt}_J \Gamma}, \quad (31)$$

where  $\Gamma(g)$  is the matrix representation of the group element  $g$ , and  $\mathbb{1}_{\text{mlt}_J \Gamma}$  is the identity matrix. Not all  $G$ -irreps participate in a given rotation matrix, and the shorthand notation  $\Gamma \uparrow J$  denotes the subset of irreps that are present in the above decomposition; such irreps are determined by “branching” or “subduction” rules.

**Example 6** ( $G = C_\infty$  isotypic decomposition). For example, rotation matrices  $D^J$ , when restricted to the group  $G = C_\infty$  of  $z$ -axis rotations, are already diagonal w.r.t. the  $C_\infty$ -irrep basis,

$$D^{J*}(z, \phi) = \sum_{|k| \leq J} e^{ik\phi} |k\rangle \langle k|, \quad (32)$$

where  $\phi$  denotes the angle of the  $z$ -axis rotation.<sup>1</sup>

The set of distinct  $C_\infty$ -irreps is in one-to-one correspondence with the integers  $\lambda \in \mathbb{Z}$  (with  $\lambda = 0$  the trivial irrep  $A$ ), and each one-dimensional block houses the irrep  $\Gamma_{\lambda=k}(\phi) = e^{ik\phi}$ . The set of participating irreps is thus

$$\Gamma \uparrow J = \{\Gamma_{\lambda=k} \text{ such that } |k| \leq J\}. \quad (33)$$

The multiplicity space is trivial in this case since each participating irrep is featured only once for each  $J$ .

<sup>1</sup> We abuse notation by substituting a rotation’s axis-angle  $(\mathbf{v}, \phi)$  or Euler-angle  $(\alpha, \beta, \gamma)$  parameterizations [36] for the rotation itself as the argument of the rotation matrix  $D^J$ .

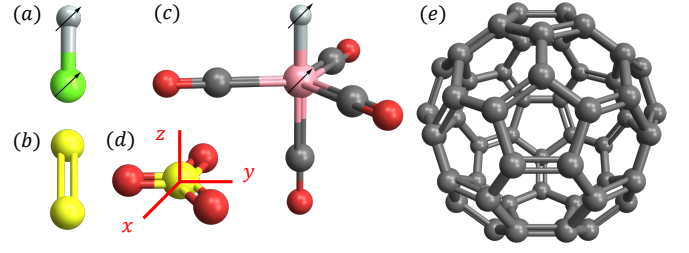


FIG. 8. Rotationally symmetric molecules (a) HCl, (b)  $S_2$ , (c)  $HCo(CO)_4$ , (d)  $SO_3$ , and (e)  $C_{60}$  from Examples 8-12. Proper rotations in a symmetry group  $G$  leave the positions of these molecules invariant.  $SO_3$  (d) is shown in the reference position state chosen in Example 11.

Plugging the decomposition (31) into Eq. (19b) yields

$$\widehat{X}_g \cong \bigoplus_{J \geq 0} \mathbb{1}_{2J+1} \otimes \bigoplus_{\Gamma \uparrow J} \Gamma(g) \otimes \mathbb{1}_{\text{mlt}_J \Gamma} \otimes \mathbb{1}_{\text{nuc}}. \quad (34)$$

The next step is to apply the symmetry restriction (30), which means keeping only the blocks corresponding to trivial irreps,  $\Gamma = A$ . We do this with the help of a Kronecker  $\delta$ -function:  $\delta_{\Gamma,A} = 1$  when  $\Gamma = A$  and zero otherwise. The trivial irrep is one-dimensional,  $\dim A = 1$ , so the first factor in the decomposition (34) reduces to a scalar factor,  $A(g) = 1$ . The second multiplicity factor remains nontrivial because each  $J$  can, in general, contain more than one copy of the trivial irrep.

All of the trivial-irrep blocks can be combined into a projection onto the state space of a  $G$ -symmetric molecule,

$$\mathbb{1}_{\text{mol}}^G = \bigoplus_{J \geq 0} \mathbb{1}_{2J+1} \otimes \bigoplus_{\Gamma \uparrow J} \delta_{\Gamma,A} \mathbb{1}_{\text{mlt}_J A} \otimes \mathbb{1}_{\text{nuc}}. \quad (35)$$

Expressing the first two factors in terms of a basis, Eq. (35) becomes

$$\mathbb{1}_{\text{mol}}^G = \sum_{J \downarrow A} \sum_{|m| \leq J} \sum_{\kappa=1}^{\text{mlt}_J A} |m_\kappa\rangle \langle m_\kappa| \otimes \mathbb{1}_{\text{nuc}}, \quad (36)$$

where  $m$  and  $\kappa$  index the two factors for each  $J$  whose  $D$ -matrix contains  $A$  in its decomposition. The sum over  $J$  becomes restricted to the subset of angular momenta which subduce to the trivial irrep. In (Frobenius [136]) reciprocity to the notation used in Eq. (31), we denote this subset by the shorthand  $J \downarrow A$ .

The symmetric rotational states  $|m_\kappa\rangle$  are the angular momentum states of a  $G$ -symmetric rigid body. The key difference from the asymmetric case is the second factor in Eq. (35), spanned by the basis  $\{|\kappa\rangle\}$  of states that transform as the trivial  $G$ -irrep. Hamiltonian eigenstates and, more generally, any molecular states can be expressed as superpositions of the symmetric rotational states.

**Example 7** (calcium monohydrosulfide). The procedure for determining the state space of a symmetric molecule

can also be applied to asymmetric molecules, such as the bent triatomic CaSH [61, 261] [see Fig. 6(a)]. The symmetry group of such molecules is trivial, containing only the identity element,  $G = C_1 = \langle e \rangle$ . This group has only one irrep, the trivial irrep A. Each rotation matrix  $D^J$ , when restricted to  $G$ , evaluates to the identity matrix whose dimension,  $2J + 1 = \text{mlt}_J A$ , indexes the multiplicity of the trivial irrep for that angular momentum. We wind up with a re-expression of the asymmetric rotational states from Eq. (22c),  $|^J_{m\kappa}\rangle = |^J_m, k = \kappa - J - 1\rangle$  for all  $J, m$  and for  $1 \leq \kappa \leq 2J + 1$ .

**Example 8** (hydrogen chloride). Aligning the HCl molecule along the  $\mathbf{z}$ -axis, we observe that any rotation around the  $\mathbf{z}$ -axis leaves it invariant. There are no other rotations that do this, so  $G = C_\infty$ .

Group elements  $g$  of  $C_\infty$  are rotations by angle  $\phi \in [-\pi, \pi)$ , and their corresponding irreps,  $e^{i\lambda\phi}$ , are indexed by integers  $\lambda$ . The case  $\lambda = 0$  corresponds to the trivial irrep.

Recalling Example 6, the  $\mathbf{z}$ -axis projection eigenstate  $|k\rangle$  houses a copy of the  $\lambda = k$  irrep. The trivial irrep is featured only once, at  $k = 0$ , so there is no need for a  $\kappa$  index. The  $C_\infty$ -symmetric rotational states are the subset of the asymmetric rotational states  $\{|^J_m, k\rangle\}$  from Eq. (22c) with zero  $k$ ,  $|^J_{m\kappa}\rangle \equiv |^J_m, k = 0\rangle$  for all  $J, m$ . This basis corresponds to the spherical harmonics [3].

The states  $\{|^J_m\rangle\}$  span the rotational state space of any diatomic whose atoms are distinct, even in cases when its nuclei admit non-zero nuclear spin. They also describe the state space of any  $C_\infty$ -symmetric linear *polyatomic* molecule, including N–N–O or C–C–N.

**Example 9** (disulfur). The  $S_2$  molecule is a symmetric molecule with symmetry group  $G = D_\infty$ . Aligning this dumbbell-like molecule along the  $\mathbf{z}$  axis, the rotations correspond to  $\mathbf{z}$ -axis rotations by arbitrary angles and form the subgroup  $C_\infty$ , while “reflections” correspond to  $\pi$ -rotations around any equatorial axis. Symmetry-group rotations *do* exchange identical sulfur nuclei, but these nuclei do not have any nuclear spin, so this molecule is rotationally symmetric.

The  $D_\infty$  group admits a trivial irrep  $A_1$ , and a “sign” irrep  $A_2$ , which represents  $\mathbf{z}$ -axis rotations by  $+1$  and equatorial-axis rotations by  $-1$ . The group also admits a countably infinite set of two-dimensional irreps, indexed by  $\lambda \in \mathbb{Z}$ , for which  $\mathbf{z}$ -axis rotations by angle  $\phi$  are represented by  $\exp(i\lambda\phi\sigma_z)$ , and the  $\mathbf{y}$ -axis “reflection” is represented by  $\sigma_x$  (given the usual Pauli matrices  $\sigma_{x,z}$ ).

Since  $C_\infty$  is a subgroup of  $D_\infty$ , we can first apply the analysis of the previous example and consider which of the admissible states from that case,  $\{|^J_m, k = 0\rangle\}$ , transform as the trivial irrep of the larger group.

Since we have already determined how the  $\mathbf{z}$ -axis rotations act via Eq. (32), we are left to determine the remaining equatorial rotations. Each such rotation is a product of a  $\mathbf{z}$ -axis rotation and a “fiducial”  $\mathbf{y}$ -axis  $\pi$ -

rotation. The latter is simply represented for each  $J$ ,<sup>1</sup>

$$D^{J*}(\mathbf{y}, \pi) = \sum_{|k| \leq J} (-1)^{J+k} |-k\rangle \langle k|, \quad (37)$$

implying that the trivial irrep occurs only in  $k = 0$  states with *even* momenta, with the remaining *odd* angular momentum states realizing the sign irrep. The basis  $\{|^J_m, k = 0\rangle\}$  for even  $J$  corresponds to the even-momentum spherical harmonics.

The above basis spans the rotational state space of any  $D_\infty$ -symmetric linear molecule with spinless identical nuclei, e.g., C–N–C or the closed-shell  $O_2^2-$ .

**Example 10** (cobalt tetracarbonyl hydride). The  $HCo(CO)_4$  molecule is symmetric under rotations by  $\pm 2\pi/3$ , which form the group  $G = C_3$  [262]. Symmetry-group rotations *do* permute identical C and O nuclei, but none of these nuclei have any nuclear spin, so this molecule is rotationally symmetric.

The group  $C_3$  has three elements, denoted by angles  $\phi \in \{0, 2\pi/3, 4\pi/3\}$ , and three irreps, with the trivial one denoted as A. Picking the rotations to be around the (principal)  $\mathbf{z}$ -axis, we can utilize the decomposition from Eq. (32) and determine that the trivial irrep occurs whenever  $k$  is a multiple of three. For example, when  $J = 4$ , there are three states,  $|\kappa = 1\rangle \equiv |k = -3\rangle$ ,  $|\kappa = 2\rangle \equiv |k = 0\rangle$ , and  $|\kappa = 3\rangle \equiv |k = 3\rangle$ .

More generally, for  $C_N$ -symmetric molecules that are aligned so that the symmetry group consists of  $\mathbf{z}$ -axis rotations, the basis  $\{|^J_{m\kappa}\rangle\}$  is a subset of the asymmetric rotational states  $\{|^J_m, k\rangle\}$  from Eq. (22c) for which  $k$  is zero modulo  $N$ . The basis states are

$$|^J_{m\kappa}\rangle \equiv |^J_m, k = N(\kappa - 1 - n)\rangle \quad (38)$$

for all  $J, m$ , and for  $\kappa$  ranging from one to the multiplicity  $\text{mlt}_J A = 2n + 1$ , where  $n = \lfloor J/N \rfloor$ .

**Example 11** (sulfur trioxide). The symmetry group of the planar  $SO_3$  molecule is  $G = D_3$  [263, 264], the symmetry group of an equilateral triangle and the permutation group of the triangle’s three vertices. This group is generated by two elements, the cyclic permutation (123), which maps vertex  $1 \rightarrow 2$ ,  $2 \rightarrow 3$ , and  $3 \rightarrow 1$ , and the swap permutation (23), which swaps vertices 2 and 3. The permutation resulting from applying both of these generating permutations depends on the order in which the two are applied, making  $D_3$  the smallest *non-Abelian* symmetry group.

Symmetry-group rotations leave  $SO_3$  invariant while also permuting its three indistinguishable oxygen nuclei. These nuclei can be thought of as the three vertices acted on by the group’s permutation representation. Since the nuclei are spinless, we can treat the molecule as rotationally symmetric and project to the group’s trivial irrep  $A_1$ .

We place the molecule in the  $\mathbf{xy}$ -plane such that the cyclic nuclear permutation is performed by a  $\mathbf{z}$ -axis rotation by  $2\pi/3$ . We further orient the molecule within the

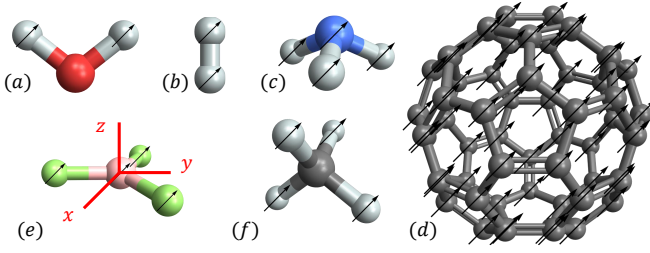


FIG. 9. Perrotationally symmetric molecules (a)  $\text{H}_2\text{O}$ , (b)  $\text{D}_2$ , (c)  $\text{NH}_3$ , (d)  $^{13}\text{C}_{60}$ , (e)  $\text{BF}_3$ , and (f)  $\text{CH}_4$  from Examples 13-24. Proper rotations in a symmetry group  $G$  leave the positions of these molecules invariant but can permute identical spinful nuclei.

$\mathbf{xy}$ -plane such that the swap of the 2nd and 3rd nuclei is performed by a  $\mathbf{y}$ -axis rotation by  $\pi$  [see Fig. 8(d)]. Using the axis-angle representation of rotations [36], the two generating elements of the group correspond to  $(\mathbf{z}, 2\pi/3)$  and  $(\mathbf{y}, \pi)$ , respectively.

The actions of the two generating rotations are described in Eqs. (32) and (37), respectively. The asymmetric molecular states need to be superposed to yield states that transform according to the trivial irrep, yielding symmetric rotational states (cf. Wang functions [22, 25, 37])

$$|_{m\kappa}^J\rangle = \frac{1}{\sqrt{2}} \left( |_{m, k=3(\kappa-1)}^J\rangle - (-1)^{J+\kappa} |_{m, k=3(1-\kappa)}^J\rangle \right), \quad (39)$$

where  $1 \leq \kappa \leq m(J)$ , and where the multiplicity is listed in [140, Table 23.10]. One can verify that  $D^{J*}(\mathbf{z}, 2\pi/3)|_{m\kappa}^J\rangle = D^{J*}(\mathbf{y}, \pi)|_{m\kappa}^J\rangle = |_{m\kappa}^J\rangle$ , as desired.

**Example 12** ( $\text{C}_{60}$  fullerene). The proper rotational symmetry group of the fullerene [265–267] is the icosahedral group,  $G = I$ . Carbon-12 has no nuclear spin, so the molecule is rotationally symmetric.

The trivial irrep of  $I$ , denoted by  $A$ , is present only for certain angular momenta. For example, the smallest nonzero momentum which houses this irrep is  $J = 6$ , and the set of momenta that contain a trivial irrep, along with their multiplicities, are tabulated in [141, Table 74.10]. Basis states  $\{|\kappa\rangle\}$  are not proportional to the  $\mathbf{z}$ -axis basis states  $|k\rangle$ , and their explicit expressions [268] are not particularly illuminating.

## B. Perrotationally symmetric molecules

Some symmetry transformations leave a molecule invariant while also permuting a set of indistinguishable molecular nuclei of nonzero spin [15–17, 19]. A simple example is water, which admits a proper rotation that exchanges the two spin-half hydrogen atoms while leaving the oxygen atom intact.

In order to enforce the required nuclear-spin statistics, the definition (19b) of molecule-frame rotations can be

modified for the case of molecule-based symmetry-group rotations. Each symmetry-group element corresponds to a rotation  $\hat{X}$  (19b) tensored with a unitary matrix,  $\text{Perm}$ , that permutes the tensor factors in the nuclear spin space according to how the rotation permutes the nuclei. We denote the full *perrotation* operation [128–130][24, Eq. (2.25)] by a different overhead arrow,

$$\overleftarrow{X}_g = \overleftarrow{X}_g \otimes \text{Perm}(g), \quad \forall g \in G. \quad (40)$$

Lab-based symmetry-group rotations,  $\overleftarrow{X}$ , are not appended with nuclear-spin permutations as the nuclei are merely moved from one position to another.

Not all molecule-frame symmetries permute identical spinful nuclei. Those that do not have an identity permutation acting on the spin factor, and are still included in the symmetry group  $G$  because they are necessary for enforcing rigid-body symmetry constraints.

Application of rotations  $g$  that also permute nuclei needs to yield a  $\pm 1$  factor determined by the bosonic or fermionic spin statistics of permuted nuclei. This sign is realized by a particular one-dimensional  $G$ -irrep, which we call  $\Gamma_{\text{mol}}$ . Taken together, symmetry and spin-statistics require that

$$\overleftarrow{X}_g|\psi_{\text{mol}}\rangle = \Gamma_{\text{mol}}(g)|\psi_{\text{mol}}\rangle, \quad \forall g \in G. \quad (41)$$

The rotational state space of a symmetric molecule with nontrivial nuclear permutations is the subspace of the space defined by  $\mathbb{1}_{\text{mol}} \otimes \mathbb{1}_{\text{nuc}}$  (22) that satisfies the restriction from Eq. (41).

In cases where no spinful nuclei are permuted by any symmetry-group rotations, the above reduces to the symmetry-only constraint in Eq. (30), for which  $\Gamma_{\text{mol}}$  is the trivial irrep. In the general case, our task is to find all states in the decomposition of  $\mathbb{1}_{\text{mol}} \otimes \mathbb{1}_{\text{nuc}}$  that transform as the irrep  $\Gamma_{\text{mol}}$ . We do so by decomposing perrotations (40) into irreps of  $G$  and keeping any copies of  $\Gamma_{\text{mol}}$ .

The permutation piece “Perm” of the perrotations decomposes in the same way as each rotation matrix  $D^J$  does in Eq. (31). We index the set of distinct  $G$ -irreps present in the “Perm” representation of  $G$  by  $\Lambda$ , with  $\text{mlt } \Lambda$  denoting the multiplicity of each irrep,

$$\text{Perm}(g) = \bigoplus_{\Lambda} \Lambda(g) \otimes \mathbb{1}_{\text{mlt } \Lambda}. \quad (42)$$

The nuclear-spin space is independent of angular momentum, so all above parameters are  $J$ -independent.

Plugging both the above Perm-matrix decomposition and the  $\Gamma$ -decomposition of the rotation  $\overleftarrow{X}$  from Eq. (34) into the perrotation (40) yields

$$\overleftarrow{X}_g = \bigoplus_{J \geq 0} \mathbb{1}_{2J+1} \otimes \bigoplus_{\Gamma \uparrow J} \bigoplus_{\Lambda} [\Gamma \otimes \Lambda](g) \otimes \mathbb{1}_{\text{mlt } J, \Gamma} \otimes \mathbb{1}_{\text{mlt } \Lambda}, \quad (43)$$

where we have collected the rotational and nuclear irrep spaces into the collective representation  $[\Gamma \otimes \Lambda](g) = \Gamma(g) \otimes \Lambda(g)$ . The joint symmetry and spin statistics restriction from Eq. (41) implies that we need to further



decompose the tensor-product representation  $\Gamma \otimes \Lambda$  into irreps and keep any copies of  $\Gamma_{\text{mol}}$  in that decomposition.

There are multiple ways to obtain  $\Gamma_{\text{mol}}$ , each one falling out from the tensor product of a particular  $\Gamma$  and  $\Lambda$ . Each distinct pair ( $\Gamma = \Gamma_{\text{rot}}, \Lambda = \Gamma_{\text{nuc}}$ ) of admissible irreps yields a subspace of rotational states called a *molecular species*, or species for short. All admissible combinations can be extracted from direct-product tables [141, Appx. E] and are tabulated in Table II.

Given a symmetry group, there turn out to be only two possible values for  $\Gamma_{\text{mol}}$  for each group, either trivial or not. Additionally, fixing  $\Gamma_{\text{mol}}$  and  $\Gamma_{\text{rot}}$  uniquely determines  $\Gamma_{\text{nuc}}$ . As such, each species  $s$  in Table II can be unambiguously and succinctly denoted by its rotational irrep only, either as  $s = \Gamma_{\text{rot}}$  or as  $s = \Gamma_{\text{rot}}^*$ . The non-primed labels are for species for which  $\Gamma_{\text{mol}}$  is trivial, while the labels with an asterisk are for a nontrivial  $\Gamma_{\text{mol}}$ .

From now on, we focus on a single species, noting that the full set of states of a given molecule corresponds to the span of all of the molecule's species.

For each species  $s$ , corresponding to the irrep triple  $[\Gamma_{\text{rot}} \otimes \Gamma_{\text{nuc}}] \downarrow \Gamma_{\text{mol}}$ , the dimensions of  $\Gamma_{\text{rot}}$  and  $\Gamma_{\text{nuc}}$  turn out to be always the same. We define the following shorthand,

$$\mathfrak{d} \equiv \dim \Gamma_{\text{rot}} = \dim \Gamma_{\text{nuc}} \quad (44a)$$

$$\mathfrak{m}(J) \equiv \text{mlt}_J \Gamma_{\text{rot}} \quad (44b)$$

$$\mathfrak{m}_{\text{nuc}} \equiv \text{mlt} \Gamma_{\text{nuc}}. \quad (44c)$$

The identity on the state space of  $s$  decomposes in a similar way as the identity for a symmetric molecule in Eq. (36) in terms of momentum states  $|^J_{m\kappa}\rangle$ ,

$$\mathbb{1}_{\text{mol}}^{\text{G},s} = \sum_{J \downarrow \Gamma_{\text{rot}}} \sum_{|m| \leq J} \sum_{\kappa=1}^{\mathfrak{m}(J)} |^J_{m\kappa}\rangle \langle^J_{m\kappa}| \otimes \sum_{\chi=1}^{\mathfrak{m}_{\text{nuc}}} |\chi\rangle \langle\chi|. \quad (45)$$

The indices  $J$  and  $m$  correspond to the standard lab-frame total angular momentum and its  $\mathbf{z}$ -axis projection, respectively. The first sum is only over those angular momenta which contain  $\Gamma_{\text{rot}}$  in the decomposition of the rotation matrices  $D^J$  via Eq. (31); we denote this set by  $J \downarrow \Gamma_{\text{rot}}$ . The third index  $\kappa$  labels the multiplicity space of  $\Gamma_{\text{rot}}$  for each  $J$ . The fourth  $\chi$  index labels the multiplicity subspace of  $\Gamma_{\text{nuc}}$  inside the nuclear-spin space, as only states in this subspace are allowed to accompany the species' rotational states due to the spin-statistics requirement. The multiplicity  $\mathfrak{m}_{\text{nuc}}$  is known as the statistical weight [29].

The key difference from the symmetric case is that the definition, and corresponding degree of rotation-spin entanglement, of each basis state  $|^J_{m\kappa}\rangle$  depends heavily on the dimension of the  $\Gamma_{\text{rot}}$  irrep, specifically, on whether  $\mathfrak{d} = 1$  or  $\mathfrak{d} > 1$ .

### 1. $\mathfrak{d} = 1$ separable species

In this case, both irreps  $\Gamma_{\text{rot}}$  and  $\Gamma_{\text{nuc}}$  are one-dimensional, and their tensor product directly yields the correct spin statistics,  $\Gamma_{\text{rot}} \otimes \Gamma_{\text{nuc}} = \Gamma_{\text{mol}}$ . To identify the state space, we can separately project the rotational and nuclear-spin space onto subspaces transforming as the two respective irreps.

Utilizing the Kronecker  $\delta$ -function from Eq. (35) for each space, we obtain

$$\mathbb{1}_{\text{mol}}^{\text{G},s} = \bigoplus_{J \geq 0} \mathbb{1}_{2J+1} \otimes \bigoplus_{\Gamma \uparrow J} \bigoplus_{\Lambda} \delta_{\Gamma, \Gamma_{\text{rot}}} \mathbb{1}_{\mathfrak{m}(J)} \otimes \delta_{\Lambda, \Gamma_{\text{nuc}}} \mathbb{1}_{\mathfrak{m}_{\text{nuc}}}. \quad (46)$$

Since both irreps are one-dimensional, the two factors  $\Gamma \otimes \Lambda$  in Eq. (43) reduce to a scalar, leaving three remaining factors — the lab-frame  $\mathbf{z}$ -axis projection factor and the two multiplicity spaces — and thereby confirming Eq. (45).

In correspondence with the three factors in Eq. (46) and generalizing Eq. (23), the basis states are then

$$|^J_{m\kappa}\rangle_{\text{rot}} |\chi\rangle_{\text{nuc}}, \quad (47)$$

where we explicitly split each basis state into a factor coming from the rotational space and a factor coming from the nuclear space. Each basis state is expressible in tensor-product form, so each basis state is separable w.r.t. the rotation-spin decomposition. Possible entangled states include superpositions of such states for a given species or of states belonging to different species.

**Example 13** (water,  $A^*$  para species). Water is a symmetric molecule with proper-rotation symmetry group  $G = C_2$ . Its only element corresponds to a  $\pi$ -rotation around some axis  $\mathbf{v}$  such that the two hydrogen atoms and the oxygen are left intact. This symmetry group has two irreps, the trivial irrep  $A$  and the sign irrep  $B$ , for which the rotation is represented by  $-1$ .

The molecule's sole perrotation from Eq. (40) with a non-identity permutation component is<sup>1</sup>

$$\widehat{X}_{\mathbf{v},\pi} = \bigoplus_{J \geq 0} \mathbb{1}_{2J+1} \otimes D^{J*}(\mathbf{v}, \pi) \otimes \text{nuc}(12), \quad (48)$$

where  $\text{Perm}(\mathbf{v}, \pi) = \text{nuc}(12)$  denotes the swap operation acting on the two nuclear-spin factors.

Since hydrogen nuclei are spin-1/2, i.e., fermionic, the nuclear exchange yields a  $-1$  sign. Admissible molecular states should satisfy Eq. (41) with  $\Gamma_{\text{mol}} = B$ , the sign irrep of the symmetry group. According to Table II, one way to achieve this is to pick  $\Gamma_{\text{rot}} = A$  and  $\Gamma_{\text{nuc}} = B$ , corresponding to the  $A^*$  species of water.

Since the rotational side transforms as the trivial irrep, identifying the basis  $\{|\kappa\rangle\}$  is done in the same way as for symmetric molecules in Sec. VIII A. We align the molecule so that the symmetry-group rotation is around the  $\mathbf{z}$ -axis, which allows us to apply Eq. (38) for  $N = 2$ . In other words, the  $C_2$ -symmetric rotational states are

symmetry	species s	$\Gamma_{\text{rot}}$	$\Gamma_{\text{nuc}}$	$\Gamma_{\text{mol}}$	$\mathfrak{d}$
$C_{2N}$	A	A	A	A	1
	B	B	B	A	1
	$^1E_i$	$^1E_i$	$^2E_i$	A	1
	$^2E_i$	$^2E_i$	$^1E_i$	A	1
	$A^*$	A	B	B	1
	$B^*$	B	A	B	1
$C_{2N+1}$	$^jE_i^*$	$^jE_i$	$^jE_{N-i}$	B	1
	A	A	A	A	1
	$^1E_i$	$^1E_i$	$^2E_i$	A	1
T	$^2E_i$	$^2E_i$	$^1E_i$	A	1
	A	A	A	A	1
	$^1E$	$^1E$	$^2E$	A	1
	$^2E$	$^2E$	$^1E$	A	1
O	T	T	T	A	3
	$A_i$	$A_i$	$A_i$	$A_1$	1
	E	E	E	$A_1$	2
	$T_i$	$T_i$	$T_i$	$A_1$	3
	$A_i^*$	$A_i$	$A_{3-i}$	$A_2$	1
	$E^*$	E	E	$A_2$	2
I	$T_i^*$	$T_i$	$T_{3-i}$	$A_2$	3
	A	A	A	A	1
	$T_i$	$T_i$	$T_i$	A	3
	G	G	G	A	4
	H	H	H	A	5

symmetry	species s	$\Gamma_{\text{rot}}$	$\Gamma_{\text{nuc}}$	$\Gamma_{\text{mol}}$	$\mathfrak{d}$
$D_2$	A	A	A	A	1
	$B_i$	$B_i$	$B_i$	A	1
$D_{4N}$	$A_i$	$A_i$	$A_i$	$A_1$	1
	$B_i$	$B_i$	$B_i$	$A_1$	1
	$E_i$	$E_i$	$E_i$	$A_1$	2
	$A_i^*$	$A_i$	$B_{3-i}$	$B_2$	1
	$B_i^*$	$B_i$	$A_{3-i}$	$B_2$	1
	$E_i^*$	$E_i$	$E_{2N-i}$	$B_2$	2
$D_{4N+1}$	$A_i$	$A_i$	$A_i$	$A_1$	1
	$E_i$	$E_i$	$E_i$	$A_1$	2
$D_{4N+2}$	$A_i$	$A_i$	$A_i$	$A_1$	1
	$B_i$	$B_i$	$B_i$	$A_1$	1
	$E_i$	$E_i$	$E_i$	$A_1$	2
	$A_i^*$	$A_i$	$B_i$	$B_1$	1
	$B_i^*$	$B_i$	$A_i$	$B_1$	1
	$E_i^*$	$E_i$	$E_{2N+1-i}$	$B_1$	2
$D_{4N+3}$	$A_i$	$A_i$	$A_i$	$A_1$	1
	$E_i$	$E_i$	$E_i$	$A_1$	2
	$A_i^*$	$A_i$	$A_{3-i}$	$A_2$	1
	$E_i^*$	$E_i$	$E_i$	$A_2$	2
$D_\infty$	$A_i$	$A_i$	$A_i$	$A_1$	1
	$A_1^*$	$A_1$	$A_2$	$A_2$	1
	$A_2^*$	$A_2$	$A_1$	$A_2$	1

TABLE II. Table of all possible species of perrotationally symmetric molecular species. Given a symmetry group, the species corresponding to the triple  $\Gamma_{\text{rot}} \otimes \Gamma_{\text{nuc}} \downarrow \Gamma_{\text{mol}}$  is unambiguously labeled by its rotational irrep (see Tab. I) for trivial  $\Gamma_{\text{mol}}$ , with an “\*” present in the superscript in case  $\Gamma_{\text{mol}}$  is non-trivial. The irrep dimension,  $\mathfrak{d} \equiv \dim \Gamma_{\text{rot}}$ , serves as the Schmidt rank, which quantifies the amount of entanglement of the species’ rotational basis states.

the subset of the asymmetric states  $\{|^J_m, k\rangle\}$  for even  $k$ , with multiplicity  $\mathfrak{m}(J) = 2\lfloor J/2 \rfloor + 1$ .

The nuclear-spin states  $\{|\chi\rangle\}$  that are paired up with the above rotational states span the multiplicity space of the  $\Gamma_{\text{nuc}} = B$  irrep. The  $-1$  factor upon exchange comes from this irrep, meaning that this space consists of all anti-symmetric states.

Each hydrogen nucleus is spanned by spin up and down states,  $|\uparrow\rangle$  and  $|\downarrow\rangle$ , respectively. The composite four-dimensional space admits one anti-symmetric “singlet” state,  $(|\uparrow\downarrow\rangle - |\downarrow\uparrow\rangle)/\sqrt{2}$ , and there is no need for the index  $\chi$  since nuclear-spin multiplicity  $\mathfrak{m}_{\text{nuc}} = 1$ . Species whose nuclei are in a singlet state are called para species. The singlet state is tensored with an arbitrary nuclear-spin state of the oxygen.

The fact that only some nuclear-spin states pair up with the trivial-irrep rotational states highlights a difference from the symmetric rigid-body case from Sec. VIII A. In that case, the overall irrep  $\Gamma_{\text{mol}}$  is also the trivial irrep, but *all* nuclear states are allowed since symmetry rotations do not permute identical spinful nuclei.

**Example 14** (water,  $B^*$  ortho species). According to Table II, there is a second way to obtain the  $\Gamma_{\text{mol}} = B$  irrep for water, namely, by picking  $\Gamma_{\text{rot}} = B$  and  $\Gamma_{\text{nuc}} = A$ .

This choice corresponds to the  $B^*$  species of water.

For this species, the rotational side transforms as the non-trivial irrep  $\Gamma_{\text{rot}} = B$ . The  $-1$  factor upon exchange comes from this irrep. Observing Eq. (32), this irrep occurs in all asymmetric states  $\{|^J_m, k\rangle\}$  for which  $k$  is odd. The lowest angular momentum of this species is thus  $J = 1$ .

The hydrogen nuclear-spin states  $\{|\chi\rangle\}$  that are paired up with the above rotational states span the multiplicity space of  $\Gamma_{\text{nuc}} = A$ , i.e., the trivial irrep. This space, with multiplicity  $\mathfrak{m}_{\text{nuc}} = 3$ , consists of all nuclear-spin triplet states and is spanned by  $|\chi = 1\rangle \equiv |\uparrow\uparrow\rangle$ ,  $|\chi = 2\rangle \equiv |\downarrow\downarrow\rangle$ , and  $|\chi = 3\rangle \equiv (|\uparrow\downarrow\rangle + |\downarrow\uparrow\rangle)/\sqrt{2}$ . Species whose nuclei are in triplet states are called ortho species. The triplet hydrogen-nuclei states are tensored with an arbitrary nuclear-spin state of the oxygen.

**Example 15** (deuterated hydrogen,  $A_1$  ortho species). A simple species with bosonic nuclei is  $D_2$ , where “D” stands for deuterium. This is a symmetric molecule with the same symmetry group as disulfur from Example 9,  $G = D_\infty$ . However, the equatorial-axis rotations exchange the two spin-1 deuterium nuclei, resulting in a  $+1$  spin-statistics factor that is realized by the trivial irrep. Admissible molecular states should satisfy Eq. (41) with  $\Gamma_{\text{mol}} = A_1$ . According to Table II, one way to achieve

this is to pick  $\Gamma_{\text{rot}} = \Gamma_{\text{nuc}} = A_1$ , corresponding to the  $A_1$  species of  $D_2$ .

Since the rotational side transforms as the trivial irrep, identifying the basis  $\{|\kappa\rangle\}$  is done in the same way as for symmetric molecules in Sec. VIII A. Per Example 9, asymmetric states  $\{|_m^J, k=0\rangle\}$  for even  $J$  transform as the trivial irrep of  $D_\infty$ .

The nuclear-spin states also transform as the trivial irrep, and so are in the same triplet subspace as in Example 14, with multiplicity  $\mathbf{m}_{\text{nuc}} = 3$ .

**Example 16** (deuterated hydrogen,  $A_2$  para species). The  $D_2$  molecule admits another para species — the  $A_2$  species from Table II — which corresponds to picking the 1D irreps  $\Gamma_{\text{rot}} = \Gamma_{\text{nuc}} = A_2$ . A basis for this species consists of tensor products of rotational states  $|_m^J, k=0\rangle$  with  $J$  odd and singlet nuclear states (with multiplicity  $\mathbf{m}_{\text{nuc}} = 1$ ).

None of the two-dimensional  $D_\infty$ -irreps feature in either the ortho or para species of this molecule. This trend extends to all  $D_\infty$ -symmetric molecules, including ordinary hydrogen, because no combination of two-dimensional irreps yields the irreps  $A_{1,2}$  that describe the spin statistics.

In the case of ordinary  $H_2$ , the spin statistics are fermionic ( $\Gamma_{\text{mol}} = A_2$ ), and there are two species —  $A_1^*$  and  $A_2^*$ . These admit the same two respective sets of rotational states as the  $A_1$  and  $A_2$  deuterium species. However, the ortho-para jargon is switched: the  $A_1^*$  admits a nuclear-spin singlet and so is called para-hydrogen, while the  $A_2^*$  hydrogen species is ortho.

**Example 17** (ammonia,  ${}^2E$  species). The  $NH_3$  molecule is not planar, admitting the cyclic  $C_3$  symmetry. We ignore any tunneling effects for clarity [26], noting that this example applies to any linear molecule that has been appended with three hydrogens in a  $C_3$  symmetric way, e.g., calcium monomethoxide ( $CaOCH_3$ ) [60].

Rotations in this group are by angles 0,  $2\pi/3$ , and  $4\pi/3$ , which wind up cyclically permuting the three hydrogen atoms. This group has three irreps, the trivial one  $A$ , and two irreps  ${}^{j=1,2}E$  that are complex conjugate to each other and for which  ${}^jE(2\pi/3) = \exp(i\frac{2\pi}{3}j)$ .

A cyclic permutation of nuclei is equivalent to performing two exchanges, yielding a +1 spin-statistics factor. This corresponds to the trivial irrep  $\Gamma_{\text{mol}} = A$ . According to Table II, one way to achieve this is to pick  $\Gamma_{\text{rot}} = {}^2E$  and  $\Gamma_{\text{nuc}} = {}^1E$ , corresponding to the  ${}^2E$  species.

Aligning the molecule such that symmetry-group rotations are around the  $\mathbf{z}$  axis and observing Eq. (32), we see that the  $|k\rangle$  states of this species are all those for which  $k \equiv 2$  modulo 3. The first momentum that harbors such states is  $J = 1$ . More generally, for  $C_N$ -symmetric molecules, the momenta of the  ${}^2E_i$  species satisfy  $J \geq i$ .

**Example 18** (boron trifluoride,  $A_2^*$  species). The  $BF_3$  molecule has the same dihedral ( $D_3$ ) symmetry [269] as sulfur trioxide from Example 11. Symmetry-group rotations leave both molecules invariant while also permuting

their three indistinguishable nuclei. In contrast to  $SO_3$ , the fluorine nuclei of  $BF_3$  are spinful, making the latter molecule perrotationally symmetric.

The  $D_3$  group — the permutation group of three objects — has three irreps. The two one-dimensional irreps are the trivial irrep  $A_1$  and the “sign” irrep  $A_2$ , in which all two-object swaps are mapped to  $-1$  while remaining elements are mapped to  $+1$ . The remaining two-dimensional irrep is called  $E$ , for which we let  $\sigma = e^{-i\frac{2\pi}{3}}$  and pick a basis  $\{|\nu=1\rangle, |\nu=2\rangle\}$  such that

$$E(123) = \begin{pmatrix} \sigma & 0 \\ 0 & \sigma^* \end{pmatrix} \quad \text{and} \quad E(23) = \begin{pmatrix} 0 & 1 \\ 1 & 0 \end{pmatrix}. \quad (49)$$

The spin statistics of the spin-half fluorine nuclei of  $BF_3$  require a  $-1$  to be produced every time a symmetry-group rotation swaps any two nuclei. This corresponds to the sign  $D_3$ -irrep, meaning that  $\Gamma_{\text{mol}} = A_2$ . According to Table II, one way to achieve this is to pick  $\Gamma_{\text{rot}} = A_2$  and  $\Gamma_{\text{nuc}} = A_1$ . This corresponds to the  $A_2^*$  species of  $BF_3$ .

We orient the molecule within the  $\mathbf{xy}$ -plane in the same way as we did with  $SO_3$ . The cyclic nuclear permutation (123) is performed by a  $\mathbf{z}$ -axis rotation by  $2\pi/3$ , with corresponding perrotation<sup>1</sup>

$$\overleftarrow{X}_{\mathbf{z}, 2\pi/3} = \bigoplus_{J \geq 0} \mathbb{1}_{2J+1} \otimes D^{J^*}(\mathbf{z}, 2\pi/3) \otimes \text{nuc}(123), \quad (50)$$

where  $\text{Perm}(\mathbf{z}, 2\pi/3) = \text{nuc}(123)$  denotes the matrix that cyclically permutes the three nuclear-spin tensor factors. The swap (23) of the 2nd and 3rd nuclei is performed by a  $\mathbf{y}$ -axis rotation by  $\pi$  [see Fig. 9(d)].

The rotations corresponding to the two generating permutations, (123) and (23), act on the asymmetric rotational states (22c) as

$$D^{J^*}(\mathbf{z}, 2\pi/3)|_m^J, k\rangle = \sigma^k |_m^J, k\rangle \quad (51a)$$

$$D^{J^*}(\mathbf{y}, \pi)|_m^J, k\rangle = (-1)^{J+k} |_m^J, -k\rangle, \quad (51b)$$

respectively. The asymmetric molecular states  $|k\rangle$  need to be superposed to yield states that transform according to the sign irrep [cf. the trivial-irrep states in Eq. (39)]. The resulting rotational states of the species are

$$|_{m\kappa}^J\rangle = \frac{1}{\sqrt{2}} \left( |_m^J, k=3(\kappa-1)\rangle + (-1)^{J+\kappa} |_m^J, k=3(1-\kappa)\rangle \right), \quad (52)$$

where  $1 \leq \kappa \leq \mathbf{m}(J)$ , and where the multiplicity is listed in [140, Table 23.10].

The  $2^3 = 8$ -dimensional space of the three fluorine nuclei decomposes into four copies of the trivial irrep  $A_1$ , with the entire admissible subspace spanned by the states  $|\uparrow\uparrow\uparrow\rangle$  and  $|\uparrow\downarrow\downarrow\rangle + |\downarrow\uparrow\uparrow\rangle + |\downarrow\downarrow\uparrow\rangle$ , along with their two counterparts obtained by flipping all spins. The quadruplet fluorine-nuclei states are then tensored with an arbitrary nuclear-spin state of the boron to form the species’ nuclear-spin states.

Interestingly, the nuclear states do not decompose into any copies of the sign irrep  $A_2$ , thereby eliminating the possibility of the  $A_2 = A_1 \otimes A_2$  species for this molecule.

This is known as having “missing levels” in the spectroscopy literature [26, 27, 173]. Since the  $A_2$  species houses the  $J = 0$  state, which transforms according to  $\Gamma_{\text{rot}} = A_1$ , symmetry and spin statistics make sure that  $\text{BF}_3$  never has zero angular momentum.

**Example 19** ( $^{13}\text{C}_{60}$  fullerene, A species). Fullerenes made up of carbon-12 have no nuclear spin and can thus be treated as rotationally symmetric molecules with icosahedral ( $G = I$ ) symmetry; we study this case in Example 12. On the other hand, isotopic  $^{13}\text{C}_{60}$  fullerenes are perrotationally symmetric since carbon-13 has a nuclear spin of  $1/2$ .

Each symmetry-group rotation acts in a way that permutes an even subset of the 60 carbon-13 nuclei, resulting in a  $+1$  spin-statistics factor that is realized by the trivial icosahedral irrep,  $\Gamma_{\text{mol}} = A$ . According to Table II, one way to achieve this is to pick  $\Gamma_{\text{rot}} = \Gamma_{\text{nuc}} = A$ , corresponding to the A species.

The rotational states transform as the trivial irrep,  $\Gamma_{\text{rot}} = A$ , so identifying the basis  $\{|\kappa\rangle\}$  is done in the same way as in Example 12.

The nuclear-spin space is restricted to only states  $\{|\chi\rangle\}$  that transform under the trivial irrep. The full space is of dimension  $2^{60}$ , and finding a basis for the states is not the most tractable of tasks. We can, however, numerically determine the nuclear multiplicity of  $\mathbf{m}_{\text{nuc}} = 19\,215\,358\,678\,900\,736$  (see Table V), confirming earlier studies [270–274].

The other species of  $^{13}\text{C}_{60}$  use any of the four other I-irreps,  $\{T_1, T_2, G, H\}$ , for both  $\Gamma_{\text{rot}}$  and  $\Gamma_{\text{nuc}}$ . All such species have  $\mathfrak{d} > 1$ .

## 2. $\mathfrak{d} > 1$ entangled species

In general, the resulting tensor-product representation  $\Gamma \otimes \Lambda$  from Eq. (43) with  $\Gamma = \Gamma_{\text{rot}}$  and  $\Lambda = \Gamma_{\text{nuc}}$  is of dimension  $\mathfrak{d}^2$ , per the notation defined in Eq. (44). In cases where the dimension  $\mathfrak{d} > 1$ , this tensor-product irrep has to be *restricted* to any copies of the one-dimensional  $\Gamma_{\text{mol}}$  irrep that yield the correct spin statistics defined in Eq. (41). For the  $\text{SU}(2)$  Lie group, performing this restriction is analogous to coupling angular momentum vectors and then restricting to a particular total angular momentum sector [275].

Let  $\{|\nu\rangle_{\text{rot}}\}_{\nu=1}^{\mathfrak{d}}$  and  $\{|\nu\rangle_{\text{nuc}}\}_{\nu=1}^{\mathfrak{d}}$  define bases for the irrep spaces of  $\Gamma_{\text{rot}}$  and  $\Gamma_{\text{nuc}}$ , respectively. The task is to find any states in the composite space, spanned by  $\{|\nu\rangle_{\text{rot}}|\nu'\rangle_{\text{nuc}}\}$ , that transform according to the scalar irrep  $\Gamma_{\text{mol}}$ . In all cases (see Table II), there turns out to be only one such state, which we denote by  $|\Gamma_{\text{mol}}\rangle$  and which can be written as

$$|\Gamma_{\text{mol}}\rangle = \frac{1}{\sqrt{\mathfrak{d}}} \sum_{\nu=1}^{\mathfrak{d}} s_{\nu} |\nu\rangle_{\text{rot}} |\nu\rangle_{\text{nuc}}, \quad (53)$$

whose Clebsch-Gordan coupling coefficients  $s_{\nu} = \pm 1$  depend on  $\Gamma_{\text{rot}}$ ,  $\Gamma_{\text{nuc}}$ , and  $\Gamma_{\text{mol}}$ .

When  $\Gamma_{\text{rot}} = \Gamma_{\text{nuc}}$  and  $\Gamma_{\text{mol}}$  are trivial, we can prove the above result by writing down the projection onto the above state,

$$\Pi_{\text{mol}} \equiv |\Gamma_{\text{mol}}\rangle\langle\Gamma_{\text{mol}}|, \quad (54)$$

as a sum over symmetry group elements and applying Schur orthogonality *a.k.a.* the “Grand Orthogonality Theorem” [250, Sec. 2.4]. More generally, the above result can be obtained by consulting Clebsch-Gordan tables [141, Appx. F].

Incorporating the above into the decomposition from Eq. (43), we first select the species corresponding to  $\Gamma = \Gamma_{\text{rot}}$  and  $\Lambda = \Gamma_{\text{nuc}}$  and then project the tensor-product irrep into the above state,

$$[\Gamma \otimes \Lambda](\mathbf{g}) \rightarrow \delta_{\Gamma, \Gamma_{\text{rot}}} \delta_{\Lambda, \Gamma_{\text{nuc}}} \Gamma_{\text{mol}}(\mathbf{g}) \Pi_{\text{mol}}. \quad (55)$$

Backing out the identity on the resulting space, we have

$$\mathbb{1}_{\text{mol}}^{\text{G}, \text{S}} = \bigoplus_{J \geq 0} \mathbb{1}_{2J+1} \otimes \bigoplus_{\Gamma \uparrow J} \bigoplus_{\Lambda} \Pi_{\text{mol}} \otimes \delta_{\Gamma, \Gamma_{\text{rot}}} \mathbb{1}_{\mathbf{m}(J)} \otimes \delta_{\Lambda, \Gamma_{\text{nuc}}} \mathbb{1}_{\mathbf{m}_{\text{nuc}}}, \quad (56)$$

where we have split the rotational and nuclear-spin multiplicity factors and plugged in Eqs. (44).

Re-expressing the above identity factor as Eq. (45) yields basis states

$$|_{m\kappa}^J|\chi\rangle \equiv \frac{1}{\sqrt{\mathfrak{d}}} \sum_{\nu=1}^{\mathfrak{d}} s_{\nu} |_{m\kappa}^J, \nu\rangle_{\text{rot}} |\nu, \chi\rangle_{\text{nuc}}, \quad (57)$$

where we have incorporated the state  $|\Gamma_{\text{mol}}\rangle$  (53) and explicitly split each state in the superposition on the right-hand side into a factor coming from the rotational space and a factor coming from the nuclear space. This notation is different from that in Eq. (3), where we explicitly write the fixed entangled state; we continue to absorb it henceforth for notational simplicity.

When  $\mathfrak{d} = 1$ , the internal  $\nu$  irrep index disappears, and Eq. (57) reduces to the separable case from Eq. (47). When  $\mathfrak{d} \geq 2$ , the basis state for each  $J$ ,  $m$ ,  $\kappa$ , and  $\chi$  is a *completely* rotation-spin entangled state with  $\mathfrak{d}$  components, i.e., Schmidt rank  $\mathfrak{d}$  [142]. This entanglement is enforced by the combination of symmetry and spin statistics, manifest in the restriction from Eq. (41), and is impossible to separate without breaking the symmetry/spin-statistics requirement or transitioning to another species. We can pick superpositions of the above states that yield a different basis with different labels, but there is no way to remove the sum over  $\nu$  in this way because it is its own separate factor.

**Example 20** (boron trifluoride,  $E^*$  species). Recalling Example 18, we know that the spin statistics of the spin- $1/2$  fluorine nuclei of  $\text{BF}_3$  require a  $-1$  to be produced every time a symmetry-group rotation swaps any two nuclei. This corresponds to the sign  $D_3$ -irrep, meaning that  $\Gamma_{\text{mol}} = A_2$ . According to Table II, the way to achieve this using multi-dimensional irreps is to pick  $\Gamma_{\text{rot}} = \Gamma_{\text{nuc}} = E$



and restrict their product to  $A_2$ . This corresponds to the  $E^*$  entangled species of  $BF_3$ .

By comparing Eq. (51) to Eq. (49), we observe that a pair of states  $\{|^J_{m,\pm|k|}\rangle\}$  form a basis for the  $E$  irrep whenever  $|k|$  is 1 modulo 3. Taking care of our chosen order of the irrep basis, we also observe that  $\{|^J_{m,\mp|k|}\rangle\}$  form a basis for the  $E$  irrep whenever  $|k|$  is 2 modulo 3. The multiplicity  $\mathbf{m}(J)$  for each angular momentum  $J$  is tabulated in [140, Table 23.10].

For example, for  $|m| \leq J = 1$ , we have only  $\mathbf{m}(1) = 1$  copy of  $E$ , so there is no need for the multiplicity index  $\kappa$ . We can then define the following basis,

$$|^J=1, \nu=1\rangle_{\text{rot}} = |^J=1, k=1\rangle \quad (58a)$$

$$|^J=1, \nu=2\rangle_{\text{rot}} = |^J=1, k=-1\rangle, \quad (58b)$$

and verify that the two rotations from Eq. (51), when expressed in this basis, reduce to the two matrices from Eq. (49).

On the nuclear side, we omit the factor due to the boron spin for simplicity since that state is unrestricted by spin statistics. The  $2^3 = 8$  dimensional spin space of the three spin-half fluorine nuclei houses two copies of  $E$ , so the multiplicity  $\mathbf{m}_{\text{nuc}} = 2$ . The first copy is spanned by the basis states

$$\begin{aligned} |\nu=1, \chi=1\rangle_{\text{nuc}} &= (|\uparrow\downarrow\downarrow\rangle + \sigma^* |\downarrow\uparrow\downarrow\rangle + \sigma |\downarrow\downarrow\uparrow\rangle) / \sqrt{3} \\ |\nu=2, \chi=1\rangle_{\text{nuc}} &= (|\uparrow\downarrow\downarrow\rangle + \sigma |\downarrow\uparrow\downarrow\rangle + \sigma^* |\downarrow\downarrow\uparrow\rangle) / \sqrt{3}, \end{aligned} \quad (59)$$

where one can verify that permuting the nuclei is equivalent to applying a corresponding product of powers of the matrices from Eq. (49). The basis for the second copy,  $\{|\nu, \chi=2\rangle_{\text{nuc}}\}_{\nu=1,2}$ , can be obtained from Eq. (59) by flipping all spins.

To construct the state  $|\Gamma_{\text{mol}} = A_2\rangle$  from Eq. (53), we consult Clebsch-Gordan tables for  $D_3$  [140, 23.11, 3rd table]. This yields the entangled “rotation-spin singlet” state of Schmidt rank 2,

$$|A_2\rangle = (|\nu=1\rangle_{\text{rot}} |\nu=2\rangle_{\text{nuc}} - |\nu=2\rangle_{\text{rot}} |\nu=1\rangle_{\text{nuc}}) / \sqrt{2}. \quad (60)$$

Plugging this into Eq. (57) and using the bases for the “rot” and “nuc”  $E$ -irreps defined above yields the basis  $\{|^J_{m\kappa}, \chi\rangle\}$  for this species. For example,

$$|^1_{m}, \chi\rangle = (|^1_{m}, 1\rangle_{\text{rot}} |2, \chi\rangle_{\text{nuc}} - |^1_{m}, 2\rangle_{\text{rot}} |1, \chi\rangle_{\text{nuc}}) / \sqrt{2} \quad (61)$$

for  $|m| \leq J = 1$ ,  $\chi \in \{1, 2\}$ , and without a  $\kappa$  index since the multiplicity  $\mathbf{m}(J = 1) = 1$ . One can verify that these yield the correct spin statistics and transform as the  $\Gamma_{\text{mol}} = A_2$  irrep under symmetry-group perrotations, such as the one from Eq. (50).

**Example 21** (methane,  $T$  species). Methane  $CH_4$  has tetrahedral symmetry  $T$  [23, 32, 276], with perrotations exchanging the four hydrogen atoms in the same way as the four corners of a tetrahedron are permuted by tetrahedral-group rotations. Using Table II, we see there

are four species of  $T$ :  $A$ ,  ${}^1E$ ,  ${}^2E$ , and  $T$ . Each of these is separable except for  $T$ , which is entangled with  $\mathfrak{d} = 3$ .

The rotational state factor is not easy to track analytically, but they have been studied in related work by Harter and Patterson [21, 171–175].

The  $2^4 = 16$  dimensional spin space of the three spin-half hydrogen nuclei houses three copies of  $T$ , so the multiplicity  $\mathbf{m}_{\text{nuc}} = 3$ . The first copy is spanned by the basis states

$$|\nu=1, \chi=1\rangle_{\text{nuc}} = (|\downarrow\downarrow\downarrow\uparrow\rangle - |\uparrow\downarrow\downarrow\downarrow\rangle) / \sqrt{2} \quad (62a)$$

$$|\nu=2, \chi=1\rangle_{\text{nuc}} = (|\downarrow\downarrow\uparrow\downarrow\rangle - |\uparrow\downarrow\downarrow\downarrow\rangle) / \sqrt{2} \quad (62b)$$

$$|\nu=3, \chi=1\rangle_{\text{nuc}} = (|\downarrow\downarrow\downarrow\downarrow\rangle - |\uparrow\downarrow\downarrow\downarrow\rangle) / \sqrt{2}. \quad (62c)$$

The second copy is spanned by the basis states

$$|\nu=1, \chi=2\rangle_{\text{nuc}} = (|\downarrow\downarrow\uparrow\uparrow\rangle - |\uparrow\uparrow\downarrow\downarrow\rangle) / \sqrt{2} \quad (62d)$$

$$|\nu=2, \chi=2\rangle_{\text{nuc}} = (|\downarrow\uparrow\uparrow\downarrow\rangle - |\uparrow\downarrow\uparrow\downarrow\rangle) / \sqrt{2} \quad (62e)$$

$$|\nu=3, \chi=2\rangle_{\text{nuc}} = (|\downarrow\uparrow\uparrow\uparrow\rangle - |\uparrow\downarrow\uparrow\uparrow\rangle) / \sqrt{2}. \quad (62f)$$

The third copy is spanned by the basis states

$$|\nu=1, \chi=3\rangle_{\text{nuc}} = (|\downarrow\uparrow\uparrow\uparrow\rangle - |\uparrow\uparrow\uparrow\downarrow\rangle) / \sqrt{2} \quad (62g)$$

$$|\nu=2, \chi=3\rangle_{\text{nuc}} = (|\uparrow\downarrow\uparrow\uparrow\rangle - |\uparrow\uparrow\uparrow\downarrow\rangle) / \sqrt{2} \quad (62h)$$

$$|\nu=3, \chi=3\rangle_{\text{nuc}} = (|\uparrow\uparrow\uparrow\uparrow\rangle - |\uparrow\uparrow\uparrow\downarrow\rangle) / \sqrt{2}. \quad (62i)$$

Notice that  $\chi = i$  corresponds to a superposition of those states with exactly  $i$   $\uparrow$ -spins and  $(4-i)$   $\downarrow$ -spins.

As with  $BF_3$ , admissible states include the factor  $|\Gamma_{\text{mol}}\rangle$ , which consists of the above states summed over  $\mu$  for each  $J$ ,  $m$ ,  $\kappa$ , and  $\chi$ . Exact expressions are no more illuminating than the general case.

### 3. Relative fraction of entanglement

A particular perrotationally  $G$ -symmetric molecule admits a set  $\{S\}$  of species, each with dimension  $\mathfrak{d}^S$ , rotational multiplicities  $\mathbf{m}^S(J)$ , and statistical weight  $\mathbf{m}_{\text{nuc}}^S$ . The identity of the entire molecular state space is a sum over the projections onto all of the molecule’s species,

$$\mathbb{1}_{\text{mol}} = \sum_S \mathbb{1}_{\text{mol}}^{G,S}, \quad (63)$$

where each term on the right-hand side is determined by the prescription from earlier in this subsection.

Each species’ state space is infinite-dimensional. However, by counting the total number of basis states for the entangled cases ( $\mathfrak{d}^S > 1$ ) and dividing by the total number of states, we can determine the *relative entangled-state fraction*,

$$F_{\text{ent}} = \frac{\sum_{J \downarrow \Gamma_{\text{rot}}} \sum_{S: \mathfrak{d}^S > 1} \mathbf{m}^S(J) \mathbf{m}_{\text{nuc}}^S}{\sum_{J \downarrow \Gamma_{\text{rot}}} \sum_S \mathbf{m}^S(J) \mathbf{m}_{\text{nuc}}^S} \quad (64a)$$

$$= \frac{\sum_{S: \mathfrak{d}^S > 1} \mathfrak{d}^S \mathbf{m}_{\text{nuc}}^S}{\sum_S \mathfrak{d}^S \mathbf{m}_{\text{nuc}}^S}. \quad (64b)$$

The second equality is the result of calculating the same relative fraction in position space (see Sec. IX), which allows us to obtain a closed-form expression. The middle sum can be cut off at some momentum  $J \leq J_{\max}$  to obtain the relative fraction for a momentum-constrained subspace.

**Example 22** (boron trifluoride). Combining all species of  $\text{BF}_3$  and calculating the relative entangled-state fraction reveals that exactly *half* of all basis states are entangled. This value, along with those of other molecules with dihedral perrotation symmetry, is listed in Table III.

symmetry	molecule	entangled-state fraction, $F_{\text{ent}}$			
		$J \leq 2$	$J \leq 4$	$J \leq 8$	$J \leq \infty$
D <sub>3</sub>	$\text{BF}_3$	0.429	0.444	0.491	$1/2 = 0.5$
D <sub>4</sub>	$\text{XeF}_4$	0.273	0.333	0.361	$3/8 = 0.375$
D <sub>5</sub>	$\text{C}_5\text{H}_5^-$	0.529	0.714	0.727	$3/4 = 0.75$
D <sub>6</sub>	$\text{C}_6\text{H}_6$	0.518	0.567	0.611	$5/8 = 0.625$
D <sub>7</sub>	$\text{C}_7\text{H}_7^+$	0.587	0.756	0.816	$27/32 \approx 0.844$
D <sub>8</sub>	$\text{C}_8\text{H}_8^{2-}$	0.585	0.672	0.710	$93/128 \approx 0.727$

TABLE III. Fraction of states that are entangled [see Eq. (64)] for planar molecules with dihedral perrotation symmetry.

**Example 23** (methane). Methane admits four species — A,  $^1\text{E}$ ,  $^2\text{E}$ , and T — with only the last one being completely entangled. We count the entangled-state fraction (64) of methane to be  $F_{\text{ent}} \approx 0.56$ , meaning that just over half of methane’s rotational states are completely entangled.

**Example 24** ( $^{13}\text{C}_{60}$  fullerene). The molecule  $^{13}\text{C}_{60}$  has icosahedral I symmetry. From Table II we see there are five species A, T<sub>1</sub>, T<sub>2</sub>, G, and H. All of these are entangled except A (which has  $\mathfrak{d} = 1$ ), with Schmidt ranks of  $\mathfrak{d} = 3, 3, 4, 5$  respectively. The species G and H have the highest degree of entanglement of any species because I is the only group that contains irreps of dimension greater than 3.

Multiplicities  $\mathbf{m}(J)$  are listed in Table IV for the first few momenta, while statistical weights are listed in Table V. Combining these yields  $F_{\text{ent}} \approx 0.98$ , meaning that one is hard-pressed to find a separable state in the entire molecule.

$J$	A	T <sub>1</sub>	T <sub>2</sub>	G	H
0	1	0	0	0	0
1	0	1	0	0	0
2	0	0	0	0	1
3	0	0	1	1	0
4	0	0	0	1	1
5	0	1	1	0	0

$J$	A	T <sub>1</sub>	T <sub>2</sub>	G	H
6	1	1	0	1	1
7	0	1	1	1	1
8	0	0	1	1	2
9	0	1	1	2	1
10	1	1	1	1	2

TABLE IV. Multiplicities  $\mathbf{m}(J)$  for each choice of rotational irrep  $\Gamma_{\text{rot}}$  for  $^{13}\text{C}_{60}$  from Example 24.

S	$\mathfrak{d}$	$\mathbf{m}_{\text{nuc}}$
A	1	19 215 358 678 900 736
T <sub>1</sub>	3	57 646 074 961 907 712
T <sub>2</sub>	3	57 646 074 961 907 712
G	4	76 861 433 640 804 352
H	5	96 076 792 318 656 512

TABLE V. Irrep  $\mathfrak{d}$  dimensions and nuclear-spin multiplicities  $\mathbf{m}_{\text{nuc}}$  of the five species of  $^{13}\text{C}_{60}$  [26, 270–274]. The statistical weights are large because the entire nuclear state space has dimension  $\sum_S \mathfrak{d}^S \mathbf{m}_{\text{nuc}}^S = 2^{60}$ . They roughly follow the ratio  $1 : 3 : 3 : 4 : 5$ .

## IX. SYMMETRIC POSITION STATES

In this section, we formulate the state space of general rotationally and perrotationally symmetric molecules in terms of position states, culminating in Eqs. (110) and (115) for a general induced representation. The formulation yields the same state space as that derived in Sec. VIII, and we develop the Fourier transform that relates position states of this section and momentum states from the previous section.

### A. Asymmetric molecules

The position state space of a symmetric molecule can be thought of as a subspace of the asymmetric molecular state space defined in Eq. (22). For such purposes, it is more convenient for us to express the factor spanned by the molecule-frame  $\mathbf{z}$ -axis projection states  $|k\rangle$  using a more general, G-adapted basis  $|\nu\kappa\rangle$  stemming from the isotypic decomposition from Eq. (31). The basis change is

$$|_m^J, k\rangle \rightarrow |_{m\kappa}^J, \nu\rangle, \quad (65)$$

where we group indices in a way that is consistent with the previous section.

Recalling Eq. (31), the G-adapted basis  $\{|\nu\kappa\rangle\}$  block diagonalizes the rotation matrices  $D^J$ , with each block corresponding to a distinct G-irrep  $\Gamma$ , and the entire set of participating irreps denoted by  $\Gamma \uparrow J$  (see Example 6). For each  $\Gamma$ , the index  $\nu$  (along with Greek indices  $\mu, \sigma$ ) labels the internal irrep space (and is removed when  $\dim \Gamma = 1$ ), and the index  $\kappa$  goes over the multiplicity space (and is removed when  $\text{mlt}_J \Gamma = 1$ ). We suppress the  $\Gamma$  index in the  $\{|\nu\kappa\rangle\}$  basis label set because, in all cases of interest, we will be selecting a particular irrep — the trivial irrep A for rotationally symmetric molecules, and a general irrep  $\Gamma_{\text{rot}}$  for perrotationally symmetric molecular species.

Indices of the original  $|_m^J, k\rangle$  rotational states are in one-to-one correspondence with the Wigner  $D$ -matrix elements  $D_{mk}^J$  (21), i.e., matrix elements of rotations  $D^J$  in the  $\mathbf{z}$ -axis basis. Generalizing the molecule-frame momentum factor, we define the corresponding G-adapted

matrix elements (cf. [2, Eq. (2.33)]),

$$\langle m_\kappa, \nu | r \rangle = \sqrt{\frac{2J+1}{8\pi^2}} D_{m;\nu\kappa}^J(r) = \sqrt{\frac{2J+1}{8\pi^2}} \langle m | D^J(r) | \nu \kappa \rangle, \quad (66a)$$

which are proportional to rotation matrix elements in two *different* bases: the original  $z$ -axis projection basis for the left index, and the  $G$ -adapted basis for the right index.

If the irrep is one-dimensional, then there is no internal irrep index, and the matrix elements are

$$\langle m_\kappa | r \rangle = \sqrt{\frac{2J+1}{8\pi^2}} D_{m;\kappa}^J(r) \quad (1D \text{ irrep}) \quad , \quad (66b)$$

with the semicolon and Greek index distinguishing them from the ordinary Wigner  $D$ -matrices  $D_{mk}^J$  from Eq. (21). The latter are recovered by picking  $G$  to be the trivial group (see Example 7). For groups such as  $C_N$ , the adapted matrix elements are a subset of the Wigner elements, in which case we default to the Wigner set.

The above change of basis yields the following expression for the  $G$ -adapted rotational states in terms of position states,

$$|m_\kappa, \nu\rangle = \sqrt{\frac{2J+1}{8\pi^2}} \int_{SO(3)} dr D_{m;\nu\kappa}^{J*}(r) |r\rangle. \quad (67a)$$

The inverse expression,

$$|r\rangle = \sum_{J \geq |m| \geq 0} \sqrt{\frac{2J+1}{8\pi^2}} \sum_{\Gamma \uparrow J} \sum_{\nu=1}^{\dim \Gamma} \sum_{\kappa=1}^{\text{mlt}_J \Gamma} D_{m;\nu\kappa}^J(r) |m_\kappa, \nu\rangle, \quad (67b)$$

is easily obtained by remembering that the orthogonality and completeness properties of the Wigner  $D$ -matrices [101, 146] are maintained under basis changes.

These bases provide an alternative decomposition of the rotation-spin state space of an asymmetric molecule, decomposing the identity from Eq. (22) as

$$\mathbb{1}_{\text{mol}} = \int_{SO(3)} dr |r\rangle \langle r| \otimes \mathbb{1}_{\text{nuc}}, \quad (68a)$$

$$= \sum_{J \geq |m| \geq 0} \sum_{\Gamma \uparrow J} \sum_{\nu=1}^{\dim \Gamma} \sum_{\kappa=1}^{\text{mlt}_J \Gamma} |m_\kappa, \nu\rangle \langle m_\kappa, \nu| \otimes \mathbb{1}_{\text{nuc}}. \quad (68b)$$

## B. Rotationally symmetric molecules

The position states of an asymmetric molecule are in one-to-one correspondence with elements of  $SO(3)$  since any proper rotation, by definition, rotates the molecule from some initial position into a *different* final position. Rotationally symmetric molecules (see Sec. VIII for a definition) admit a proper-rotation subgroup  $G$  that leaves the molecule invariant per the restriction from Eq. (30), so not all  $SO(3)$  rotations are needed to label distinct orientations of a symmetric molecule.

Re-stating the symmetry restriction in terms of group theory, given a label  $a$  for a molecular position state, any labels of the form  $ag$  for symmetry-group rotations

$g \in G$  correspond to the same position and are therefore redundant. This redundancy implies that each  $a$  is representative of its corresponding *left coset* of  $G$  in  $SO(3)$ ,

$$aG = \{ag | g \in G\}. \quad (69)$$

The set of labels for distinct position states of a  $G$ -symmetric molecule thus corresponds to elements of  $SO(3)/G$ , the space of left cosets of  $G$  in  $SO(3)$ . Each coset can be represented by only one of its elements, and particular choices of representatives are referred to as “sections”, “gauges”, or “transversals”.

Position states  $|a\rangle$  of  $G$ -symmetric molecules form a subspace of the state space of an asymmetric molecule and can be expressed as equal superpositions of elements of their corresponding cosets,

$$|a\rangle \equiv \frac{1}{\sqrt{|G|}} \sum_{g \in G} |r = ag\rangle, \quad (70)$$

where  $|r\rangle$  is a position state of an asymmetric molecule from Eq. (67b), and where  $|G|$  is the number of elements in the group. For continuous groups  $G \in \{C_\infty, D_\infty\}$ , the sum turns into an integral, and  $|G|$  becomes the group volume; we cover such cases in the examples.

The above coset states satisfy the symmetry constraint from Eq. (30) since the application of a molecule-based rotation merely permutes the elements in the superposition. For any  $h \in G$ , we have

$$\widehat{X}_h |a\rangle = \frac{1}{\sqrt{|G|}} \sum_g |r = agh^{-1}\rangle \quad (71a)$$

$$= \frac{1}{\sqrt{|G|}} \sum_g |r = ag\rangle. \quad (71b)$$

In the first equality, we use the definition of the action of molecule-based rotations on asymmetric position states,  $\widehat{X}_g |r\rangle = |rg^{-1}\rangle$  in Eq. (15a). In the second, we use the group resummation property,

$$\sum_g f(gh) = \sum_g f(g), \quad (72)$$

for any  $h \in G$  and any function  $f$  on the group.

We now express each position state  $|r\rangle$  in the above coset states as a superposition of  $G$ -adapted rotational states using Eq. (67b). Rearranging sums, writing out the  $G$ -adapted  $D$ -matrices (66), and splitting up the product between  $a$  and  $g$  yields

$$|a\rangle = \sum_{J \geq |m| \geq 0} \sqrt{\frac{2J+1}{8\pi^2 |G|}} \sum_{\Gamma \uparrow J} \sum_{\nu=1}^{\dim \Gamma} \sum_{\kappa=1}^{\text{mlt}_J \Gamma} \left\langle m | D^J(a) \left[ \frac{1}{|G|} \sum_g D^J(g) \right] | \nu \kappa \right\rangle |m_\kappa, \nu\rangle. \quad (73)$$

This equation can be further simplified by noticing that the sum in square brackets is a projection onto all copies of the trivial irrep. In terms of the  $G$ -adapted basis,

$$\frac{1}{|G|} \sum_{g \in G} D^J(g) | \nu \kappa \rangle = \delta_{\Gamma, A} | \kappa \rangle, \quad (74)$$

where the  $\nu$  index is not present since  $\dim A = 1$ .

Plugging in the expression for the projection reduces the position-state expression (73) in the following ways. First, the sum over  $\Gamma$  goes away due to  $\Gamma = A$ . As a result, the sum over  $J$  is reduced to the sum over only those momenta which contain at least one copy of the trivial irrep; we denote this set by  $J \downarrow A$ . Second, the sums over  $\nu$  and  $\kappa$  index the irrep and multiplicity spaces of  $A$ , and the former goes away since the irrep dimension is one, i.e.,  $|_{m\kappa}^J, \nu\rangle \rightarrow |_{m\kappa}^J$ . Altogether, this yields

$$|a\rangle = \sum_{J \downarrow A} \sum_{|m| \leq J} \sqrt{\frac{2J+1}{8\pi^2/|G|}} \sum_{\kappa=1}^{\text{mlt}_J A} D_{m;\kappa}^J(a) |_{m\kappa}^J, \quad (75)$$

which expresses position states precisely in terms of the rotational states  $\{|_{m\kappa}^J\rangle\}$  that we obtained in Sec. VIII A.

The symmetric molecular position states (75) constitute an orthonormal “basis” for the state space of a  $G$ -symmetric rigid body,

$$\langle a|a'\rangle = \delta^{\text{SO}(3)/G}(a, a'), \quad (76)$$

where the coset-space Dirac  $\delta$ -function is infinite for coset representatives  $a = a'$  and zero otherwise. Position states resolve the identity on the symmetric state space as

$$\mathbb{1}_{\text{mol}}^G = \int_{\text{SO}(3)/G} da |a\rangle \langle a| \otimes \mathbb{1}_{\text{nuc}}, \quad (77)$$

dual to the rotational-state identity in Eq. (36).

The reverse Fourier transform expressing  $|_{m\kappa}^J$  in terms of position states can be derived by using the fact that cosets partition  $\text{SO}(3)$ . Given a fixed set of coset representatives, each rotation  $r \in \text{SO}(3)$  can be written as a product of a particular representative and symmetry-group element,

$$r = ag \quad \text{for some } a \in \text{SO}(3)/G \quad \text{and } g \in G. \quad (78)$$

As a result, any integral over  $\text{SO}(3)$  can be split into an integral over the coset space and a sum over the symmetry group. Applying this to Eq. (67a) and specializing to the trivial (one-dimensional) irrep yields

$$|_{m\kappa}^J\rangle = \sqrt{\frac{2J+1}{8\pi^2}} \int_{\text{SO}(3)/G} da \sum_{g \in G} D_{m;\kappa}^{J*}(ag) |r = ag\rangle, \quad (79)$$

where  $\kappa$  indexes the multiplicity of  $A$ .

Next, we simplify the  $G$ -adapted matrix elements by noticing that taking the  $\kappa$ th element is effectively evaluating  $g$  in the trivial  $G$ -irrep,

$$D_{m;\kappa}^{J*}(ag) = \langle m|D^{J*}(a)D^{J*}(g)|\kappa\rangle \quad (80a)$$

$$= \langle m|D^{J*}(a)A(g)|\kappa\rangle \quad (80b)$$

$$= \langle m|D^{J*}(a)|\kappa\rangle. \quad (80c)$$

Plugging this in, evaluating  $\sum_{g \in G} 1 = |G|$ , and expressing the sum of position states  $|r = ag\rangle$  as a symmetric position state  $|a\rangle$  from Eq. (70) yields

$$|_{m\kappa}^J\rangle = \sqrt{\frac{2J+1}{8\pi^2/|G|}} \int_{\text{SO}(3)/G} da D_{m;\kappa}^{J*}(a) |a\rangle, \quad (81)$$

completing the Fourier transform on  $\text{SO}(3)/G$ .

**Example 25** (calcium monohydrosulfide). The procedure for determining the position state space of a symmetric molecule can also be applied to asymmetric molecules. Recalling Example 7, the symmetry group of such molecules is trivial, containing only the identity element,  $G = \langle e \rangle$ . The coset space  $\text{SO}(3)/C_1 = \text{SO}(3)$ , meaning that the entire group remains as the set of labels of asymmetric molecular position states.

The trivial irrep is the only irrep, so the sum over  $\Gamma$  in the position-state expression (67b) goes away. The trivial irrep is one-dimensional, so there is also no  $\nu$  index in that equation. The  $\kappa$  index goes from 1 to  $2J + 1 = \text{mlt}_J A$ , reducing Eq. (67b) to the position states from Eq. (20b).

**Example 26** (hydrogen chloride). Position states of any  $C_\infty$ -symmetric molecules from Example 6 are labeled by points on the ordinary two-sphere  $S^2$ . In our formalism, the sphere is recovered as the coset space  $\text{SO}(3)/C_\infty \cong S^2$  and corresponds to a subset of coset representatives.

A convenient partition of  $\text{SO}(3)$ -rotations into coset representatives  $a$  and symmetry-group elements  $g$  per Eq. (78) can be done using the Euler angle parameterization,  $r = (\alpha\beta\gamma) = ag$ , when  $C_\infty$  is the group of rotations around the  $z$ -axis. In that case, the  $\gamma$  angle is reserved for labeling the subgroup elements  $g$ , while the pair  $(\alpha\beta)$  is retained for the position states  $a$ .

For  $C_\infty$ , the position state sum in Eq. (70) becomes an integral,

$$|a\rangle \equiv \frac{1}{\sqrt{|G|}} \int_G dG |r = ag\rangle, \quad (82)$$

where the group volume is  $C_\infty = \int_0^{2\pi} d\gamma = 2\pi$ . When  $C_\infty$  is the subgroup of  $z$ -axis rotations in the Euler-angle parameterization, the above integral reduces to one over  $\gamma$ .

The  $C_\infty$ -adapted matrix elements correspond to the spherical harmonics,

$$Y_m^J(a) = \sqrt{\frac{2J+1}{4\pi}} D_{m0}^{J*}(a), \quad (83)$$

and the position and momentum states for this case are

$$|a\rangle = \sum_{J \geq 0} \sum_{|m| \leq J} Y_m^{J*}(a) |_{m}^J\rangle \quad (84a)$$

$$|_{m}^J\rangle = \int_{S^2} da Y_m^J(a) |a\rangle, \quad (84b)$$

where  $|_{m}^J\rangle = |_{m}^J, k=0\rangle$  are the rotational basis states determined in Example 6.

**Example 27** (disulfur). The  $S_2$  molecule, along with any spinless homonuclear diatomic, is a  $D_\infty$ -symmetric rigid body (see Example 9). Its symmetry group includes the rotations from the previous heteronuclear example, along with all  $\pi$ -rotations that permute the two identical (spinless) nuclei.

Position states of this case are of the form in Eq. (82), with the integral being over  $G = D_\infty$ , with group volume  $|D_\infty| = 4\pi$ .



The coset space labeling  $S_2$  positions is  $SO(3)/D_\infty \cong \mathbb{RP}^2$  — the two-dimensional real projective plane. This is also known as the two-sphere with opposite points identified, and each point can be identified with a rod in three-dimensional space [138]. In terms of the Euler-angle parameterization from the previous example, each projective-plane point  $(\alpha\beta)$  is a rod with endpoints at  $(\alpha\beta)$  and its antipode  $(\alpha + \pi, \pi - \beta)$ .

Position and momentum states for this case are,

$$|a\rangle = \sqrt{2} \sum_{J \text{ even}} \sum_{|m| \leq J} Y_m^{J*}(a) |m\rangle^J \quad (85a)$$

$$|m\rangle^J = \sqrt{2} \int_{\mathbb{RP}^2} da Y_m^J(a) |a\rangle, \quad (85b)$$

where the square root is due to a different normalization for  $G = D_\infty$ , i.e.,  $8\pi^2/|D_\infty| = 2\pi$ . These are closely related to those of the  $C_\infty$ -symmetric case from Eq. (84). The position states can even be obtained by superposing each  $C_\infty$ -symmetric state  $a = (\alpha\beta)$  with its antipode, which restricts the spherical-harmonic sum to only the even-momentum harmonics.

**Example 28** (cobalt tetracarbonyl hydride). Recalling Example 10, this molecule is  $C_3$  symmetric. The coset space labeling its positions is  $SO(3)/C_3$ , a member of the *lens space* family,  $L_{2N,1} \equiv SO(3)/C_N$ . We handle the general- $N$  case directly due to its simple generality.

Picking the group to consist of  $z$ -axis rotations, a simple parameterization for the coset space consists of Euler angles  $(\alpha\beta\gamma)$ , with  $0 \leq \gamma < 2\pi/N$ . The  $N \rightarrow \infty$  case reduces yields the  $C_\infty$ -symmetric Example 26 (cf. [101, Appx. D]).

The symmetry group  $C_N$  is discrete, so Eq. (70) applies directly. Position and momentum states (with the latter worked out in Example 10) can be expressed in terms of the standard Wigner  $D$ -matrix elements,

$$|a\rangle = \sum_{J \geq 0} \sqrt{\frac{2J+1}{8\pi^2/N}} \sum_{|m| \leq J} \sum_{\kappa=1}^{2n+1} D_{m,N(\kappa-n-1)}^J(a) |m\kappa\rangle^J \quad (86a)$$

$$|m\kappa\rangle^J = \sqrt{\frac{2J+1}{8\pi^2/N}} \int_{L_{2N,1}} da D_{m,N(\kappa-n-1)}^{J*}(a) |a\rangle, \quad (86b)$$

where  $n = \lfloor J/N \rfloor$ .

**Example 29** (sulfur trioxide). Recalling Example 11, this molecule is  $D_3$  symmetric. The coset space labeling its positions is  $SO(3)/D_3$ , a member of the *prism space* family,  $SO(3)/D_N$ . The  $N \rightarrow \infty$  case of such spaces yields the real projective plane from Example 27.

Recalling the form of the rotational states from Eq. (39), the corresponding  $D_3$ -adapted rotation matrix elements from Eq. (66b), expressed in terms of the standard Wigner  $D$ -matrix elements, are

$$D_{m;\kappa}^{J*}(a) = \frac{1}{\sqrt{2}} (D_{m,3(\kappa-1)}^{J*}(a) - (-1)^{J+\kappa} D_{m,3(1-\kappa)}^{J*}(a)), \quad (87)$$

for  $a \in SO(3)/D_3$ . These are then plugged into the Fourier transform on this prism space,

$$|a\rangle = \sum_{J \geq 0} \sqrt{\frac{2J+1}{4\pi^2/3}} \sum_{|m| \leq J} \sum_{\kappa=1}^{m(J)} D_{m;\kappa}^J(a) |m\kappa\rangle^J \quad (88a)$$

$$|m\kappa\rangle^J = \sqrt{\frac{2J+1}{4\pi^2/3}} \int_{SO(3)/D_3} da D_{m;\kappa}^{J*}(a) |a\rangle. \quad (88b)$$

**Example 30** ( $C_{60}$  fullerene). The position-state space of this icosahedrally symmetric molecule is the Poincare homology sphere  $SO(3)/I$  [277, 278]. This space was once a candidate model for the shape of an assumed-to-be-periodic universe [279]. Position states are difficult to express in terms of icosahedral harmonics, but admit a simple coset-state expression,

$$|a\rangle \equiv \frac{1}{\sqrt{60}} \sum_{g \in I} |r = ag\rangle. \quad (89)$$

### C. Perrotationally symmetric molecules

Molecular position states of perrotationally symmetric molecules have to satisfy the joint symmetry and spin-statistics condition from Eq. (41), under which the collective rotation-spin space transforms according to the 1D  $G$ -irrep  $\Gamma_{\text{mol}}$ . In Sec. VIII B, we showed that there are various combinations of rotational irreps  $\Gamma_{\text{rot}}$  and nuclear irreps  $\Gamma_{\text{nuc}}$  such that their direct product restricts to  $\Gamma_{\text{mol}}$ .

Here, we develop position states for a single species  $S$ , which corresponding to the triple  $\Gamma_{\text{rot}} \otimes \Gamma_{\text{nuc}} \downarrow \Gamma_{\text{mol}}$ . This requires generalizing the procedure for rotationally symmetric molecules from the previous subsection. The resulting states are still parameterized, in part, by coset-space labels  $a \in SO(3)/G$ , but the non-Abelian nature of  $\Gamma_{\text{rot}}$  irrep attaches extra internal degrees of freedom to each position state in the entangled case.

#### 1. $\mathfrak{d} = 1$ separable species

In the separable case, both irreps  $\Gamma_{\text{rot}}$  and  $\Gamma_{\text{nuc}}$  are one-dimensional, and their tensor product directly yields the correct spin statistics,  $\Gamma_{\text{rot}} \otimes \Gamma_{\text{nuc}} = \Gamma_{\text{mol}}$ . To identify the position state space, we have to formulate position states on the rotational factor that transform according to  $\Gamma_{\text{rot}}$ .

The result is obtained by a simple modification of the coset-state superposition in Eq. (70) to a superposition whose coefficients are evaluations of the symmetry-group elements in the desired irrep. For each position-state label  $a \in SO(3)/G$ , the state is

$$|a\rangle \equiv \frac{1}{\sqrt{|G|}} \sum_{g \in G} \Gamma_{\text{rot}}(g) |r = ag\rangle. \quad (90)$$

These states are Dirac- $\delta$  orthogonal, satisfying Eq. (76) for any one-dimensional  $\Gamma_{\text{rot}}$ . When  $\Gamma_{\text{rot}} = A$ , they reduce to the rotationally symmetric case in Eq. (70).

The above generalized coset states transform correctly under the rotational part of the perrotation from Eq. (40). Generalizing Eq. (71), we have, for any  $\mathbf{h} \in \mathbf{G}$ ,

$$\widehat{X}_{\mathbf{h}}|\mathbf{a}\rangle = \frac{1}{\sqrt{|\mathbf{G}|}} \sum_{\mathbf{g}} \Gamma_{\text{rot}}(\mathbf{g}) |r = \mathbf{a}\mathbf{g}\mathbf{h}^{-1}\rangle \quad (91a)$$

$$= \frac{1}{\sqrt{|\mathbf{G}|}} \sum_{\mathbf{g}} \Gamma_{\text{rot}}(\mathbf{g}\mathbf{h}) |r = \mathbf{a}\mathbf{g}\rangle \quad (91b)$$

$$= \frac{1}{\sqrt{|\mathbf{G}|}} \sum_{\mathbf{g}} \Gamma_{\text{rot}}(\mathbf{g}) \Gamma_{\text{rot}}(\mathbf{h}) |r = \mathbf{a}\mathbf{g}\rangle \quad (91c)$$

$$= \Gamma_{\text{rot}}(\mathbf{h})|\mathbf{a}\rangle. \quad (91d)$$

In the third equality, we recall that  $\Gamma_{\text{rot}}$  is a scalar representing the group and split the product of  $\mathbf{g}$  and  $\mathbf{h}$ . In the fourth, we re-express the result in terms of the original coset states.

The generalized coset states (90) can be expressed in terms of the rotational states  $\{|_{m\kappa}^J\rangle\}$  from Eq. (47), where  $\kappa$  indexes the multiplicity of  $\Gamma_{\text{rot}}$ . The derivation is a slight generalization of the rotationally symmetric ( $\Gamma_{\text{rot}} = \mathbf{A}$ ) derivation in Eqs. (73-75). We omit it for brevity, noting that the entangled species derivation done in the next subsection encompasses both.

Position and rotational states for the rotational factor of a separable species are

$$|\mathbf{a}\rangle = \sum_{J \downarrow \Gamma_{\text{rot}}} \sum_{|m| \leq J} \sqrt{\frac{2J+1}{8\pi^2/|\mathbf{G}|}} \sum_{\kappa=1}^{m(J)} D_{m,\kappa}^J(\mathbf{a}) |_{m\kappa}^J\rangle \quad (92a)$$

$$|_{m\kappa}^J\rangle = \sqrt{\frac{2J+1}{8\pi^2/|\mathbf{G}|}} \int_{\text{SO}(3)/\mathbf{G}} d\mathbf{a} D_{m,\kappa}^{J*}(\mathbf{a}) |\mathbf{a}\rangle. \quad (92b)$$

Tacking on the nuclear states  $\{|\chi\rangle\}$ , which are required to transform according to  $\Gamma_{\text{nuc}}$ , the species' identity decomposes as

$$\mathbb{1}_{\text{mol}}^{\mathbf{G},\mathbf{S}} = \int_{\text{SO}(3)/\mathbf{G}} d\mathbf{a} |\mathbf{a}\rangle \langle \mathbf{a}| \otimes \sum_{\chi=1}^{m_{\text{nuc}}} |\chi\rangle \langle \chi|, \quad (93)$$

dual to the rotational-state decomposition from Eq. (45).

**Example 31** (water,  $\mathbf{A}^*$  para species). Recalling Example 13,  $\text{H}_2\text{O}$  is  $\mathbf{C}_2$ -symmetric, so its position states are parameterized by points in the lens space  $\mathbf{L}_{4,1} \equiv \text{SO}(3)/\mathbf{C}_2$ . Using the Euler-angle parameterization from Example 28, each coset consists of only two elements,  $(\alpha\beta\gamma)$  and  $(\alpha, \beta, \gamma + \pi)$ . Coset representatives are parameterized by  $(\alpha\beta\gamma)$  with  $\alpha = [0, 2\pi)$ ,  $\beta = [0, \pi]$ , and  $\gamma = [0, \pi)$ .

Since  $\Gamma_{\text{rot}} = \mathbf{A}$  is the trivial irrep for this species, we have  $\mathbf{A}(\gamma = 0) = \mathbf{A}(\gamma = \pi) = +1$ . The coset states from (90) are

$$|\mathbf{a} = (\alpha\beta\gamma)\rangle = \frac{1}{\sqrt{2}} (|r = (\alpha, \beta, \gamma)\rangle + |r = (\alpha, \beta, \gamma + \pi)\rangle), \quad (94)$$

where we abuse notation and use a coset representative's Euler-angle parameterization as a stand-in for the representative  $\mathbf{a}$  itself. Applying the symmetry-group rotation  $\widehat{X}_{00\pi}$  to this state yields +1, confirming that the state transforms according to the trivial irrep.

The Fourier transform between these states and the rotational states is that from Eq. (85) for  $N = 2$ . Per Example 13, a basis for the species consists of tensor products of the above states with the singlet state  $(|\uparrow\downarrow\rangle - |\downarrow\uparrow\rangle)/\sqrt{2}$  of the two hydrogen nuclei and an arbitrary state of the oxygen nucleus.

**Example 32** (water,  $\mathbf{B}^*$  ortho species). The other species of water, considered in Example 14, admit the  $\Gamma_{\text{rot}} = \mathbf{B}$  irrep, for which  $\mathbf{B}(\gamma = 0) = +1$  and  $\mathbf{B}(\gamma = \pi) = -1$ . Plugging this data into the generalized coset states in Eq. (90) yields

$$|\mathbf{a} = (\alpha\beta\gamma)\rangle = \frac{1}{\sqrt{2}} (|r = (\alpha, \beta, \gamma)\rangle - |r = (\alpha, \beta, \gamma + \pi)\rangle). \quad (95)$$

Applying  $\widehat{X}_{00\pi}$  to this state yields -1, confirming that the state transforms according to the  $\mathbf{B}$  irrep.

Per Example 14, the rotational states transforming according to the  $\mathbf{B}$  irrep are the asymmetric states  $|_{m,k}^J\rangle$  for which  $k$  is odd. The number of such states for a given  $J$  is  $m(J) = 2[(J+1)/2]$ , and the symmetric rotational states are  $|_{m\kappa}^J\rangle = |_{m,k}^J, k = 2\kappa - m(J) - 1\rangle$  for  $1 \leq \kappa \leq m(J)$ . The Fourier transform between position and rotational states for this species is then expressible using the Wigner  $D$ -matrix elements,

$$|\mathbf{a}\rangle = \sum_{J>0} \sqrt{\frac{2J+1}{4\pi^2}} \sum_{|m| \leq J} \sum_{\kappa=1}^{m(J)} D_{m,2\kappa-m(J)-1}^J(\mathbf{a}) |_{m\kappa}^J\rangle \quad (96a)$$

$$|_{m\kappa}^J\rangle = \sqrt{\frac{2J+1}{4\pi^2}} \int_{\mathbf{L}_{4,1}} d\mathbf{a} D_{m,2\kappa-m(J)-1}^{J*}(\mathbf{a}) |\mathbf{a}\rangle. \quad (96b)$$

Note that all momenta participate except  $J = 0$ , which has no odd values of its  $\mathbf{z}$ -axis component.

A basis for the species consists of tensor products of the above states with any triplet-subspace state of the two hydrogen nuclei and an arbitrary state of the oxygen.

**Example 33** (deuterated hydrogen,  $\mathbf{A}_1$  ortho species). Recalling Example 15,  $\text{D}_2$  is  $\text{D}_{\infty}$ -symmetric, so its position states are parameterized by points in the projective plane  $\text{RP}^2 = \text{SO}(3)/\text{D}_{\infty}$ . This is the same set of labels as for disulfur in Example 27. The rotational-state irrep participating in this species is also trivial,  $\Gamma_{\text{rot}} = \mathbf{A}_1$ , so the Fourier transform on the rotational part of this species is the same as that of  $\text{S}_2$  in Eq. (85).

A basis for the species consists of tensor products of the above states with any triplet-subspace state of the two deuterium nuclei.

**Example 34** (deuterated hydrogen,  $\mathbf{A}_2$  para species). Recalling Example 16, the other species of  $\text{D}_2$  is constructed by setting both the rotational and nuclear-spin states to transform according to the sign irrep,  $\Gamma_{\text{rot}} = \Gamma_{\text{nuc}} = \mathbf{A}_2$ . While the position-state labels,  $\mathbf{a} \in \text{RP}^2$ , remain the same as those of the  $\mathbf{A}_1$  species, the rotational-state irrep is different.

Since the irrep is nontrivial, the coset-state superposition is no longer uniform like it was in Eq. (82). Parameterizing  $\mathbf{z}$ -axis rotations by angle  $\gamma$  by the Euler-angle

triple  $(00\gamma)$  and equatorial rotations by  $(0\pi\gamma)$ , position states are parameterized by  $\mathbf{a} = (\alpha\beta)$  (see Example 27), and position states from Eq. (90) are

$$|(\alpha\beta)\rangle \equiv \frac{1}{4\pi} \int_0^{2\pi} d\gamma \, |\mathbf{r} = (\alpha, \beta, \gamma)\rangle - |\mathbf{r} = (\alpha + \pi, \pi - \beta, \gamma)\rangle, \quad (97)$$

where the relative phase is due to the fact that that all equatorial rotations evaluate to  $-1$  in the irrep.

The Fourier transform between position and momentum states (worked out in Example 16) is

$$|\mathbf{a}\rangle = \sqrt{2} \sum_{J \text{ odd}} \sum_{|m| \leq J} Y_m^{J*}(\mathbf{a}) |m\rangle^J \quad (98a)$$

$$|m\rangle^J = \sqrt{2} \int_{\text{RP}^2} d\mathbf{a} Y_m^J(\mathbf{a}) |\mathbf{a}\rangle. \quad (98b)$$

A basis for the species consists of tensor products of the above states with the singlet state of the two deuterium nuclei.

**Example 35** (ammonia,  ${}^2\text{E}$  species). Recalling Example 15,  $\text{NH}_3$  is  $\text{C}_3$ -symmetric, so its position states are parameterized by points in the lens space  $\text{L}_{6,1} \cong \text{SO}(3)/\text{C}_3$ . The symmetry group contains three rotations by  $\frac{2\pi}{3}p$  for  $p \in \{0, 1, 2\}$ , which evaluate to  $\exp(-i\frac{2\pi}{3}p)$  in the  ${}^2\text{E}$  irrep. Position states from Eq. (90) are

$$|\mathbf{a} = (\alpha\beta\gamma)\rangle = \sum_{p=0}^2 e^{-i\frac{2\pi}{3}p} |\mathbf{r} = (\alpha, \beta, \gamma + \frac{2\pi}{3}p)\rangle, \quad (99)$$

parameterized by  $\alpha \in [0, 2\pi)$ ,  $\beta \in [0, \pi]$ , and  $\gamma \in [0, 2\pi/3)$ . States for the  $\text{C}_N$ -symmetric  ${}^2\text{E}_1$  species are obtained by letting  $3 \rightarrow N$  and iterating  $p$  from 0 to  $N-1$ .

Per Example 17, the rotational states transforming according to the  ${}^2\text{E}$  irrep are the asymmetric states  $|m, k\rangle^J$  for which  $k \equiv 2 \pmod{3}$ . The admissible rotational states are

$$|m, k\rangle^J = |m, k = 3\kappa - 1 - 3[(J+2)/3]\rangle \quad (100)$$

for  $|m| \leq J$  and  $1 \leq \kappa \leq \mathbf{m}(J) = J - \lfloor J/3 \rfloor$ . The Fourier transform between position and rotational states for this species is then expressible using the Wigner  $D$ -matrix elements,

$$|\mathbf{a}\rangle = \sum_{J>0} \sqrt{\frac{2J+1}{4\pi^2}} \sum_{|m| \leq J} \sum_{\kappa=1}^{\mathbf{m}(J)} D_{m, 3\kappa-1-3[(J+2)/3]}^J(\mathbf{a}) |m, k\rangle^J$$

$$|m, k\rangle^J = \sqrt{\frac{2J+1}{4\pi^2}} \int_{\text{SO}(3)/\text{C}_3} d\mathbf{a} D_{m, 3\kappa-1-3[(J+2)/3]}^{J*}(\mathbf{a}) |\mathbf{a}\rangle. \quad (101)$$

## 2. $\mathfrak{d} \geq 2$ entangled species

The collective rotational and nuclear-spin wavefunction of an entangled species transforms according the irrep  $\Gamma_{\text{mol}}$ , which is present in the tensor product of its corresponding  $\mathfrak{d}$ -dimensional rotational irrep  $\Gamma_{\text{rot}}$  and a nuclear-spin irrep  $\Gamma_{\text{nuc}}$ . We first formulate “uncoupled”

position states on the rotational factor that transform as  $\Gamma_{\text{rot}}$ , and then perform the projection onto the  $\Gamma_{\text{mol}}$  irrep according to the prescription of Sec. VIII B.

Since the rotational irrep is no longer one-dimensional,  $\Gamma_{\text{rot}}(\mathbf{g})$  is a  $\mathfrak{d}$ -dimensional matrix with matrix elements

$$\Gamma_{\text{rot}}^{\mu\nu}(\mathbf{g}) = \langle \mu | \Gamma_{\text{rot}}(\mathbf{g}) | \nu \rangle, \quad (102)$$

where  $\mu, \nu \in \{1, 2, \dots, \mathfrak{d}\}$ , and where  $\mathbf{g} \in \mathbf{G}$ . Defining these elements requires a choice of orthonormal basis  $|\mu\rangle$  for the irrep space, but the results below hold for any choice.

Extending the coset-state construction from Eq. (90) to this case yields  $\mathfrak{d}^2$  states for each representative  $\mathbf{a} \in \text{SO}(3)/\text{G}$ ,

$$|\mathbf{a}; \Gamma_{\text{rot}}^{\mu\nu}\rangle = \sqrt{\frac{\mathfrak{d}}{|\mathbf{G}|}} \sum_{\mathbf{g} \in \mathbf{G}} \Gamma_{\text{rot}}^{\mu\nu}(\mathbf{g}) |\mathbf{r} = \mathbf{a}\mathbf{g}\rangle, \quad (103)$$

with each state corresponding to a particular matrix element.

Molecule-based rotations in the symmetry group leave the position-state label  $\mathbf{a}$  invariant, but transform the internal degrees of freedom at each position. More precisely, rotations act on the  $\nu$  index according to  $\Gamma_{\text{rot}}$ . Generalizing Eq. (91) yields, for any  $\mathbf{h} \in \mathbf{G}$ ,

$$\widehat{X}_{\mathbf{h}} |\mathbf{a}; \Gamma_{\text{rot}}^{\mu\nu}\rangle = \sqrt{\frac{\mathfrak{d}}{|\mathbf{G}|}} \sum_{\mathbf{g} \in \mathbf{G}} \Gamma_{\text{rot}}^{\mu\nu}(\mathbf{g}\mathbf{h}) |\mathbf{r} = \mathbf{a}\mathbf{g}\rangle \quad (104a)$$

$$= \sqrt{\frac{\mathfrak{d}}{|\mathbf{G}|}} \sum_{\mathbf{g} \in \mathbf{G}} \sum_{\sigma=1}^{\mathfrak{d}} \Gamma_{\text{rot}}^{\mu\sigma}(\mathbf{g}) \Gamma_{\text{rot}}^{\sigma\nu}(\mathbf{h}) |\mathbf{a}\mathbf{g}\rangle \quad (104b)$$

$$= \sum_{\sigma=1}^{\mathfrak{d}} \Gamma_{\text{rot}}^{\sigma\nu}(\mathbf{h}) |\mathbf{a}; \Gamma_{\text{rot}}^{\mu\sigma}\rangle, \quad (104c)$$

where we have resolved the identity on the internal  $\Gamma_{\text{rot}}$ -irrep space in order to split up the product of  $\mathbf{g}$  and  $\mathbf{h}$ .

We now express Eq. (103) in terms of rotational states  $\{|m, \mu\rangle^J\}$  from Eq. (67a). The derivation proceeds analogously to the rotationally symmetric case in Eqs. (73-75) whilst taking into account the internal  $\mu, \nu$ -labeled degrees of freedom.

After plugging in the  $\mathbf{G}$ -adapted expressions for asymmetric position states  $|\mathbf{r}\rangle$  from Eq. (67b), writing out the  $\mathbf{G}$ -adapted matrix elements from Eq. (66), and splitting up the product between  $\mathbf{a}$  and  $\mathbf{g}$ , Eq. (103) becomes

$$|\mathbf{a}; \Gamma_{\text{rot}}^{\mu\nu}\rangle = \sum_{J \geq |m| \geq 0} \sqrt{\frac{(2J+1)/\mathfrak{d}}{8\pi^2/|\mathbf{G}|}} \sum_{\Gamma \uparrow J}^{\dim \Gamma} \sum_{\sigma=1}^{\text{mlt}_J \Gamma} \sum_{\kappa=1}^{\Gamma} \langle m | D^J(\mathbf{a}) \left[ \frac{\mathfrak{d}}{|\mathbf{G}|} \sum_{\mathbf{g}} \Gamma_{\text{rot}}^{\mu\nu}(\mathbf{g}) D^J(\mathbf{g}) \right] | \sigma \kappa \rangle |m, \kappa, \sigma\rangle^J. \quad (105)$$

This equation can be further simplified by noticing that  $\mathbf{g}$  is evaluated in the  $\Gamma$  irrep, i.e.,

$$D^J(\mathbf{g}) |\sigma \kappa\rangle = \Gamma^*(\mathbf{g}) |\sigma\rangle \otimes |\kappa\rangle, \quad (106)$$

per the convention chosen in the isotypic decomposition from Eq. (31). Inserting another resolution of identity on the irrep space and simplifying yields

$$|\mathbf{a}; \Gamma_{\text{rot}}^{\mu\nu}\rangle = \sum_{J \geq |m| \geq 0} \sqrt{\frac{(2J+1)/\mathfrak{d}}{8\pi^2/|\mathbf{G}|}} \sum_{\Gamma \uparrow J}^{\dim \Gamma} \sum_{\sigma, \tau=1}^{\text{mlt}_J \Gamma} \sum_{\kappa=1}^{\Gamma} \langle m | D^J(\mathbf{a}) \left[ \frac{\mathfrak{d}}{|\mathbf{G}|} \sum_{\mathbf{g}} \Gamma_{\text{rot}}^{\mu\sigma}(\mathbf{g}) \Gamma_{\text{rot}}^{\tau\nu}(\mathbf{g}) \right] | \sigma \kappa \rangle |m, \kappa, \sigma\rangle^J. \quad (107)$$

$$D_{m;\tau\kappa}^J(\mathbf{a}) \left[ \frac{\mathfrak{d}}{|\mathcal{G}|} \sum_{\mathbf{g}} \Gamma_{\text{rot}}^{\mu\nu}(\mathbf{g}) \Gamma^{\tau\sigma*}(\mathbf{g}) \right] |_{m\kappa}^J, \sigma \rangle.$$

The sum in square brackets is then evaluated using Schur orthogonality, yielding three  $\delta$ -functions,  $\delta_{\Gamma_{\text{rot}}\Gamma}\delta_{\mu\tau}\delta_{\nu\sigma}$ .

The first  $\delta$ -function kills the sum over  $\Gamma$  by selecting  $\Gamma = \Gamma_{\text{rot}}$ . Conversely, the sum over  $J$  is reduced to a sum over only those momenta which contain at least one copy of the desired irrep; we denote this set by  $J \downarrow \Gamma_{\text{rot}}$ . The latter two  $\delta$ -functions kill the sums over  $\tau$  and  $\sigma$ , respectively, leaving only the multiplicity sum over  $\kappa$ . Altogether, Eq. (105) is simplified to

$$| \mathbf{a}; \Gamma_{\text{rot}}^{\mu\nu} \rangle = \sum_{J \downarrow \Gamma_{\text{rot}}} \sum_{|m| \leq J} \sqrt{\frac{(2J+1)/\mathfrak{d}}{8\pi^2/|\mathcal{G}|}} \sum_{\kappa=1}^{\mathfrak{m}(J)} D_{m;\mu\kappa}^J(\mathbf{a}) |_{m\kappa}^J, \nu \rangle. \quad (108)$$

expressing position states precisely in terms of the uncoupled rotational states  $\{|_{m\kappa}^J, \nu \rangle\}$  from Eq. (67a).

We now couple the above position states to the  $\Gamma_{\text{nuc}}$ -irrep nuclear-spin subspace and restrict the result to the collective  $\Gamma_{\text{mol}}$  irrep in order to obtain the correct spin statistics. According to Sec. VIII B, we couple internal irrep space (indexed above by  $\nu$ ) to its partner, the  $\Gamma_{\text{nuc}}$ -irrep space, and project onto the admissible rotational states from Eq. (57),

$$|_{m\kappa}^J \rangle = \frac{1}{\sqrt{\mathfrak{d}}} \sum_{\nu=1}^{\mathfrak{d}} s_{\nu} |_{m\kappa}^J, \nu \rangle_{\text{rot}} | \nu \rangle_{\text{nuc}}. \quad (109)$$

This coupling takes in the set  $\{ | \mathbf{a}; \Gamma_{\text{rot}}^{\mu\nu} \rangle \}_{\nu=1}^{\mathfrak{d}}$  of  $\mathfrak{d}$  states and yields a single entangled species' position state,

$$| \mathbf{a}, \mu \rangle \equiv \frac{1}{\sqrt{\mathfrak{d}}} \sum_{\nu=1}^{\mathfrak{d}} s_{\nu} | \mathbf{a}; \Gamma_{\text{rot}}^{\mu\nu} \rangle_{\text{rot}} | \nu \rangle_{\text{nuc}} \quad (110a)$$

$$= \sum_{J \downarrow \Gamma_{\text{rot}}} \sum_{|m| \leq J} \sqrt{\frac{(2J+1)/\mathfrak{d}}{8\pi^2/|\mathcal{G}|}} \sum_{\kappa=1}^{\mathfrak{m}(J)} D_{m;\mu\kappa}^J(\mathbf{a}) |_{m\kappa}^J, \nu \rangle, \quad (110b)$$

for each  $\mathbf{a}$  and  $\mu$ . While the  $\nu$ -labeled degree of freedom has been eliminated due to the enforcement of spin statistics, the  $\mu$ -labeled degree of freedom remains!

Together with the nuclear basis states indexing copies of  $\Gamma_{\text{nuc}}$ , the identity on an entangled species  $\mathbf{s}$  decomposes in terms of position states as

$$\mathbb{1}_{\text{mol}}^{\mathbf{G},\mathbf{s}} = \int_{\text{SO}(3)/\mathcal{G}} d\mathbf{a} \sum_{\mu=1}^{\mathfrak{d}} | \mathbf{a}, \mu \rangle \langle \mathbf{a}, \mu | \otimes \sum_{\chi=1}^{\mathfrak{m}_{\text{nuc}}} | \chi \rangle \langle \chi |, \quad (111)$$

where the tensor product is *not* between the rotational and nuclear-spin factors since the molecular position states contain a nuclear-spin component. Each molecular position  $\mathbf{a} \in \text{SO}(3)/\mathcal{G}$  carries with it, not only the requisite  $\mathfrak{m}_{\text{nuc}}$ -dimensional nuclear multiplicity space, but also an internal  $\mathfrak{d}$ -dimensional pseudo-spin factor, spanned by  $\{ | \mu \rangle \}_{\mu=1}^{\mathfrak{d}}$ , that we call the species' *fiber*.

Position states and their fibers form an orthonormal “basis” for the species, satisfying

$$\langle \mathbf{a}, \mu | \mathbf{a}', \mu' \rangle = \delta_{\mu\mu'} \delta^{\text{SO}(3)/\mathcal{G}}(\mathbf{a}, \mathbf{a}'). \quad (112)$$

Orthogonality and completeness can be proven by observing that the uncoupled position states  $\{ | \mathbf{a}; \Gamma^{\mu\nu} \rangle \}$  from Eq. (103) — when collected over all irreps, matrix elements, and coset representatives — form an orthonormal “basis” for the state space of an asymmetric molecule that is a special case of the *Zak basis* [101, 176–178]. Orthogonality and completeness relations for the Zak basis [101, Eq. (125)] imply analogous relations for the coupled states from Eqs. (111) and (112).

The reverse Fourier transform expressing rotational states  $|_{m\kappa}^J \rangle$  in terms of position states  $| \mathbf{a}, \mu \rangle$  can be derived as follows. We start with expression (67a) of the uncoupled rotational states for  $\Gamma = \Gamma_{\text{rot}}$  in terms of an integral superposition over the asymmetric position states,

$$|_{m\kappa}^J, \nu \rangle = \sqrt{\frac{2J+1}{8\pi^2}} \int_{\text{SO}(3)/\mathcal{G}} d\mathbf{a} \sum_{\mathbf{g} \in \mathcal{G}} D_{m;\nu\kappa}^{J*}(\mathbf{a}\mathbf{g}) | \mathbf{r} = \mathbf{a}\mathbf{g} \rangle, \quad (113)$$

where we have split the integral into one over the coset space and a sum over the symmetry group according to Eq. (78).

The product  $\mathbf{a}\mathbf{g}$  inside the matrix element of  $D^J$  can be split such that Eq. (106) can be applied. This yields

$$\begin{aligned} |_{m\kappa}^J, \nu \rangle &= \sqrt{\frac{2J+1}{8\pi^2}} \int_{\text{SO}(3)/\mathcal{G}} d\mathbf{a} \sum_{\mathbf{g} \in \mathcal{G}} \sum_{\mu=1}^{\mathfrak{d}} D_{m;\mu\kappa}^{J*}(\mathbf{a}) \Gamma_{\text{rot}}^{\mu\nu}(\mathbf{g}) | \mathbf{r} \rangle \\ &= \sqrt{\frac{(2J+1)/\mathfrak{d}}{8\pi^2/|\mathcal{G}|}} \int_{\text{SO}(3)/\mathcal{G}} d\mathbf{a} \sum_{\mu=1}^{\mathfrak{d}} D_{m;\mu\kappa}^{J*}(\mathbf{a}) | \mathbf{a}; \Gamma_{\text{rot}}^{\mu\nu} \rangle. \end{aligned} \quad (114)$$

We then plug in the above into Eq. (109), eliminating the  $\nu$  index, and use Eq. (110) to obtain

$$|_{m\kappa}^J \rangle = \sqrt{\frac{(2J+1)/\mathfrak{d}}{8\pi^2/|\mathcal{G}|}} \int_{\text{SO}(3)/\mathcal{G}} d\mathbf{a} \sum_{\mu=1}^{\mathfrak{d}} D_{m;\mu\kappa}^{J*}(\mathbf{a}) | \mathbf{a}, \mu \rangle, \quad (115)$$

completing the Fourier transform for entangled species.

Absorbing the constants into a  $\mathcal{G}$ -adapted “harmonic”,

$$H_{m\kappa}^J(\mathbf{a}, \mu) = \sqrt{\frac{(2J+1)/\mathfrak{d}}{8\pi^2/|\mathcal{G}|}} D_{m;\mu\kappa}^J(\mathbf{a}), \quad (116)$$

yields Eq. (5) from Sec. II. The  $\mathcal{G}$ -adapted orthogonality and completeness relations become

$$\int_{\text{SO}(3)/\mathcal{G}} d\mathbf{a} \sum_{\mu=1}^{\mathfrak{d}} H_{m\kappa}^J(\mathbf{a}, \mu) H_{m'\kappa'}^{J'*}(\mathbf{a}, \mu) = \delta_{JJ'} \delta_{mm'} \delta_{\kappa\kappa'} \quad (117a)$$

$$\sum_{J \downarrow \Gamma_{\text{rot}}} \sum_{|m| \leq J} \sum_{\kappa=1}^{\mathfrak{m}(J)} H_{m\kappa}^J(\mathbf{a}, \mu) H_{m\kappa}^{J*}(\mathbf{a}', \mu') = \delta_{\mu\mu'} \delta^{\text{SO}(3)/\mathcal{G}}(\mathbf{a}, \mathbf{a}'). \quad (117b)$$

**Example 36** (boron trifluoride,  $E^*$  species). Recalling Example 20, this  $D_3$ -symmetric molecule is the simplest example of a rotation-spin entangled species. Position states are labeled by points in the prism space  $\text{SO}(3)/D_3$ . Because the species is entangled, the molecule's position



states  $|\mathbf{a}, \mu\rangle$  have a fiber degree of freedom, with internal index  $\mu \in \{1, 2\}$ .

The species' Fourier transform is in Eqs. (110) and (115), with  $G = D_3$ . We will see in the next section that, since the fiber degree of freedom comes from the rotational state space, it will transform in a nontrivial way under lab-based rotations.

## X. HOLONOMY OF POSITION STATES

In Sec. IX, we developed admissible position states of rotationally and perrotationally symmetric molecular species and obtained the rotation-spin states  $|\mathbf{a}, \mu\rangle$ , tensored with a nuclear-spin factor spanned by appropriately transforming nuclear-spin states  $|\chi\rangle$ . Here, we derive the holonomy of such states arising from a closed adiabatic path in position state space, showing that it depends only on the “global” or “topological” details of the path. Motivated by our results, we also make a conjecture about holonomy in more general situations.

We omit the residual  $|\chi\rangle$  factor in the position-state expressions from now on because it is decoupled from and not relevant to the calculation. Since we deal only with the (dressed) rotational factor, we also drop the “rot” subscript, i.e.  $\Gamma_{\text{rot}} \rightarrow \Gamma$ .

### A. Induced representations

We derive the holonomy only for the case of a general entangled perrotational species. Its position states are

$$\{ |\mathbf{a}, \mu\rangle \text{ s.t. } \mathbf{a} \in \text{SO}(3)/G \text{ and } \mu \in \{1, \dots, \mathfrak{d}\} \}, \quad (118)$$

where  $\mu$  labels the internal degrees of freedom of the rotational  $G$ -irrep  $\Gamma$ , and where  $\mathfrak{d} = \dim \Gamma$ . This general case can then be specialized to all other cases of interest. States of separable species are obtained by setting  $\Gamma$  to a one-dimensional irrep and removing the  $\mu$  index. Any rotationally symmetric case is obtained by setting  $\Gamma$  to be the trivial irrep.

Interpreting the above state set from a geometric perspective, each point  $\mathbf{a} \in \text{SO}(3)/G$  can be thought of as housing the fiber's  $\mathfrak{d}$ -dimensional vector space. Such a space transforms under lab-based rotations  $\vec{X}_{\mathbf{g}}$  according to what is known as the induced representation,  $\Gamma \uparrow \text{SO}(3)$  [36, 131–136].

For all trivial-irrep cases considered here, the vector space has effectively zero dimension, and each state  $|\mathbf{a}\rangle$  can be thought of as a point. This corresponds to the representation  $\mathbf{A} \uparrow \text{SO}(3)$ , encompassing the  $G$ -symmetric cases and the  $G = C_1$  asymmetric case.

The  $\mathfrak{d} = 1$  case for a nontrivial one-dimensional irrep  $\Gamma$  yields  $\Gamma \uparrow \text{SO}(3)$ , corresponding to separable species of perrotationally symmetric molecules. In that case, the space is one-dimensional, and lab-based rotations change the global phase of the position states.

The  $\mathfrak{d} > 1$  case corresponds to the entangled species, and the fiber degrees of freedom transform under lab-based symmetry rotations according to the inducing irrep [101, Eq. (131)]. More generally, assuming sufficiently slow (i.e., adiabatic) movement along *any* path, the resulting transformations from symmetry rotations depend only on the “global” details of the path and not on any small deformations.

### B. Non-Abelian connection and holonomy

Consider evolving in an adiabatic path in the coset space  $\text{SO}(3)/G$  of the set of states above parameterized by Eq. (118). We determine the holonomy for all closed (piece-wise) continuous paths,

$$\{ \mathbf{a}(t) \text{ s.t. } t \in [0, 1] \}. \quad (119)$$

By closed, we mean that the final point  $\mathbf{a}(1)$  is identified in the coset space with the initial point  $\mathbf{a}(0)$  because of the symmetry of the molecule. Following Sec. VII D, we parameterize the path using the same coset-state parameterization for all points except, potentially, the last point  $\mathbf{a}(1)$ .

Upon traversing a closed path, the molecular basis state  $|\mathbf{a}, \mu\rangle$  undergoes a holonomy,

$$|\mathbf{a}(0), \mu\rangle \rightarrow U_{\text{hol}} |\mathbf{a}(0), \mu\rangle. \quad (120)$$

Since there is a vector space for each  $\mathbf{a}$ , the holonomy is a  $\mathfrak{d}$ -dimensional unitary Berry-Wilczek-Zee matrix [97]. Generalizing Eq. (25),

$$U_{\text{hol}} = U_{\text{mono}} \mathcal{P} \exp \left( - \int_{\mathbf{a}(0)}^{\mathbf{a}(1)} d\mathbf{a} A(\mathbf{a}) \right). \quad (121)$$

The second term on the right-hand side is the path-ordered integral of exponentials of the Berry-Wilczek-Zee connection  $A(\mathbf{a})$  (we call this the Berry connection from now on). The connection is now matrix-valued, with elements

$$A_{\mu\nu}(\mathbf{a}) = \frac{i\langle \mathbf{a}, \mu | \partial \mathbf{a}, \nu \rangle}{\sqrt{\langle \mathbf{a}, \mu | \mathbf{a}, \mu \rangle \langle \mathbf{a}, \nu | \mathbf{a}, \nu \rangle}}, \quad (122)$$

all defined for points  $\mathbf{a}(t < 1)$ . Path-ordering, denoted by  $\mathcal{P}$ , means that matrix exponentials of  $A$  earlier in the path  $\mathbf{a}(t)$  are written before those later in the path.

The monodromy  $U_{\text{mono}}$  is a compensating matrix that is the result of re-expressing the label  $\mathbf{a}(1)$  of the final state in terms of the label  $\mathbf{a}(0)$  of the initial state. The monodromy is only an issue when the path is non-contractible, but such paths exist in  $\text{SO}(3)/G$  for any  $G$  that admits perrotationally symmetric molecules (see Tab. II).

The set of holonomies for closed paths starting and ending at a particular *base point*  $\mathbf{a}(0)$  forms a group called the *holonomy group* at that point. It is sufficient to know the holonomy group at the identity base point,

$\mathbf{a}(0) = \mathbf{e}$ , to obtain the group at all other basepoints. This is because the space  $\text{SO}(3)$  admits a path connecting any two points, so if we know the holonomy group at  $\mathbf{e}$ , we can obtain other holonomy groups by shifting via lab-based rotations  $\vec{X}_{\mathbf{g}}$  (for some  $\mathbf{g}$ ) to some other desired base point [100, Eq. (16)].

We verify that the Berry connection from Eq. (121) is zero for all spaces considered in this work. In Sec. XD, we prove this claim for some cases either via a brute-force analytical calculation or via symmetry arguments, and provide numerical evidence for the rest of the cases. Our results are summarized in Table VI.

Since the work on the connection is technical, we assume the connection is zero and proceed directly to calculating the monodromy in the next subsection. Given such a locally flat connection, the holonomy group is equal to the *monodromy group* — the group formed by all monodromies.

### C. Nontrivial monodromy

Fixing  $\mathbf{a}(0) = \mathbf{e}$ , we begin with the “identity” coset subspace from Eq. (110),

$$|\mathbf{a} = \mathbf{e}, \mu\rangle = \sum_{J \downarrow \Gamma} \sum_{|m| \leq J} \sqrt{\frac{(2J+1)/\mathfrak{d}}{8\pi^2/|\mathbf{G}|}} \sum_{\kappa=1}^{\mathfrak{m}(J)} D_{m;\mu\kappa}^J(\mathbf{e}) |_{m\kappa}^J, \quad (123)$$

where  $\mu \in \{1, 2, \dots, \mathfrak{d}\}$ . We consider paths obtained by applying lab-based rotations in the symmetry group, i.e.,  $\vec{X}_{\mathbf{g}}$  for any  $\mathbf{g} \in \mathbf{G}$ . Such rotations parameterize a “direct” path (w.r.t. some metric on the group) from  $\mathbf{a}(0) = \mathbf{e}$  to  $\mathbf{a}(1) = \mathbf{g}$ . Since the underlying molecule is  $\mathbf{G}$ -symmetric, such paths are in fact closed in the coset space despite  $\mathbf{g} \neq \mathbf{e}$ .

For example, a  $\pi$ -rotation around an axis perpendicular to the primary axis of  $\text{H}_2$  exchanges the molecule’s nuclei and yields a non-contractible path in its position state space,  $\text{SO}(3)/\text{D}_{\infty} = \text{RP}^2$ . Such a path would be considered open if the nuclei were distinguishable, but it is instead closed in the state space because the nuclei are *indistinguishable*. This rotation maps the spatial coordinates of one nucleus to those of the other, but acts purely on the rotational factor and *does not* permute any nuclear-spin factors.

When the connection  $A = 0$ , the monodromy for any other path between  $\mathbf{e}$  and  $\mathbf{g}$  is the same as that for the “direct” path from  $\mathbf{e}$  to  $\mathbf{g}$  since the monodromy is independent of smooth path deformations [99, 100].

Applying  $\vec{X}_{\mathbf{g}}$  to the state from Eq. (123), we recall from Eq. (19a) that lab-based rotations act on the  $|_m^J\rangle$  factor of each rotational state,

$$\vec{X}_{\mathbf{g}} |_{m\kappa}^J = \sum_{|n| \leq J} D_{nm}^J(\mathbf{g}) |_{n\kappa}^J. \quad (124)$$

molecule	symmetry	species	$\mathfrak{d}$	connection		monodromy	
				flat	reason	$\mathbf{G}_{\text{mono}}$	non-Ab.
$\text{C}_N$		$\text{A}, \text{A}^*$	1	✓	analytics	$\text{C}_1$	
		$\text{B}, \text{B}^*$	1	✓	analytics	$\text{C}_2$	
		${}^j\text{E}_i, {}^j\text{E}_i^*$	1	✓	analytics	$\text{C}_M$	
$\text{D}_N$		$\text{A}, \text{A}_1, \text{A}_1^*$	1	✓	symmetry	$\text{C}_1$	
		$\text{A}_2, \text{A}_2^*$	1	✓	symmetry	$\text{C}_2$	
		$\text{B}_i, \text{B}_i^*$	1	✓	symmetry	$\text{C}_2$	
		$\text{E}_1, \text{E}_1^*$	2	✓	analytics	$\text{D}_N$	☆
		$\text{E}_{i>1}, \text{E}_{i>1}^*$	2	✓	analytics	$\text{D}_M$	★
$\text{D}_{\infty}$		$\text{A}_1, \text{A}_1^*$	1	✓	symmetry	$\text{C}_1$	
		$\text{A}_2, \text{A}_2^*$	1	✓	symmetry	$\text{C}_2$	
$\text{T}$		$\text{A}$	1	✓	symmetry	$\text{C}_1$	
		${}^j\text{E}$	1	✓	symmetry	$\text{C}_3$	
		$\text{T}$	3	✓	numerics	$\text{T}$	☆
$\text{O}$		$\text{A}_1, \text{A}_1^*$	1	✓	symmetry	$\text{C}_1$	
		$\text{A}_2, \text{A}_2^*$	1	✓	symmetry	$\text{C}_2$	
		$\text{E}, \text{E}^*$	2	✓	symmetry	$\text{D}_3$	★
		$\text{T}_1, \text{T}_1^*$	3	✓	numerics	$\text{O}$	☆
		$\text{T}_2, \text{T}_2^*$	3	✓	numerics	$\text{O}$	★
$\text{I}$		$\text{A}$	1	✓	symmetry	$\text{C}_1$	
		$\text{T}_1$	3	✓	numerics	$\text{I}$	☆
		$\text{T}_2$	3	✓	symmetry	$\text{I}$	★
		$\text{G}$	4	✓	numerics	$\text{I}$	★
		$\text{H}$	5	✓	numerics	$\text{I}$	★

TABLE VI. Table listing reasons why the Berry connection (122) is proven to be locally flat as well as the monodromy group  $\mathbf{G}_{\text{mono}}$  (127) for the perrotationally symmetric molecular species from Table II. The species  $\text{s}^*$  has the same monodromy group as  $\text{s}$  since the rotational states of both transform under the same induced representation,  $\text{s} \uparrow \text{SO}(3)$ . The parameter  $M = \text{GCD}(N, i)$  for the groups  $\text{C}_M$  and  $\text{D}_M$ . Flatness of the connection in the cases marked by “✓” is proven by symmetry arguments (see Sec. XD 1), proven by explicit analytical calculation (see Sec. XD 2), or supported by numerical evidence (see Sec. XD 4). Species with a star in the last column have non-Abelian monodromy groups, while the fibers of those with a filled-in star also form protected encodings (see Sec. XI).

Plugging this in and simplifying yields

$$\begin{aligned} \vec{X}_{\mathbf{g}} |\mathbf{e}, \mu\rangle &= \sum_{J \downarrow \Gamma} \sqrt{\frac{(2J+1)/\mathfrak{d}}{8\pi^2/|\mathbf{G}|}} \sum_{\kappa=1}^{\mathfrak{m}(J)} \sum_{n,m} D_{nm}^J(\mathbf{g}) D_{m;\mu\kappa}^J(\mathbf{e}) |_{n\kappa}^J \\ &= \sum_{J \downarrow \Gamma} \sum_{|n| \leq J} \sqrt{\frac{(2J+1)/\mathfrak{d}}{8\pi^2/|\mathbf{G}|}} \sum_{\kappa=1}^{\mathfrak{m}(J)} D_{n;\mu\kappa}^J(\mathbf{g}) |_{n\kappa}^J \\ &= |\mathbf{g}, \mu\rangle. \end{aligned} \quad (125)$$

Since  $\mathbf{g}$  is a symmetry rotation, both  $|\mathbf{e}, \mu\rangle$  and  $|\mathbf{g}, \mu\rangle$  describe a molecule in the same physical position. Mathematically, both  $\mathbf{g}$  and  $\mathbf{e}$  are in the same (identity) coset,  $\mathbf{e}\mathbf{G} = \{\mathbf{h} \in \mathbf{G}\}$ .

However, the  $|\mathbf{g}, \mu\rangle$  state is representing the coset by  $\mathbf{g}$ , while the  $|\mathbf{e}, \mu\rangle$  state is using the identity  $\mathbf{e}$ . We have to pick *one* parameterization to be consistent with our

expression of the holonomy, and we pick the representative of each coset to be the element closest to the identity (w.r.t. to some metric on the group). Given such a parameterization, we have to re-express  $|\mathbf{g}, \mu\rangle$  in terms of  $|\mathbf{e}, \mu\rangle$ .

Applying Eq. (106) and using the fact that  $\Gamma^{\nu\mu*}(\mathbf{g}) = \Gamma^{\mu\nu}(\mathbf{g}^{-1})$ , we obtain

$$\begin{aligned} |\mathbf{g}, \mu\rangle &= \sum_{J \downarrow \Gamma} \sum_{|n| \leq J} \sqrt{\frac{(2J+1)/\mathfrak{d}}{8\pi^2/|\mathbf{G}|}} \sum_{\kappa=1}^{m(J)} \sum_{\nu=1}^{\mathfrak{d}} D_{n;\nu\kappa}^J(\mathbf{e}) \Gamma^{\nu\mu*}(\mathbf{g}) |_{n\kappa}^J \rangle \\ &= \sum_{\nu=1}^{\mathfrak{d}} \Gamma^{\mu\nu}(\mathbf{g}^{-1}) |\mathbf{e}, \nu\rangle, \end{aligned} \quad (126)$$

resulting in an operation on the fiber degrees of freedom  $\{|\mu\rangle\}$ . This change in the internal state is precisely the monodromy, which in this case realizes the  $\Gamma$  irrep of the symmetry group.

The above is true for any  $\mathbf{g} \in \mathbf{G}$ , so there are at most  $|\mathbf{G}|$  different types of monodromies. The actual number of distinct monodromies is equal to the number of distinct irrep elements. For example, in the case of rotationally symmetric molecules, all monodromies are +1.

**Example 37** (rotationally symmetric molecules). In these cases,  $\mathbf{G}$  is any group, but the induced representation is induced by the trivial irrep,  $\Gamma = \mathbf{A}$ . The states  $|\mathbf{a}, \mu\rangle$  reduce to the coset states  $|\mathbf{a}\rangle$  from Eq. (70). The fiber is one-dimensional ( $\mathfrak{d} = 1$ ), so there is no  $\mu$  index. Since  $\Gamma(\mathbf{g}) = \mathbf{A}(\mathbf{g}) = 1$  for any  $\mathbf{g}$ , the states  $|\mathbf{a} = \mathbf{g}\rangle$  and  $|\mathbf{a} = \mathbf{e}\rangle$  are directly identified, and there is no monodromy.

The above applies also to the asymmetric case, for which  $\mathbf{G} = \mathbf{C}_1$ , and any perrotationally symmetric species for which  $\Gamma$  is the trivial irrep. Hence, the monodromy group in the first line of each symmetry group in Table VI is the trivial group,  $\mathbf{G}_{\text{mono}} = \mathbf{C}_1$ .

On the other hand, perrotationally symmetric molecular species exhibit nontrivial monodromy for all  $\Gamma$  but the trivial one. Their monodromy group is the group formed by the distinct elements  $\{\Gamma(\mathbf{g}), \mathbf{g} \in \mathbf{G}\}$ . This is a normal subgroup of  $\mathbf{G}$ , obtained by taking the quotient of  $\mathbf{G}$  by the kernel of  $\Gamma$ ,

$$\mathbf{G}_{\text{mono}} = \mathbf{G} / \ker \Gamma, \quad (127)$$

where  $\ker \Gamma$  is the subset of elements of  $\mathbf{G}$  which evaluate to the identity in the  $\Gamma$  irrep.

**Example 38** (water,  $\mathbf{B}^*$  ortho species). This species, with symmetry group  $\mathbf{G} = \mathbf{C}_2$  and irrep  $\Gamma = \mathbf{B}$ , admits the simplest nontrivial monodromy. The irrep is one-dimensional, so there is no  $\mu$  index. The only non-identity symmetry rotation,  $\mathbf{g} = (00\pi)$  in the Euler-angle prescription, exchanges the two hydrogen nuclei and evaluates to  $-1$  in the  $\mathbf{B}$  irrep (see Example 32). This yields a monodromy of  $-1$ , which is not present in the para species since  $\Gamma$  is trivial for that species. The monodromy group is the symmetry group itself,  $\mathbf{G}_{\text{mono}} = \mathbf{C}_2$ .

The  $-1$  monodromy can alternatively be derived using the coset-state expression from Eq. (95). Beginning with the identity coset state,  $\mathbf{a} = \mathbf{e} = (000)$ , and applying the symmetry rotation yields

$$\begin{aligned} \vec{X}_{(00\pi)} |(000)\rangle &= \vec{X}_{(00\pi)} \frac{1}{\sqrt{2}} (|r = (000)\rangle - |r = (00\pi)\rangle) \\ &= \frac{1}{\sqrt{2}} (|r = (00\pi)\rangle - |r = (000)\rangle) \\ &= -|(000)\rangle. \end{aligned} \quad (128)$$

Above, we continue to abuse notation and use a rotation's Euler-angle parameterization as a stand-in for the rotation  $\mathbf{r}$  (or  $\mathbf{a}$ ) itself.

**Example 39** (deuterated hydrogen,  $\mathbf{A}_2$  para species). The coset states of this  $\mathbf{D}_\infty$ -symmetric molecule are labeled by points in the projective plane,  $\text{SO}(3)/\mathbf{D}_\infty = \mathbf{RP}^2$  (see Example 34). The  $\mathbf{A}_2$  irrep is one-dimensional, so there is no  $\mu$  index in the position states  $|\mathbf{a}\rangle$  [see Eq. (98)].

A  $\pi$ -rotation around any equatorial axis yields a monodromy of  $-1$ , while the  $\mathbf{C}_\infty$  subgroup of  $\mathbf{z}$ -axis rotations is mapped to  $+1$ . The monodromy group is  $\mathbf{G}_{\text{mono}} = \mathbf{D}_\infty / \mathbf{C}_\infty = \mathbf{C}_2$ . This is the same monodromy group as that for the  $\mathbf{A}_2^*$  (ortho) species of ordinary  $\text{H}_2$  since the rotational state subspace —  $\mathbf{A}_2 \uparrow \text{SO}(3)$  — is the same for both species.

We easily extract the monodromy using momentum states. The identity position state from Eq. (98) is

$$|\mathbf{a} = \mathbf{e}\rangle = \sum_{J \text{ odd}} \sqrt{\frac{2J+1}{2\pi}} |_0^J \rangle. \quad (129)$$

Applying a  $\pi$ -rotation around the  $\mathbf{y}$  axis and using the fact that  $\vec{X}_{(0\pi 0)} |_0^J \rangle = (-1)^J |_0^J \rangle$  yields the  $-1$  phase. A  $\pi$ -rotation around any equatorial axis yields the same phase since such a rotation can be expressed as a product of  $\vec{X}_{(0\pi 0)}$  and a rotation around the  $\mathbf{z}$  axis.

In contrast, position states of ortho deuterium and para hydrogen are of the same form as above, except that only even momenta are present. The monodromy for those cases is trivial.

**Example 40** (ammonia,  ${}^2\text{E}$  species). This species, with symmetry group  $\mathbf{G} = \mathbf{C}_3$  and irrep  $\Gamma = {}^2\text{E}$ , is the simplest to realize a monodromy that is not  $\pm 1$ , i.e., that is not related to Bose/Fermi spin statistics.

The  ${}^2\text{E}$  irrep is one-dimensional, so there is no  $\mu$  index in the position states  $|\mathbf{a}\rangle$  [see Eq. (98)]. The irrep evaluates to third roots of unity and has a trivial kernel, yielding the monodromy group  $\mathbf{G}_{\text{mono}} = \mathbf{C}_3$ . The  $\mathbf{a} = \mathbf{e} = (000)$  position state transforms under a symmetry rotation as

$$\begin{aligned} \vec{X}_{00 \frac{2\pi}{3}} |(000)\rangle &= \sum_{p=0}^2 e^{-i \frac{2\pi}{3} p} |r = (0, 0, \frac{2\pi}{3} p - \frac{2\pi}{3})\rangle \\ &= e^{-i \frac{2\pi}{3}} |(000)\rangle. \end{aligned} \quad (130)$$

**Example 41** (boron trifluoride,  $\text{E}$  species). Per Example 20, this perrotationally  $\mathbf{D}_3$ -symmetric species admits

a  $\mathfrak{d} = 2$ -dimensional fiber — the simplest fiber with non-unity dimension. Rotations permuting its three fluorine nuclei realize the group's two-dimensional irrep E from Eq. (49) via monodromy.

**Example 42** (methane, T species). Per Example 21, the position state space of methane is parameterized by the octahedral space  $\text{SO}(3)/\Gamma$ , with fiber degrees of freedom  $|\mu\rangle$  with  $\mu \in \{1, 2, 3\}$ . Rotations permuting its four hydrogen nuclei realize the group's three-dimensional irrep T via monodromy.

**Example 43** ( $^{13}\text{C}_{60}$  fullerene, H species). Per Example 24, the position state space of isotopic fullerene is parameterized by the Poincare dodecahedral space  $\text{SO}(3)/I$ , with fiber degrees of freedom  $|\mu\rangle$  with  $\mu \in \{1, 2, 3, 4, 5\}$ . Rotations permuting its sixty hydrogen nuclei realize the group's five-dimensional irrep H via monodromy. This irrep has a trivial kernel, so the monodromy group is I.

The remaining species, with exception of the trivial-irrep species, also realize the entire icosahedral group as their monodromy group. This is because this group has no normal subgroups other than itself and the trivial group, which implies that every non-trivial irrep must have trivial kernel.

#### D. Locally flat connection

We proceed to simplify the expression for the connection in Eq. (122). The denominator is a function of state normalizations, which can be simplified to the formal sum

$$\langle a, \mu | a, \mu \rangle = \sum_{J \downarrow \Gamma} \sum_{|m| \leq J} \frac{(2J+1)/\mathfrak{d}}{8\pi^2/|\mathcal{G}|} \sum_{\kappa=1}^{m(J)} D_{m;\mu\kappa}^{J*}(a) D_{m;\mu\kappa}^J(a) \quad (131a)$$

$$= \sum_{J \downarrow \Gamma} \frac{(2J+1)/\mathfrak{d}}{8\pi^2/|\mathcal{G}|} \sum_{\kappa=1}^{m(J)} \langle \mu\kappa | D^J(a^{-1}a) | \mu\kappa \rangle \quad (131b)$$

$$= \sum_{J \downarrow \Gamma} \frac{(2J+1)/\mathfrak{d}}{8\pi^2/|\mathcal{G}|} m(J). \quad (131c)$$

This sum is formal because it does not converge — the position states are not normalizable — but this will not be relevant until we perform numerical calculations in Sec. (XD 4). For now, we merely keep in mind that the sum is independent of fiber index  $\mu$ .

The numerator is simplified to the following form,

$$\langle a, \mu | \partial a, \nu \rangle = \sum_{J \downarrow \Gamma} \frac{(2J+1)/\mathfrak{d}}{8\pi^2/|\mathcal{G}|} \sum_{\kappa=1}^{m(J)} \langle \mu\kappa | D^{J\dagger}(a) \partial D^J(a) | \nu\kappa \rangle \quad (132a)$$

$$= -i \sum_{\mathbf{q}} \partial w_{\mathbf{q}}(a) \sum_{J \downarrow \Gamma} \frac{(2J+1)/\mathfrak{d}}{8\pi^2/|\mathcal{G}|} \sum_{\kappa=1}^{m(J)} \langle \mu\kappa | L_{\mathbf{q}}^J | \nu\kappa \rangle, \quad (132b)$$

where we expand the angular velocity matrix  $D^\dagger \partial D$  in terms of  $\text{SO}(3)$  angular momentum generators  $L_{\mathbf{q}}^J$  with  $\mathbf{q} \in \{\mathbf{x}, \mathbf{y}, \mathbf{z}\}$  and coordinate vector  $\partial w_{\mathbf{q}}(a)$ .

Plugging the numerator (132) and denominator (131) into the connection Eq. (122) yields the expansion

$$A_{\mu\nu}(a) = \frac{\mathfrak{d}}{|\mathcal{G}|} \sum_{\mathbf{q}} \partial w_{\mathbf{q}}(a) \frac{\sum_{J \downarrow \Gamma} (2J+1) A_{\mu\nu}^{\mathbf{q},J}}{\sum_{J \downarrow \Gamma} (2J+1) m(J)}, \quad (133)$$

with two expressions for the  $J$ -dependent component,

$$A_{\mu\nu}^{\mathbf{q},J} = \frac{|\mathcal{G}|}{\mathfrak{d}} \sum_{\kappa=1}^{m(J)} \langle \mu\kappa | L_{\mathbf{q}}^J | \nu\kappa \rangle \quad (134a)$$

$$= \sum_{\mathbf{g} \in \mathcal{G}} \Gamma^{\nu\mu}(\mathbf{g}) \text{tr}(D^J(\mathbf{g}) L_{\mathbf{q}}^J). \quad (134b)$$

The second expression is obtained by expressing the sum over  $\kappa$  as a projection onto the  $\nu, \mu$ th matrix element of all copies of  $\Gamma$  present for a given angular momentum [250, Eq. (2.63)][3, Eq. (5.5.20)].

For each  $J$ , the component  $A_{\mu\nu}^{\mathbf{q},J}$  can be thought of as a three-dimensional vector (with components indexed by  $\mathbf{q}$ ) of  $\mathfrak{d}$ -dimensional matrices (with elements indexed by  $\mu, \nu$ ). Since  $\sum_{\mathbf{q}} \partial w_{\mathbf{q}}(a) A_{\mu\nu}^{\mathbf{q},J}$  generates a unitary holonomy,  $A^{\mathbf{q},J}$  must be an element of the Lie algebra of the unitary group  $\text{U}(\mathfrak{d})$ .

In Sec. XD 1, we show that symmetries constrain  $A^{\mathbf{q},J}$  to lie in particular Lie subalgebras and, in some cases, to be identically zero. In Sec. XD 2, we calculate  $A_{\mu\nu}^{\mathbf{q},J}$  by hand for certain cases. In Sec. XD 4, we numerically evaluate the entire sum ratio  $A_{\mu\nu}^{\mathbf{q}}$  for the remaining cases.

##### 1. Symmetries of the connection

Certain combinations of groups and irreps yield a connection of zero for each momentum  $J$ , which can be proven using various symmetry arguments.

Suppressing the  $J$  index for the component from Eq. (134b), let us define the following trace quantity,

$$A^{\mathbf{q}} = \sum_{\mu=1}^{\mathfrak{d}} A_{\mu\mu}^{\mathbf{q},J} = \sum_{\mathbf{g} \in \mathcal{G}} \chi_{\Gamma}(\mathbf{g}) \text{tr}(D^J(\mathbf{g}) L_{\mathbf{q}}^J), \quad (135)$$

where  $\chi_{\Gamma}(\mathbf{g})$  is the character of  $\mathbf{g}$  in the  $\Gamma$  irrep. This quantity is invariant under  $\mathbf{g} \rightarrow \mathbf{h}\mathbf{g}\mathbf{h}^{-1}$  for any  $\mathbf{h} \in \mathcal{G}$ .

To show this, we use the fact that characters are invariant under conjugation,  $\chi(\mathbf{h}\mathbf{g}\mathbf{h}^{-1}) = \chi(\mathbf{g})$ , and that the vector  $(L_{\mathbf{x}}^J, L_{\mathbf{y}}^J, L_{\mathbf{z}}^J)$  for any  $J$  transforms under the defining rotation-matrix representation  $R$  of  $\text{SO}(3)$  (also called the *adjoint representation* [275]),

$$D^J(\mathbf{h}^{-1}) L_{\mathbf{q}}^J D^J(\mathbf{h}) = \sum_{\mathbf{r}} R_{\mathbf{qr}}(\mathbf{h}) L_{\mathbf{r}}^J. \quad (136)$$

Above,  $R_{\mathbf{qr}}(\mathbf{h})$  are real rotation-matrix elements of the rotation corresponding to  $\mathbf{h}$ .



Letting  $g \rightarrow hgh^{-1}$  and using the above facts,

$$A^{\mathbf{q}} = \sum_{g \in G} \chi_{\Gamma}(hgh^{-1}) \text{tr}(D^J(hgh^{-1})L_{\mathbf{q}}^J) = \sum_{\mathbf{r}} R_{\mathbf{qr}}(h)A^{\mathbf{r}}. \quad (137)$$

This formula is independent of both  $\Gamma$  and  $J$ , so any consequences of it must hold for all irreps and momenta.

Explicitly expressing the connection in vector form,

$$|A\rangle = A^{\mathbf{x}}|\mathbf{x}\rangle + A^{\mathbf{y}}|\mathbf{y}\rangle + A^{\mathbf{z}}|\mathbf{z}\rangle = \sum_{\mathbf{q}} A^{\mathbf{q}}|\mathbf{q}\rangle. \quad (138)$$

Such a vector is invariant under the adjoint representation of  $G \subset \text{SO}(3)$ ,

$$R(h)|A\rangle = \sum_{\mathbf{q}, \mathbf{r}} A^{\mathbf{q}} R_{\mathbf{rq}}(h)|\mathbf{r}\rangle \quad (139a)$$

$$= \sum_{\mathbf{r}} A^{\mathbf{r}}|\mathbf{r}\rangle = |A\rangle, \quad (139b)$$

implying that  $|A\rangle$  transforms according to the trivial irrep  $\mathbf{A}$  of  $G$ .

The main consequence of the above invariance occurs for groups for which the adjoint representation of  $\text{SO}(3)$  (which is isomorphic to the  $J=1$  irrep) does *not* branch to trivial  $G$ -irrep,

$$J=1 \not\subset \mathbf{A}. \quad (140)$$

In other words, if the trivial  $G$ -irrep is not present in the adjoint representation,  $|A\rangle$  must be the zero vector, i.e.,  $A^{\mathbf{q}} = 0$ . Equation (140) holds for groups  $G \in \{\text{D}_N, \text{D}_{\infty}, \text{T}, \text{O}, \text{I}\}$ .

For 1D irreps  $\Gamma$ ,  $A^{\mathbf{q}} = 0$  means that the entire connection is zero. This concludes our proof of local flatness for all species whose rotational states transform according to representations induced by  $\Gamma$ . We have marked such cases by “symmetry” in Table VI.

For irreps of higher dimension, the tracelessness of  $A^{\mathbf{q}}$  means that the holonomy does not contain a global  $\text{U}(1)$  component, restricting  $A_{\mu\nu}^{\mathbf{q},J}$  to be an element of  $\text{SU}(\mathfrak{d})$  (as opposed to  $\text{U}(\mathfrak{d})$ ).

Another useful piece of information is obtained for groups  $\text{O}$  and  $\text{I}$  by considering higher-order invariances. We construct nine-dimensional and 27-dimensional vectors, respectively,

$$|A_2\rangle = \sum_{\mathbf{q}, \mathbf{r}} \text{tr}_{\Gamma}(A^{\mathbf{q}}.A^{\mathbf{r}})|\mathbf{q}, \mathbf{r}\rangle \quad (141a)$$

$$|A_3\rangle = \sum_{\mathbf{q}, \mathbf{r}, \mathbf{s}} \text{tr}_{\Gamma}(A^{\mathbf{q}}.A^{\mathbf{r}}.A^{\mathbf{s}})|\mathbf{q}, \mathbf{r}, \mathbf{s}\rangle, \quad (141b)$$

where the product denoted by “.” is over the irrep, i.e.,

$$\text{tr}_{\Gamma}(A^{\mathbf{q}}.A^{\mathbf{r}}) = \sum_{\mu, \nu=1}^{\mathfrak{d}} A_{\mu\nu}^{\mathbf{q},J} A_{\nu\mu}^{\mathbf{r},J} \quad (142a)$$

$$\text{tr}_{\Gamma}(A^{\mathbf{q}}.A^{\mathbf{r}}.A^{\mathbf{s}}) = \sum_{\mu, \nu, \sigma=1}^{\mathfrak{d}} A_{\mu\nu}^{\mathbf{q},J} A_{\nu\sigma}^{\mathbf{r},J} A_{\sigma\mu}^{\mathbf{s},J}. \quad (142b)$$

These vectors are invariant under tensor products of the adjoint representation,

$$R^{\otimes j}(h)|A_j\rangle = |A_j\rangle \quad \text{for} \quad j \in \{2, 3\}. \quad (143)$$

In other words,  $|A_j\rangle$  transforms under the trivial irrep of the  $j$ th tensor-product representation  $R^{\otimes j}$  of  $G$ . This invariance can be naturally extended to higher  $j$ .

The groups  $\text{O}$  and  $\text{I}$  contain only one copy of their trivial irrep in each case. In other words, the second and third tensor product of the adjoint irrep branches to only one copy of the trivial  $\text{O}$  and  $\text{I}$  irrep, respectively,

$$1 \otimes 1 \downarrow \mathbf{A} \quad (144a)$$

$$1 \otimes 1 \otimes 1 \downarrow \mathbf{A}. \quad (144b)$$

Since we know the exact form of the rotation matrices  $R$ , we can determine the corresponding form of the irrep vector [141]. The form of this vector constrains the tracial components, respectively,

$$\text{tr}_{\Gamma}(A^{\mathbf{q}}.A^{\mathbf{r}}) \propto c\delta_{\mathbf{qr}} \quad (145a)$$

$$\text{tr}_{\Gamma}(A^{\mathbf{q}}.A^{\mathbf{r}}.A^{\mathbf{s}}) \propto c'\epsilon_{\mathbf{qrs}}, \quad (145b)$$

where  $c, c'$  are  $\mathbf{q}$ -independent constants, and  $\epsilon$  is the fully anti-symmetric tensor. These two constraints restrict  $A_{\mu\nu}^{\mathbf{q},J}$  to be an element of  $\text{SU}(2)$  [275] (as opposed to  $\text{SU}(\mathfrak{d})$ ) for the groups  $\text{O}$  and  $\text{I}$ .

For the remaining exceptional subgroup —  $\text{T}$  — we contend with looser constraints [141],

$$1 \otimes 1 \downarrow 2\mathbf{A} \quad (146a)$$

$$1 \otimes 1 \otimes 1 \downarrow \mathbf{A}, \quad (146b)$$

which are not sufficient to restrict  $A_{\mu\nu}^{\mathbf{q},J}$  to be inside  $\text{SU}(2)$  (although this is something that we observe numerically).

There are two more special cases that have zero connection component for each  $\mathbf{q}$  and  $J$  due to other types of symmetry.

First, a special symmetry of occurs for the two-dimensional  $\text{E}$  irrep of the octahedral group (cf. [212]). We embed the group into  $\text{SO}(3)$  such that this irrep maps to identity the rotations  $(\mathbf{x}, \pi)$ ,  $(\mathbf{y}, \pi)$ , and  $(\mathbf{z}, \pi)$ . Each of these rotations, which generate the  $\text{D}_2$  group, switches the sign of one of the three angular momentum generators,  $L_{\mathbf{q}}^J \rightarrow -L_{\mathbf{q}}^J$  for  $\mathbf{q} \in \{\mathbf{x}, \mathbf{y}, \mathbf{z}\}$ . This means that we are free to flip the sign of each connection component,  $A_{\mu\nu}^{\mathbf{q},J} = -A_{\mu\nu}^{\mathbf{q},J}$ , implying that the entire connection is zero for this case.

Second, the  $\text{T}_2$  irrep of  $\text{I}$  admits a property — automatic protection [215, 216] — which guarantees a zero connection component. Automatic protection occurs only for certain irreps of certain groups, e.g., a particular irrep of the double icosahedral group,  $2\text{I}$  [215, Thm. 4][216]. We verify that the same property holds for the  $\text{T}_2$  irrep of  $\text{I}$ .

## 2. Analytical results

The connection  $A_{\mu\nu}^{\mathbf{q},J}$  can be evaluated analytically in certain simple cases, such as when  $G = \text{C}_N$ . We pick this group to consist of rotations by multiples of  $2\pi/N$  around the  $\mathbf{z}$ -axis, but the result is basis-independent.

All  $C_N$ -irreps  $\{A, B, {}^jE_i\}$  are one-dimensional, so there are no  $\mu, \nu$  indices. The expression (134a) for the connection component simplifies to

$$A^{\mathbf{q}, J} = N \sum_{\kappa=1}^{m(J)} \langle \kappa | L_{\mathbf{q}}^J | \kappa \rangle. \quad (147)$$

Recalling Eq. (32),  $C_N$ -irrep states  $|\kappa\rangle$  correspond directly to asymmetric states  $|k\rangle$  for some  $k$ . The sum reduces to

$$A^{\mathbf{q}, J} = N \sum_{|k| \leq J} \delta_{ki}^{\text{mod } N} \langle k | L_{\mathbf{q}}^J | k \rangle, \quad (148)$$

where  $\delta_{ki}^{\text{mod } N} = 1$  when  $k \equiv i$  modulo  $N$ , and zero otherwise.

The value of  $i$  depends on the irrep, coming from the irrep label in the case of  $\Gamma = {}^1E_i$ . The value flips sign when  $\Gamma = {}^2E_i$ , it is zero for the trivial irrep A, and it is  $N/2$  for the B irrep (for which  $N$  is even).

Recalling expressions of the angular momentum matrices in the  $|k\rangle$  basis [146],  $L_{\mathbf{x}, \mathbf{y}}$  have nonzero entries only on the bands above and below the diagonal, meaning that  $A^{\mathbf{x}, J} = A^{\mathbf{y}, J} = 0$ . Plugging in  $L_{\mathbf{z}} = \sum_k |k\rangle k \langle k|$ , we see that the connection is an element of  $U_1$ ,

$$A^{\mathbf{q}, J} = \delta_{\mathbf{qz}} N \sum_{|k| \leq J} \delta_{ki}^{\text{mod } N} k. \quad (149)$$

The trivial irrep occurs whenever  $k \equiv 0$  modulo  $N$ , while the B irrep occurs for  $k \equiv N/2$ . Both cases have the property that  $k \equiv i$  if and only if  $-k \equiv i$  modulo  $N$  for  $i \in \{N, N/2\}$ , respectively. Therefore, the positive and negative  $k$  values cancel, yielding  $A^{\mathbf{q}, J} = 0$  for these irreps. This concludes our proof for flatness of connection for all A and B  $C_N$ -species; they are marked by “analytics” in the appropriate rows of Table VI.

The above quantity is not zero for the other irreps, so we have to consider the sum over all  $J$ . Plugging in the sum for the connection components from Eq. (149) into the formula for the connection in Eq. (133) yields

$$A^{\mathbf{q}} = \delta_{\mathbf{qz}} \frac{\sum_{J \geq i} (2J+1) \sum_{|k| \leq J} \delta_{ki}^{\text{mod } N} k}{\sum_{J \geq i} (2J+1) \sum_{|k| \leq J} \delta_{ki}^{\text{mod } N}}, \quad (150)$$

valid for the  ${}^1E_i$  irreps of  $C_N$  (with  $i \rightarrow -i$  for the  ${}^2E_i$  irreps). We find that this sum is also zero [280].

The same sum occurs for the two-dimensional  $E_i$  irreps of  $D_N$ , which we take to consist of rotations around the  $\mathbf{z}$  axis as before. Each copy is spanned by two states, and we have to be consistent with the order of the internal indices  $\mu, \nu$  across all copies. Irrep copies are spanned by states  $|k = \pm s\rangle$  for any positive  $s$  such that  $s \equiv \min(i, N-i)$  modulo  $N$ , but are spanned by  $|k = \mp s\rangle$  for any positive  $s$  such that  $s \equiv \max(i, N-i)$  modulo  $N$ . Given that off-diagonal elements  $A_{12}^{\mathbf{z}} = A_{21}^{\mathbf{z}} = 0$  by the same arguments as for the  $C_N$  case, calculating the diagonal elements  $A_{\mu\mu}^{\mathbf{z}}$  yields the sum from Eq. (150), up to an overall constant. We mark the appropriate  $C_N$  and  $D_N$  cases with “analytics” in Table VI.

### 3. Approximate states

All Berry connections, including both the ones we have calculated so far and the remaining ones marked by “numerics” in Table VI, can be calculated numerically using approximate normalizable versions of molecular position states. The approximate states defined below are straightforward generalizations of finite-energy GKP states [281, 282] and their molecular-code extensions [101, 178].

Regularization proceeds by applying a damping operator to the original position states,

$$|a, \mu\rangle \rightarrow e^{-\Delta \hat{J}^2/2} |a, \mu\rangle, \quad (151)$$

where the parameter  $\Delta \geq 0$ , and where

$$\hat{J}^2 = \sum_{J, m, k} J(J+1) |J_m, k\rangle \langle J_m, k| \quad (152)$$

is the total angular momentum operator squared. This type of regularization converts delta-function-like states  $|a, \mu\rangle$  into wavepackets in position space centered around the point  $\mathbf{a}$ . These states are no longer exactly orthogonal in the coset space, but their overlap is suppressed exponentially with  $1/\Delta^2$  (cf. [101]).

Approximate states remain infinite superpositions of momentum states, but are “regularized” in a way that makes them have finite normalization, finite mean angular momentum, and finite values for all higher-order moments in momentum. The damping operator commutes with all rotations because it is a function of the total angular momentum, so moments of the momentum reduce to ratios of sums that can be bounded. For example, the average momentum squared reduces to

$$\langle \hat{J}^2 \rangle = \frac{\sum_{J \downarrow \Gamma} e^{-\Delta J(J+1)} (2J+1) \mathbf{m}(J) J(J+1)}{\sum_{J \downarrow \Gamma} e^{-\Delta J(J+1)} (2J+1) \mathbf{m}(J)}. \quad (153)$$

Each sum is finite since each multiplicity  $\mathbf{m} \leq 2J+1$ .

### 4. Numerical evidence

Connections for the remaining multi-dimensional irreps of  $G \in \{\mathbf{T}, \mathbf{O}, \mathbf{I}\}$  are neither zero for each momentum nor simple to handle analytically, so we calculate them numerically. The symmetry arguments in Sec. XD 1 dictate that we only need to determine some minimal set of matrix elements  $\{\mu, \nu\}$  since all other elements are determined from them due to the connection belonging to a particular Lie algebra.

Substituting the approximate states from Eq. (151) yields a modified, convergent ratio of sums in the connection formula (133),

$$\frac{\sum_{J \downarrow \Gamma} e^{-\Delta J(J+1)} (2J+1) A_{\mu\nu}^{\mathbf{q}, J}}{\sum_{J \downarrow \Gamma} e^{-\Delta J(J+1)} (2J+1) \mathbf{m}(J)}, \quad (154)$$

which we calculate numerically to go to zero in the  $\Delta \rightarrow 0$  limit. We mark these cases with “numerics” in Table VI.

We observe that all calculated connections converge to zero in a way that is exponential in a power of  $1/\Delta$  (cf. [101, 178]), demonstrating a robustness of our holonomy to finite-energy effects.

### E. Flat connection conjecture

Induced representation state spaces,  $\Gamma \uparrow K$  for Lie group  $K$  and  $G$ -irrep  $\Gamma$ , are examples of  $G$ -bundles — fiber bundles whose base space is  $K/G$  and whose fiber houses the irrep. Such bundles come with their own canonical or  $G$ -connection,  $A^G$ . The Berry connection  $A$  can be expressed as a sum of two terms, one of which is the  $G$ -connection [42, Eq. (4.2)],

$$A = A^G + A^\perp. \quad (155)$$

If we are dealing with Lie groups, then  $A^G$  is a projection of  $K$ 's Maurer-Cartan form into  $G$ 's Lie algebra, while  $A^\perp$  is the same projection into the remaining Lie algebra generators of  $K$ .

The Berry and  $G$ -connections are generally not equal due to the difference term  $A^\perp$ . We observe that a locally flat Berry connection seems to be synonymous with a locally flat  $G$ -connection. In other words, all three terms in Eq. (155) wind up being zero whenever either  $A$  or  $A^G$  is zero.

Locally flat  $G$ -connections on  $G$ -bundles are in one-to-one correspondence with irreps  $\rho$  of the fundamental group  $\pi_1(K/G)$  of the underlying coset space [206, Lemma 1]. These irreps generate different types of monodromies occurring after closed non-contractible paths [179, Eq. (1)]. They induce faithful irreps of their corresponding monodromy groups,  $\pi_1(K/G)/\ker \rho$ .

Per Eq. (126), our (Berry) monodromies are *also* generated by irreps  $\Gamma$ , but of a *different* group, namely,  $G$ . These irreps induce faithful irreps of their corresponding monodromy groups,  $G/\ker \Gamma = G_{\text{mono}}$ .

When the two monodromy groups are equal, the two irreps are related to each other,  $G/\ker \Gamma \cong \pi_1(K/G)/\ker \rho$ . In other words, given a  $G$ -irrep  $\Gamma$ , there exists a  $\pi_1$ -irrep  $\rho$  such that above holds, and visa versa. The  $G$ -connection is flat in this case [206, Lemma 1], but the Berry connection can nevertheless be nonzero due to the additional term  $A^\perp$ .

We observe that, not only  $A^G$ , but *all* terms in Eq. (155) are zero when the two monodromy groups are isomorphic, leading us to make the following conjecture.

**Conjecture.** *Given the state space  $\Gamma \uparrow K$ , the position-state Berry connection is locally flat iff there exists a  $\pi_1(K/G)$ -irrep  $\rho$  such that*

$$\frac{G}{\ker \Gamma} \cong \frac{\pi_1(K/G)}{\ker \rho}. \quad (156)$$

We corroborate this conjecture with some examples; see Refs. [42, 155, 217–220] for more examples.

**Example 44** ( $K = \text{SO}(3)$ ,  $G = C_\infty$ ). The coset space is the two-sphere,  $K/G = S^2$ , whose fundamental group is trivial,  $\pi_1(S^2) = C_1$ . Therefore,  $\rho = A$ , the trivial irrep.

When the  $C_\infty$ -irrep  $\Gamma$  is trivial, the monodromy group is also trivial per Eq. (126), and Eq. (156) becomes

$$\frac{C_\infty}{C_\infty} \cong C_1 \cong \frac{C_1}{C_1}. \quad (157)$$

This corresponds to a locally flat Berry connection per Table VI.

All other  $C_\infty$ -irreps  $\Gamma = \lambda$  (with  $\lambda$  a non-zero integer) have a kernel of  $C_{|\lambda|}$ . In such cases, repeating the analysis behind Eq. (126) yields a monodromy group of  $C_\infty/C_{|\lambda|} \cong C_\infty$ , and the right-hand side of Eq. (156) *cannot* be satisfied. Per our conjecture, this means the Berry connection is nonzero. Indeed, these well-known cases describe a sphere with a “monopole” of  $\lambda$ , whose Berry phase depends on the area enclosed by the path [95]. In other contexts,  $\lambda \uparrow \text{SO}(3)$  is called the spin-weighted representation [283, Sec. 12.3][284].

**Example 45** ( $K = \text{SO}(3)$ ,  $G = D_\infty$ ). The coset space is the projective plane,  $K/G = \text{RP}^2$ , whose fundamental group is  $\pi_1(\text{RP}^2) = C_2$ . Therefore,  $\rho$  can be either the trivial irrep  $A$  or the sign irrep  $B$ .

When the  $D_\infty$ -irrep  $\Gamma$  is trivial, the monodromy group is also trivial, and Eq. (156) becomes

$$\frac{D_\infty}{D_\infty} \cong C_1 \cong \frac{C_2}{\ker \rho}. \quad (158)$$

This is satisfied by picking  $\rho$  to be trivial, and corresponds to a locally flat Berry connection per Table VI.

When  $\Gamma = A_2$  (the sign irrep), the monodromy group is non-trivial. Equation (156) becomes

$$\frac{D_\infty}{C_\infty} \cong C_2 \cong \frac{C_2}{\ker \rho}, \quad (159)$$

which is satisfied for  $\rho = B$ . This corresponds to locally flat Berry connection per Table VI.

All other two-dimensional irreps of  $D_\infty$  yield a monodromy group that is neither  $C_1$  nor  $C_2$ . We *cannot* satisfy Eq. (156) because we have run out of fundamental-group irreps  $\rho$ . Per our conjecture, these must a nonzero Berry connection. This can be verified by repeating the calculations of the previous subsection for this case.

**Example 46** ( $K = \text{SO}(3)$ ,  $G = I$ ). The coset space is  $\text{SO}(3)/I$ , whose fundamental group is the binary icosahedral group,  $\pi_1 = 2I$  [138].

Any non-trivial  $I$ -irrep  $\Gamma$  “lifts” to an irrep of  $2I$  by assigning the  $-1$   $2I$ -group element to the kernel. This yields an irrep of  $2I$  whose kernel is the double cover of that of  $\Gamma$ . Equation (156) is satisfied,

$$\frac{I}{\ker \Gamma} \cong I \cong \frac{2I}{2 \ker \Gamma}, \quad (160)$$

yielding a monodromy group that is non-trivial for any  $\Gamma \neq A$ . In all cases, we have verified that the Berry connection is locally flat (see Table VI), albeit mostly using numerics. The other finite subgroups of  $SO(3)$  follow similar behavior.

## XI. FIBER CODES

Following the notation of the previous sections, we define our encoding to be in the fiber degree of freedom of the “identity” orientation,  $\mathbf{a} = \mathbf{e}$ , of an entangled species  $\Gamma_{\text{rot}} \equiv \Gamma$  (i.e., whose irrep dimension  $\mathfrak{d} = \dim \Gamma > 1$ ). A basis of code states, or codewords, for this qudit encoding consists of position states (123)

$$|\bar{\mu}\rangle \propto |\mathbf{a} = \mathbf{e}, \mu\rangle \quad \text{for} \quad \mu \in \{1, 2, \dots, \mathfrak{d}\}. \quad (161)$$

We omit the residual nuclear  $|\chi\rangle$  factor from now on since we do not use it to store information.

The above encoding lies fully in a *single* molecular orientation  $\mathbf{e}$ , and we will show that this encoding is comparable to other encodings for asymmetric molecules whose codewords are superpositions of *several* molecular orientations [101].

Errors acting on the molecule can be grouped into two types — inter-species and intra-species. *Inter-species* errors cause the information to leak out of the  $\Gamma$  species into a different species of the same molecule. Such errors can, in principle, be detected by monitoring the other species. Some errors will also be correctable, but determining correctability requires developing a physical basis of inter-species operators — an open question from both the chemical and quantum-information perspectives that is outside the scope of this work (cf. [122]).

We focus on *intra-species* errors, which cause transitions within the given species. We generalize the noise operators from Ref. [101] for asymmetric and rotationally

$C_\infty$ -symmetric molecules to rotationally and perrotationally  $G$ -symmetric species.

### A. Intra-species noise operators

Intra-species operators can shift the position of the molecule by applying some lab-frame rotation  $\mathbf{r}$  and/or kick the molecule’s angular momentum by some amount  $J$ . General noise operators are products of position shifts  $\hat{X}$  and momentum kicks  $\hat{H}$ ,

$$\hat{E}_{m\kappa}^J(\mathbf{r}) = \sqrt{\frac{\mathfrak{d}}{|\mathbf{G}|}} \hat{X}_{\mathbf{r}} \hat{H}_{m\kappa}^J. \quad (162)$$

Here,  $J$ ,  $m$ , and  $\kappa$  are indices associated with the induced representation  $\Gamma \uparrow SO(3)$ , and only kicks by these specified values keep the system within the given species.

Above, the  $X$ -type operators are lab-frame rotations acting as

$$\hat{X}_{\mathbf{r}}|\mathbf{a}, \mu\rangle = \frac{1}{\sqrt{|\mathbf{G}|}} \sum_{\tau=1}^{\mathfrak{d}} s_{\tau} \sum_{\mathbf{g} \in \mathbf{G}} \Gamma^{\mu\tau}(\mathbf{g}) |\mathbf{r}\mathbf{g}\rangle |\tau\rangle, \quad (163a)$$

where, for convenience, we have expressed the codeword in its Zak form (103) in terms of  $SO(3)$  position states  $|\mathbf{r}\rangle$ . Here and for the remainder of this subsection, every ket that contains only **sans serif** text represents an  $SO(3)$  position state.

The  $Z$ -type momentum kicks are diagonal in the position-state basis,

$$\hat{H}_{m\kappa}^J|\mathbf{a}, \mu\rangle = H_{m\kappa}^J(\mathbf{a}, \mu)|\mathbf{a}, \mu\rangle, \quad (163b)$$

whose diagonal matrix elements are  $G$ -adapted harmonics (116). One can show these form an orthonormal basis for functions on the induced representation using the  $G$ -adapted orthogonality relation (117).

Products of shifts and kicks form a complete basis for the space of all physical operators on the species, meaning that any noise operator can be expanded as a sum of such products. To show this, we need to prove the following,

$$\int_{SO(3)} d\mathbf{r} \sum_{J \uparrow \Gamma} \sum_{|m| \leq J} \sum_{\kappa=1}^{m(J)} \langle \mathbf{a}, \mu | \hat{E}_{m\kappa}^J(\mathbf{r}) | \mathbf{b}, \nu \rangle \langle \mathbf{b}', \nu' | \hat{E}_{m\kappa}^J(\mathbf{r}) | \mathbf{a}', \mu' \rangle^* = \langle \mathbf{a}, \mu | \mathbf{a}', \mu' \rangle \langle \mathbf{b}, \nu | \mathbf{b}', \nu' \rangle, \quad (164)$$

for any coset representatives  $\mathbf{a}, \mathbf{a}', \mathbf{b}, \mathbf{b}' \in SO(3)/G$  and  $\Gamma$ -irrep elements  $\mu, \mu', \nu, \nu'$ .

Using the action (163) of the two types of noise operators, we first simplify the following matrix element to

$$\langle \mathbf{a}, \mu | \hat{E}_{m\kappa}^J(\mathbf{r}) | \mathbf{b}, \nu \rangle = \sqrt{\frac{\mathfrak{d}}{|\mathbf{G}|}} H_{m\kappa}^J(\mathbf{b}, \nu) \sum_{\mathbf{g} \in \mathbf{G}} \Gamma^{\nu\mu}(\mathbf{g}) \langle \mathbf{a}\mathbf{g}^{-1} | \mathbf{r}\mathbf{b} \rangle. \quad (165)$$

Then, we plug this into two places in the left-hand side of Eq. (164) and apply the  $G$ -adapted completeness rela-

tion (117), simplifying the left-hand side to

$$\langle \mathbf{b}, \nu | \mathbf{b}', \nu' \rangle \int_{SO(3)} d\mathbf{r} \frac{\mathfrak{d}}{|\mathbf{G}|} \sum_{\mathbf{g}, \mathbf{h} \in \mathbf{G}} \Gamma^{\nu\mu}(\mathbf{g}) \Gamma^{\nu'\mu'}(\mathbf{h}) \langle \mathbf{a}\mathbf{g}^{-1} | \mathbf{r}\mathbf{b} \rangle \langle \mathbf{r}\mathbf{b} | \mathbf{a}'\mathbf{h}^{-1} \rangle. \quad (166)$$

Finally, we notice that the outer product of position kets  $|\mathbf{r}\mathbf{b}\rangle$  yields the identity on  $SO(3)$  position-state space when combined with the integral over  $\mathbf{r}$ . Removing this identity, using Eq. (78), and applying Schur orthogonality over  $G$  completes the proof.



## B. Protected encodings

A fiber code (161) detecting intra-species operators  $\hat{E}$  satisfies [285]

$$\langle \bar{\nu} | \hat{E} | \bar{\mu} \rangle = c_{\hat{E}} \delta_{\mu\nu} \quad (167)$$

for all codeword labels  $\nu, \mu$ . In words, either the error causes the information to leave the code space (corresponding to  $c_{\hat{E}} = 0$ ) or the error acts as the identity on the codespace (up to the constant  $c_{\hat{E}}$ ). The constant can be infinite since we are using the idealized, non-normalizable position states as code states. Using approximate but normalized position states will yield finite constants, and intrinsic memory errors (due to the approximate code states not being exactly orthogonal) should be suppressed with the energy of the states by the same reasoning as that from Sec. XD3.

We can utilize our holonomy calculations from Sec. X to show that all but a measure-zero set of position shifts are detectable. Since all rotations  $\bar{X}_r$ , except for those in  $G$ , map the codeword to a different coset, any rotations *not* in the symmetry group will map the codeword to an error state that is orthogonal to the original codespace. In other words, intra-species noise operators satisfy

$$\langle \bar{\nu} | \hat{E}_{m\kappa}^J(r) | \bar{\mu} \rangle = 0 \quad \forall \quad r \notin G, \quad (168)$$

detecting all rotations except those in the symmetry group (which in turn form fault-tolerant monodromy gates). Moreover, rotations  $r \in \text{SO}(3)/G$  (i.e., those that are also coset representatives closest to the identity) are correctable since one can undo them by rotating back to the codespace without inducing a monodromy.

Protecting against momentum kicks requires picking a species for which transitions between momentum states require more than a single quantum of angular momentum. The set of momentum kicks  $\hat{H}_{m\kappa}^J$  for a given species  $\Gamma$  takes values in momenta  $J \downarrow \Gamma$ , i.e., those momenta which contain the species' irrep when restricted to the symmetry group (see Sec. VIII B). This set has a minimal element  $J_{\min}$ , and the corresponding species are immune to momentum kicks by  $J < J_{\min}$  since kick operators by such amounts do not exist within the species.

We catalogue all vector irreps with  $J_{\min} > 1$ , which consist of all vector irreps in Table VI excluding those that appear at  $J = 1$  (namely, the tetrahedral  $T$  and the octahedral and icosahedral  $T_1$  irreps). All such irreps yield fiber encodings that protect against both position shifts and momentum kicks and that require only a single molecular orientation. The corresponding molecular species are marked with a filled-in star in the table.

**Example 47** ( $D_N$  symmetry). Entangled molecular species with dihedral perrotational symmetry correspond to two-dimensional rotation irreps  $\Gamma = E_i$  for some  $i \geq 1$ . Branching rules [140] reveal that the  $i$ th irrep features first at angular momentum  $i$ , corresponding to  $J_{\min} = i$ . Fiber codes of such species are immune to momentum

kicks up to  $i - 1$  and encode a qubit (since  $\mathfrak{d} = 2$ ). Such codes also correct rotations in  $\text{SO}(3)/D_N$ .

The simplest case is  $D_5$  symmetry, whose group has two 2D irreps,  $E_1$  and  $E_2$ . The  $E_2$  species of such molecules is thus immune to single momentum kicks. Perrotationally  $D_5$ -symmetric molecules include pentagonal planar molecules like  $\text{XeF}_5^-$  as well as the cyclopentadienide molecule and the rather large pentaphenylcyclopentadienyl molecule.

Dihedral fiber codes are comparable in performance to dihedral molecular codes, which are based on nested groups  $D_{N/2} \subset D_N$  (for even  $N$ ) [101]. Both codes encode a qubit and correct rotations in  $\text{SO}(3)/D_N$ , but the number of detectable momentum kicks is never larger for fiber codes since the irrep index always satisfies  $i < N/2$  (with dihedral molecular codes detecting  $< N/2$  kicks). However, fiber codes are much less “quantum”: dihedral molecular codewords consist of a superposition of  $N/2$  position states of any asymmetric molecule, while dihedral fiber codewords consist of a *single* position state of an entangled perrotationally  $D_N$ -symmetric molecular species. Moreover, the dihedral fiber code admits a fault-tolerant dihedral gate set via monodromy (see Table VI), while the only fault-tolerant operation admitted by the molecular code is the logical- $X$  codeword permutation.

**Example 48** ( $O$  symmetry). The two-dimensional  $E$  and three-dimensional  $T_2$  irreps of the octahedral group both feature first at angular momentum  $J = 2$ , meaning that fiber codes of either species are immune to single momentum kicks. The codes encode a qubit and qutrit, respectively, and correct rotations in  $\text{SO}(3)/O$ . Examples include the  $E^*$  and  $T_2^*$  species of  $\text{SF}_6$ , respectively [21, 172, 286].

Octahedral fiber codes can be compared to qubit molecular codes based on nested subgroups  $T \subset O$ . Both codes protect against rotations in  $\text{SO}(3)/O$ , but the molecular code detects up to two momentum kicks, while either fiber code is immune to only a single kick. The molecular code consists of superpositions of 12 molecular positions, while the fiber code encodes using only one. Moreover, the octahedral fiber code admits either a fault-tolerant dihedral or octahedral gate set via monodromy (see Table VI), while the only fault-tolerant operation admitted by the molecular code is the logical- $X$  codeword permutation.

**Example 49** ( $I$  symmetry). The five-dimensional  $H$  irrep of the icosahedral group features first at momentum  $J = 2$ , meaning that its corresponding five-dimensional fiber encoding is immune to single momentum kicks. At  $J = 3$ , one encounters the three-dimensional  $T_2$  and four-dimensional  $G$  irreps, yielding respective qutrit and quartit fiber codes immune to single and double momentum kicks. All such codes can correct rotations in the Poincare sphere,  $\text{SO}(3)/I$ .

Icosahedral fiber codes can be compared to molecular codes based on nested subgroups  $T \subset I$ , which encode a five-dimensional qudit. Both codes protect against rotations in  $\text{SO}(3)/I$  and admit a fault-tolerant implementation

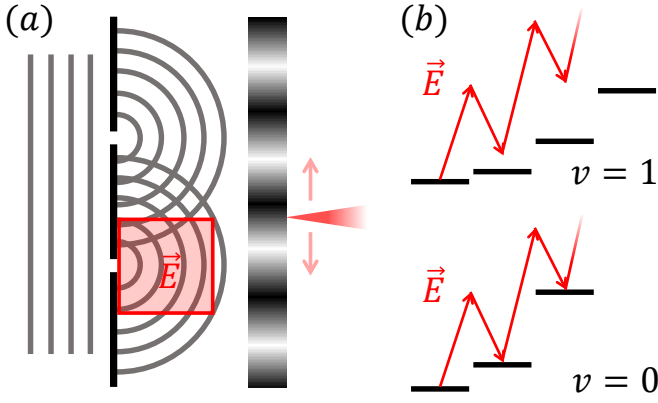


FIG. 10. (a) Sketch of the matter-wave diffraction approach to induce a monodromy. A single species of homonuclear diatomic (i.e., either para or ortho) is initialized in the span of states  $|J_{m=0}\rangle$  and diffracted by a double slit. Ultrafast laser pulses are applied to the lower arm (in the region outlined by the red square) to re-orient the molecules and induce a species-dependent monodromy of  $\pm 1$  (see Fig. 5 for details). The phase of the matter-wave interference fringes can be probed by monitoring the photo-ionization probability as a function of distance (red needle). (b) In an alternative proposal, a set of oriented molecules is driven by a  $\pi/2$ -pulse into a superposition of ground ( $v = 0$ ) and excited ( $v = 1$ ) vibrational states. The two states correspond to the two “arms” of an interferometer. The difference in rotational constants between ( $v = 0$ ) and ( $v = 1$ ) states makes one “arm” of the interferometer “dark” to the re-orienting pulse.

of the icosahedral gate group. The molecular code detects up to two momentum kicks, one more than the H-irrep and the same as the  $T_2$ -irrep and G-irrep fiber codes.

## XII. MONODROMY DETECTION VIA INTERFEROMETRY

We turn to the problem of detecting the monodromy phase of homonuclear diatomic species. One approach is molecular interferometry: conceptually, a cold beam of molecules of a particular symmetry species (e.g., ortho or para) is aligned in some fixed position state and then split into two “arms”. In practice, a fixed position state is difficult to realize, requiring a strong aligning field to be always present. We will comment on this further shortly. A lab-based rotation, as described earlier, is applied to just one of the two arms. Downstream, the two arms are then recombined, whereby they can interfere with each other. In practice, the two arms can be separated in real space using matter wave diffraction, or by using the internal degrees of freedom of the molecule such as vibrational or electronic states.

As mentioned in Sec. III F, initializing molecules in states other than position states can be used to simulate a monodromy. Initializing in the span of  $|J_{m=0}\rangle$  and applying an equatorial rotation also yields a  $\pm 1$  phase

(see Example 39), albeit a phase that can no longer be attributed to a monodromy in position-state space.

**Matter-wave diffraction** Conceptually, the matter wave diffraction is easier to visualize, but in practice may yield poorer signal and phase contrast due to loss of molecular flux at each “beamsplitter” step of the interferometer. In this approach, a beam of aligned molecules is incident on a double slit, whose two paths correspond to the arms of the interferometer [Fig. 10(a)].

Next, the molecules in the lower arm are rotated according to the stroboscopic sequence of ultrafast pulses described in Fig. 5. Hitting the molecule with an ultrafast pulse at every rotational revival time ( $T_{\text{rev}} = 2\pi/B \sim 10$  ps, with  $B$  the rotational constant) is experimentally challenging, as typical pulsed laser repetition rates are too low. Furthermore, realistic molecules can support only about 10 good rotational revivals prior to dephasing due to rovibrational coupling [158–160], so one cannot apply realigning pulses at arbitrarily large integer multiples of  $T_{\text{rev}}$ .

One solution is to split up the aligning laser beam path into  $N$  arms, with the  $j$ th arm experiencing a relative path length delay of  $jT_{\text{rev}}$ , before recombining the arms again and directing them onto the molecules. Available laser power severely limits the number of times we can split and recombine a beam, meaning that we can afford roughly  $N \sim 3$  arms.

The polarization in the  $j$ th arm would then need to be tilted by  $\pi/3 \sim 60$  degrees relative to the  $(j+1)$ -st arm. As long as the tilt is less than 90 degrees, there should be no ambiguity as to which direction the molecule should rotate. Within the three revivals, a typical diatomic molecule in a supersonic molecular beam (longitudinal speed 500 m/s) only travels  $\sim 100$  nm, allowing it to be fully reoriented well within the  $10 \mu\text{m}$  waist of a single aligning beam.

Further downstream, those rotated molecules are recombined with the un-rotated molecules in the upper arm due to diffraction. The matter-wave interference leads to fringes in the molecular flux. The fringes are phase shifted compared to those obtained in a classic double slit experiment (i.e., when no molecular rotation is induced in the lower arm). The phase of the molecular interference fringes could be observed by scanning an ionization laser vertically and recording molecular ion counts as a function of distance.

**Internal state interferometry** Another method is to use the molecular internal degrees of freedom for interferometry. Instead of a double slit, a  $\pi/2$ -pulse resonant with a transition to the first excited vibrational (or metastable electronic) state is applied. This generates a coherent superposition of aligned molecules in vibrational states  $v = 0$  and  $v = 1$ . An aligning pulse with a repetition frequency equal to the first rotational spacing in the ground state  $v = 0$  will be able to excite resonant two-photon transitions, thereby mixing states of neighboring momenta. Generally, however, the rotational constant in the  $v = 1$  state will be different, and this would make its

rotational states off resonant (and therefore “invisible”) with respect to the aligning pulse [see Fig. 10(b)]. This requires choosing a molecule whose rotational constant at  $v = 1$  is sufficiently incommensurate with that of the ground state so that only the ground-state component is affected by the aligning pulses within the excitation bandwidth.

Assuming the excited state is dark to the alignment pulses, only the ground-state component of the vibrational superposition is rotated in the lab frame. The two components can be subsequently recombined with a second  $\pi/2$ -pulse further downstream. Population in  $v = 0$  or  $v = 1$  can be measured via resonant photo ionization, and should be modulated depending on whether the re-orientation pulses are active or not. The advantage

over matter-wave diffraction is that more of the molecular beam flux can be preserved at every “beam splitter” step.

We now return to the issue of preparing the incident molecular beam. We have assumed that all molecules remain aligned in the lab frame unless actively rotated, but in reality such alignment can be only transient. Furthermore, aligned molecules are in (approximate) position states, which are superpositions of many rotational states. It remains to be checked whether the condition of incommensurability (i.e., off-resonant aligning pulses) in the vibrational-state interferometer can be met if the molecules already populate many rotational states to begin with.

- 
- [1] W. Heisenberg, Ober den anschaulichen Inhalt der quantentheoretischen Kinematik und Mechanik, *Z. Phys.* **43**, 172 (1927).
  - [2] W. G. Harter, C. W. Patterson, and F. J. Da Paixao, Frame transformation relations and multipole transitions in symmetric polyatomic molecules, *Rev. Mod. Phys.* **50**, 37 (1978).
  - [3] W. G. Harter, *Principles of symmetry, dynamics, and spectroscopy* (Wiley, New York, 1993).
  - [4] R. Schmidt and M. Lemesko, Rotation of Quantum Impurities in the Presence of a Many-Body Environment, *Phys. Rev. Lett.* **114**, 203001 (2015).
  - [5] B. Papendell, B. A. Stickler, and K. Hornberger, Quantum angular momentum diffusion of rigid bodies, *New J. Phys.* **19**, 122001 (2017).
  - [6] B. A. Stickler, F. T. Ghahramani, and K. Hornberger, Rotational Alignment Decay and Decoherence of Molecular Superrotors, *Phys. Rev. Lett.* **121**, 243402 (2017).
  - [7] L. V. Damme, D. Leiner, P. Mardesic, S. J. Glaser, and D. Sugny, Linking the rotation of a rigid body to the Schrodinger equation: The quantum tennis racket effect and beyond, *Sci. Rep.* **7**, 3998 (2017).
  - [8] B. A. Stickler, B. Schirinski, and K. Hornberger, Rotational Friction and Diffusion of Quantum Rotors, *Phys. Rev. Lett.* **121**, 040401 (2018).
  - [9] B. A. Stickler, K. Hornberger, and M. S. Kim, Quantum rotations of nanoparticles, *Nat. Rev. Phys.* **3**, 589 (2021).
  - [10] B. Friedrich and D. R. Herschbach, Spatial orientation of molecules in strong electric fields and evidence for pendular states, *Nature* **353**, 412 (1991).
  - [11] J. M. Rost, J. C. Griffin, B. Friedrich, and D. R. Herschbach, Pendular states and spectra of oriented linear molecules, *Phys. Rev. Lett.* **68**, 1299 (1992).
  - [12] A. Slenczka, B. Friedrich, and D. Herschbach, Pendular alignment of paramagnetic molecules in uniform magnetic fields, *Phys. Rev. Lett.* **72**, 1806 (1994).
  - [13] B. Friedrich and D. Herschbach, Alignment and Trapping of Molecules in Intense Laser Fields, *Phys. Rev. Lett.* **74**, 4623 (1995).
  - [14] F. Rasetti, Incoherent Scattered Radiation in Diatomic Molecules, *Phys. Rev.* **34**, 367 (1929).
  - [15] E. B. Wilson, The Statistical Weights of the Rotational Levels of Polyatomic Molecules, Including Methane, Ammonia, Benzene, Cyclopropane and Ethylene, *J. Chem. Phys.* **3**, 276 (1935).
  - [16] E. B. Wilson, Symmetry Considerations Concerning the Splitting of Vibration-Rotation Levels in Polyatomic Molecules, *J. Chem. Phys.* **3**, 818 (1935).
  - [17] H. Longuet-Higgins, The symmetry groups of non-rigid molecules, *Mol. Phys.* **6**, 445 (1963).
  - [18] J. H. Van Vleck, The Coupling of Angular Momentum Vectors in Molecules, *Rev. Mod. Phys.* **23**, 213 (1951).
  - [19] J. T. Hougen, Interpretation of Molecular-Beam Radiofrequency *ortho-para* Transitions in Methane, *J. Chem. Phys.* **55**, 1122 (1971).
  - [20] J. D. Louck and H. W. Galbraith, Eckart vectors, Eckart frames, and polyatomic molecules, *Rev. Mod. Phys.* **48**, 69 (1976).
  - [21] W. G. Harter and C. W. Patterson, Orbital level splitting in octahedral symmetry and SF<sub>6</sub> rotational spectra. I. Qualitative features of high  $J$  levels, *J. Chem. Phys.* **66**, 4872 (1977).
  - [22] J. K. Watson, Aspects of quartic and sextic centrifugal effects on rotational energy levels, in *Vibrational spectra and structure*, Vol. 6 (Elsevier, New York, NY, 1977) pp. 1–89.
  - [23] H. Berger, Classification of energy levels for polyatomic molecules, *J. Phys. France* **38**, 1371 (1977).
  - [24] G. S. Ezra, *Symmetry Properties of Molecules*, edited by G. Berthier, M. J. S. Dewar, H. Fischer, K. Fukui, G. G. Hall, H. Hartmann, H. H. Jaffé, J. Jortner, W. Kutzelnigg, K. Ruedenberg, and E. Scrocco, Lecture Notes in Chemistry, Vol. 28 (Springer, Berlin, Heidelberg, 1982).
  - [25] D. Papoušek and M. R. Aliev, *Molecular vibrational-rotational spectra*, Studies in physical and theoretical chemistry, Vol. 17 (Elsevier, Amsterdam, 1982) ISBN 0-444-99737-7.
  - [26] P. R. Bunker and P. Jensen, *Molecular symmetry and spectroscopy*, 2nd ed. (NRC Research Press, Ottawa, 1998).
  - [27] P. Bunker and P. Jensen, *Fundamentals of Molecular Symmetry* (CRC Press, 2004).
  - [28] J. M. Brown and A. Carrington, *Rotational Spectroscopy of Diatomic Molecules* (Cambridge University Press, 2003).

- [29] L. C. Biedenharn, J. D. Louck, and P. A. Carruthers, *Angular Momentum in Quantum Physics* (Cambridge University Press, 2010).
- [30] G. Herzberg, *Spectra of diatomic molecules*, Molecular spectra and molecular structure, Vol. 1 (Read Books Ltd., 2013).
- [31] G. Herzberg, *Infrared and Raman spectra of polyatomic molecules*, Molecular spectra and molecular structure, Vol. 2 (van Nostrand, New York, 1987).
- [32] G. Herzberg, *Electronic spectra and electronic structure of polyatomic molecules*, Molecular spectra and molecular structure, Vol. 3 (van Nostrand, New York, 1966).
- [33] H. G. Casimir, *Rotation of a rigid body in quantum mechanics [PhD Thesis]* (JB Wolter, 1931).
- [34] L. D. Landau and E. M. Lifshits, *Mechanics*, 3rd ed., Course of theoretical physics No. v. 1 (Pergamon Press, Oxford New York, 1976).
- [35] R. G. Littlejohn and M. Reinsch, Gauge fields in the separation of rotations and internal motions in the n-body problem, *Rev. Mod. Phys.* **69**, 213 (1997).
- [36] G. S. Chirikjian and A. B. Kyatkin, *Engineering Applications of Noncommutative Harmonic Analysis: With Emphasis on Rotation and Motion Groups* (CRC Press, 2000).
- [37] P. E. S. Wormer, *The rigid rotor in classical and quantum mechanics* (online notes).
- [38] K. M. Lynch and F. C. Park, *Modern robotics: mechanics, planning, and control* (Cambridge University Press, Cambridge, UK, 2017).
- [39] C. Isham, *Topological and global aspects of quantum theory*, Relativity, groups and topology, Vol. 2 (North-Holland, Netherlands, 1984).
- [40] N. Landsman and N. Linden, The geometry of inequivalent quantizations, *Nucl. Phys. B* **365**, 121 (1991).
- [41] S. Tanimura and T. Iwai, Reduction of quantum systems on Riemannian manifolds with symmetry and application to molecular mechanics, *J. Math. Phys.* **41**, 1814 (2000).
- [42] P. Levay, D. McMullan, and I. Tsutsui, The canonical connection in quantum mechanics, *J. Math. Phys.* **37**, 625 (1996).
- [43] S. Ospelkaus, A. Pe'er, K.-K. Ni, J. J. Zirbel, B. Neyenhuis, S. Kotochigova, P. S. Julienne, J. Ye, and D. S. Jin, Efficient state transfer in an ultracold dense gas of heteronuclear molecules, *Nat. Phys.* **4**, 622 (2008).
- [44] K.-K. Ni, S. Ospelkaus, M. H. G. De Miranda, A. Pe'er, B. Neyenhuis, J. J. Zirbel, S. Kotochigova, P. S. Julienne, D. S. Jin, and J. Ye, A High Phase-Space-Density Gas of Polar Molecules, *Science* **322**, 231 (2008).
- [45] T. Takekoshi, L. Reichsollner, A. Schindewolf, J. M. Hutson, C. R. Le Sueur, O. Dulieu, F. Ferlaino, R. Grimm, and H.-C. Nagerl, Ultracold Dense Samples of Dipolar RbCs Molecules in the Rovibrational and Hyperfine Ground State, *Phys. Rev. Lett.* **113**, 205301 (2014).
- [46] J. F. Barry, D. J. McCarron, E. B. Norrgard, M. H. Steinecker, and D. DeMille, Magneto-optical trapping of a diatomic molecule, *Nature* **512**, 286 (2014).
- [47] J. W. Park, S. A. Will, and M. W. Zwierlein, Ultracold Dipolar Gas of Fermionic Na 23 K 40 Molecules in Their Absolute Ground State, *Phys. Rev. Lett.* **114**, 205302 (2015).
- [48] T. M. Rvachov, H. Son, A. T. Sommer, S. Ebadi, J. J. Park, M. W. Zwierlein, W. Ketterle, and A. O. Jamison, Long-Lived Ultracold Molecules with Electric and Magnetic Dipole Moments, *Phys. Rev. Lett.* **119**, 143001 (2017).
- [49] L. Anderegg, B. L. Augenbraun, E. Chae, B. Hemmerling, N. R. Hutzler, A. Ravi, A. Collopy, J. Ye, W. Ketterle, and J. M. Doyle, Radio Frequency Magneto-Optical Trapping of CaF with High Density, *Phys. Rev. Lett.* **119**, 103201 (2017).
- [50] S. Truppe, H. J. Williams, M. Hambach, L. Caldwell, N. J. Fitch, E. A. Hinds, B. E. Sauer, and M. R. Tarbutt, Molecules cooled below the Doppler limit, *Nat. Phys.* **13**, 1173 (2017).
- [51] A. L. Collopy, S. Ding, Y. Wu, I. A. Finneran, L. Anderegg, B. L. Augenbraun, J. M. Doyle, and J. Ye, 3D Magneto-Optical Trap of Yttrium Monoxide, *Phys. Rev. Lett.* **121**, 213201 (2018).
- [52] F. Seeßelberg, N. Buchheim, Z.-K. Lu, T. Schneider, X.-Y. Luo, E. Tiemann, I. Bloch, and C. Gohle, Modeling the adiabatic creation of ultracold polar 23 Na 40 K molecules, *Phys. Rev. A* **97**, 013405 (2018).
- [53] L. R. Liu, J. D. Hood, Y. Yu, J. T. Zhang, N. R. Hutzler, T. Rosenband, and K.-K. Ni, Building one molecule from a reservoir of two atoms, *Science* **360**, 900 (2018).
- [54] L. De Marco, G. Valtolina, K. Matsuda, W. G. Tobias, J. P. Covey, and J. Ye, A degenerate Fermi gas of polar molecules, *Science* **363**, 853 (2019).
- [55] L. R. Liu, J. D. Hood, Y. Yu, and J. T. Zhang et al., Molecular Assembly of Ground-State Cooled Single Atoms, *Phys. Rev. X* **9**, 21039 (2019).
- [56] E. Urban, N. Glikin, S. Mouradian, K. Krimmel, B. Hemmerling, and H. Haefner, Coherent Control of the Rotational Degree of Freedom of a Two-Ion Coulomb Crystal, *Phys. Rev. Lett.* **123**, 133202 (2019).
- [57] K. K. Voges, P. Gersema, M. Meyer Zum Alten Borgloh, T. A. Schulze, T. Hartmann, A. Zenesini, and S. Ospelkaus, Ultracold Gas of Bosonic Na 23 K 39 Ground-State Molecules, *Phys. Rev. Lett.* **125**, 083401 (2020).
- [58] S. Ding, Y. Wu, I. A. Finneran, J. J. Burau, and J. Ye, Sub-Doppler Cooling and Compressed Trapping of YO Molecules at microK Temperatures, *Phys. Rev. X* **10**, 021049 (2020).
- [59] G. Valtolina, K. Matsuda, W. G. Tobias, J.-R. Li, L. De Marco, and J. Ye, Dipolar evaporation of reactive molecules to below the Fermi temperature, *Nature* **588**, 239 (2020).
- [60] D. Mitra, N. B. Vilas, C. Hallas, L. Anderegg, B. L. Augenbraun, L. Baum, C. Miller, S. Raval, and J. M. Doyle, Direct laser cooling of a symmetric top molecule, *Science* **369**, 1366 (2020).
- [61] B. L. Augenbraun, J. M. Doyle, T. Zelevinsky, and I. Kozyryev, Molecular Asymmetry and Optical Cycling: Laser Cooling Asymmetric Top Molecules, *Phys. Rev. X* **10**, 031022 (2020).
- [62] A. Schindewolf, R. Bause, X.-Y. Chen, M. Duda, T. Karman, I. Bloch, and X.-Y. Luo, Evaporation of microwave-shielded polar molecules to quantum degeneracy, *Nature* **607**, 677 (2022).
- [63] I. Stevenson, A. Z. Lam, N. Bigagli, C. Warner, W. Yuan, S. Zhang, and S. Will, Ultracold Gas of Dipolar NaCs Ground State Molecules, *Phys. Rev. Lett.* **130**, 113002 (2023).
- [64] J. Lin, G. Chen, M. Jin, Z. Shi, F. Deng, W. Zhang, G. Quémener, T. Shi, S. Yi, and D. Wang, Microwave Shielding of Bosonic NaRb Molecules, *Phys. Rev. X* **13**,



- 031032 (2023).
- [65] L. Anderegg, N. B. Vilas, C. Hallas, P. Robichaud, A. Jadbabaie, J. M. Doyle, and N. R. Hutzler, Quantum control of trapped polyatomic molecules for eEDM searches, *Science* **382**, 665 (2023).
  - [66] N. Glikin, B. A. Stickler, R. Tollefsen, S. Mouradian, N. Yadav, E. Urban, K. Hornberger, and H. Häffner, *Systematic study of rotational decoherence with a trapped-ion planar rotor* (2023), arXiv:2310.13293.
  - [67] N. B. Vilas, C. Hallas, L. Anderegg, P. Robichaud, A. Winnicki, D. Mitra, and J. M. Doyle, Magneto-optical trapping and sub-Doppler cooling of a polyatomic molecule, *Nature* **606**, 70 (2022).
  - [68] M. Koller, F. Jung, J. Phrompao, M. Zeppenfeld, I. Rabey, and G. Rempe, Electric-Field-Controlled Cold Dipolar Collisions between Trapped CH<sub>3</sub>F Molecules, *Phys. Rev. Lett.* **128**, 203401 (2022).
  - [69] N. B. Vilas, P. Robichaud, C. Hallas, G. K. Li, L. Anderegg, and J. M. Doyle, *An optical tweezer array of ultracold polyatomic molecules* (2023), arXiv:2311.07529.
  - [70] Y. Lu, S. J. Li, C. M. Holland, and L. W. Cheuk, *Raman Sideband Cooling of Molecules in an Optical Tweezer Array* (2023), arXiv:2306.02455.
  - [71] Y. Bao, S. S. Yu, J. You, L. Anderegg, E. Chae, W. Ketterle, K.-K. Ni, and J. M. Doyle, *Raman sideband cooling of molecules in an optical tweezer array to the 3-D motional ground state* (2023), arXiv:2309.08706.
  - [72] C. M. Holland, Y. Lu, and L. W. Cheuk, On-demand entanglement of molecules in a reconfigurable optical tweezer array, *Science* **382**, 1143 (2023).
  - [73] Y. Bao, S. S. Yu, L. Anderegg, E. Chae, W. Ketterle, K.-K. Ni, and J. M. Doyle, Dipolar spin-exchange and entanglement between molecules in an optical tweezer array, *Science* **382**, 1138 (2023).
  - [74] A. Singh, L. Maisenbacher, Z. Lin, J. Axelrod, C. Panda, and H. Müller, Dynamics of a buffer-gas-loaded, deep optical trap for molecules, *Phys. Rev. Research* **5**, 033008 (2023).
  - [75] H. J. Loesch and A. Remscheid, Brute force in molecular reaction dynamics: A novel technique for measuring steric effects, *J. Chem. Phys.* **93**, 4779 (1990).
  - [76] T. Seideman, Rotational excitation and molecular alignment in intense laser fields, *J. Chem. Phys.* **103**, 7887 (1995).
  - [77] W. Kim and P. M. Felker, Spectroscopy of pendular states in optical-field-aligned species, *J. Chem. Phys.* **104**, 1147 (1996).
  - [78] S. Fleischer, Y. Zhou, R. W. Field, and K. A. Nelson, Molecular Orientation and Alignment by Intense Single-Cycle THz Pulses, *Phys. Rev. Lett.* **107**, 163603 (2011).
  - [79] H. Stapelfeldt and T. Seideman, Colloquium: Aligning molecules with strong laser pulses, *Rev. Mod. Phys.* **75**, 543 (2003).
  - [80] S. A. Malinovskaya and I. Novikova, *From Atomic to Mesoscale: The Role of Quantum Coherence in Systems of Various Complexities* (World Scientific, 2015).
  - [81] N. Fitch and M. Tarbutt, Laser-cooled molecules, in *Advances In Atomic, Molecular, and Optical Physics*, Vol. 70 (Elsevier, 2021) pp. 157–262.
  - [82] Committee on Identifying Opportunities at the Interface of Chemistry and Quantum Information Science, Board on Chemical Sciences and Technology, Board on Life Sciences, Division on Earth and Life Studies, and National Academies of Sciences, Engineering, and Medicine, *Advancing Chemistry and Quantum Information Science: An Assessment of Research Opportunities at the Interface of Chemistry and Quantum Information Science in the United States* (National Academies Press, Washington, D.C., 2023) pages: 26850.
  - [83] B. L. Augenbraun, L. Anderegg, C. Hallas, Z. D. Lاسner, N. B. Vilas, and J. M. Doyle, Direct laser cooling of polyatomic molecules, in *Advances In Atomic, Molecular, and Optical Physics*, Vol. 72 (Elsevier, 2023) pp. 89–182.
  - [84] S. L. Cornish, M. R. Tarbutt, and K. R. A. Hazzard, *Quantum Computation and Quantum Simulation with Ultracold Molecules* (2024), arXiv:2401.05086.
  - [85] C. P. Koch, M. Lemesko, and D. Sugny, Quantum control of molecular rotation, *Rev. Mod. Phys.* **91**, 035005 (2019).
  - [86] E. Pozzoli, Classical and Quantum Controllability of a Rotating Asymmetric Molecule, *Appl. Math. Optim.* **85**, 8 (2022).
  - [87] M. Leibscher, E. Pozzoli, C. Pérez, M. Schnell, M. Sigalotti, U. Boscain, and C. P. Koch, Full quantum control of enantiomer-selective state transfer in chiral molecules despite degeneracy, *Commun. Phys.* **5**, 110 (2022).
  - [88] Y. Lin, D. R. Leibbrandt, D. Leibfried, and C.-w. Chou, Quantum entanglement between an atom and a molecule, *Nature* **581**, 273 (2020).
  - [89] S. Todaro, V. Verma, K. McCormick, D. Allcock, R. Mirin, D. Wineland, S. Nam, A. Wilson, D. Leibfried, and D. Slichter, State Readout of a Trapped Ion Qubit Using a Trap-Integrated Superconducting Photon Detector, *Phys. Rev. Lett.* **126**, 010501 (2021).
  - [90] N. E. Frattini, U. Vool, S. Shankar, A. Narla, K. M. Sliwa, and M. H. Devoret, 3-wave mixing Josephson dipole element, *Appl. Phys. Lett.* **110**, 222603 (2017).
  - [91] M. Elliott, J. Joo, and E. Ginossar, Designing Kerr interactions using multiple superconducting qubit types in a single circuit, *New J. Phys.* **20**, 023037 (2018).
  - [92] K. R. Parthasarathy, On the maximal dimension of a completely entangled subspace for finite level quantum systems, *Proceedings Mathematical Sciences* **114**, 365 (2004).
  - [93] K. Parthasarathy, Extremal quantum states in coupled systems, in *Annales de l'IHP Probabilités et statistiques*, Vol. 41 (2005) pp. 257–268.
  - [94] J. Walgate and A. J. Scott, Generic local distinguishability and completely entangled subspaces, *Journal of Physics A: Mathematical and Theoretical* **41**, 375305 (2008).
  - [95] M. V. Berry, Quantal Phase Factors Accompanying Adiabatic Changes, *Proc. R. Soc. A* **392**, 45 (1984).
  - [96] B. Simon, Holonomy, the Quantum Adiabatic Theorem, and Berry's Phase, *Phys. Rev. Lett.* **51**, 2167 (1983).
  - [97] F. Wilczek and A. Zee, Appearance of Gauge Structure in Simple Dynamical Systems, *Phys. Rev. Lett.* **52**, 2111 (1984).
  - [98] P. Zanardi and M. Rasetti, Holonomic quantum computation, *Phys. Lett. A* **264**, 94 (1999).
  - [99] N. Read, Non-Abelian adiabatic statistics and Hall viscosity in quantum Hall states and px+ipy paired superfluids, *Phys. Rev. B* **79**, 045308 (2009).
  - [100] D. Gottesman and L. L. Zhang, *Fibre bundle framework for unitary quantum fault tolerance* (2017), arXiv:1309.7062.
  - [101] V. V. Albert, J. P. Covey, and J. Preskill, Robust En-

- coding of a Qubit in a Molecule, *Phys. Rev. X* **10**, 031050 (2020).
- [102] S. L. Braunstein and P. van Loock, Quantum information with continuous variables, *Rev. Mod. Phys.* **77** (2005).
- [103] A. Micheli, G. K. Brennen, and P. Zoller, A toolbox for lattice-spin models with polar molecules, *Nature Physics* **2**, 341 (2006).
- [104] A. V. Gorshkov, S. R. Manmana, G. Chen, E. Demler, M. D. Lukin, and A. M. Rey, Quantum magnetism with polar alkali-metal dimers, *Phys. Rev. A* **84**, 033619 (2011).
- [105] M. L. Wall, K. Maeda, and L. D. Carr, Simulating quantum magnets with symmetric top molecules, *Ann. Phys. (Berlin)* **525**, 845 (2013).
- [106] M. L. Wall, K. Maeda, and L. D. Carr, Realizing unconventional quantum magnetism with symmetric top molecules, *New J. Phys.* **17**, 025001 (2015).
- [107] V. Karle, A. Ghazaryan, and M. Leshchko, Topological Charges of Periodically Kicked Molecules, *Phys. Rev. Lett.* **130**, 103202 (2023).
- [108] D. DeMille, J. M. Doyle, and A. O. Sushkov, Probing the frontiers of particle physics with tabletop-scale experiments, *Science* **357**, 990 (2017).
- [109] S. S. Kondov, C.-H. Lee, K. H. Leung, C. Liedl, I. Majewska, R. Moszynski, and T. Zelevinsky, Molecular lattice clock with long vibrational coherence, *Nature Physics* **15**, 1118 (2019).
- [110] K. Leung, B. Iritani, E. Tiberi, I. Majewska, M. Borkowski, R. Moszynski, and T. Zelevinsky, Terahertz Vibrational Molecular Clock with Systematic Uncertainty at the 10<sup>-14</sup> Level, *Phys. Rev. X* **13**, 011047 (2023).
- [111] B. R. Heazlewood and T. P. Softley, Towards chemistry at absolute zero, *Nat. Rev. Chem.* **5**, 125 (2021).
- [112] Y.-X. Liu, L. Zhu, J. Luke, J. J. A. Houwman, M. C. Babin, M.-G. Hu, and K.-K. Ni, Quantum interference and entanglement in ultracold atom-exchange reactions (2023), arXiv:2310.07620.
- [113] L. W. Cheuk, L. Anderegg, Y. Bao, S. Burchesky, S. S. Yu, W. Ketterle, K.-K. Ni, and J. M. Doyle, Observation of Collisions between Two Ultracold Ground-State CaF Molecules, *Phys. Rev. Lett.* **125**, 043401 (2020).
- [114] D. DeMille, Quantum Computation with Trapped Polar Molecules, *Phys. Rev. Lett.* **88**, 067901 (2002).
- [115] C. M. Tesch and R. de Vivie-Riedle, Quantum Computation with Vibrationally Excited Molecules, *Phys. Rev. Lett.* **89**, 157901 (2002).
- [116] S. F. Yelin, K. Kirby, and R. Côté, Schemes for robust quantum computation with polar molecules, *Phys. Rev. A* **74**, 050301 (2006).
- [117] Q. Wei, S. Kais, B. Friedrich, and D. Herschbach, Entanglement of polar symmetric top molecules as candidate qubits, *J. Chem. Phys.* **135**, 154102 (2011).
- [118] K.-K. Ni, T. Rosenband, and D. D. Grimes, Dipolar exchange quantum logic gate with polar molecules, *Chem. Sci.* **9**, 6830 (2018).
- [119] P. Yu, L. W. Cheuk, I. Kozyryev, and J. M. Doyle, A scalable quantum computing platform using symmetric-top molecules, *New J. Phys.* **21**, 093049 (2019).
- [120] R. Sawant, J. A. Blackmore, P. D. Gregory, J. Mur-Petit, D. Jaksch, J. Aldegunde, J. M. Hutson, M. R. Tarbutt, and S. L. Cornish, Ultracold polar molecules as qudits, *New J. Phys.* **22**, 013027 (2020).
- [121] M. Zeppenfeld, A robust framework for quantum computation using quasi-hidden molecular degrees of freedom (2023), arXiv:2311.14133.
- [122] S. P. Jain, E. R. Hudson, W. C. Campbell, and V. V. Albert, Absorption-emission codes for atomic and molecular quantum information platforms, *Phys. Rev. Lett.* **133**, 260601 (2024).
- [123] M. Freedman, M. Shokrian-Zini, and Z. Wang, Quantum Computing with Octonions, *Peking Math. J.* **2**, 239 (2019).
- [124] M. P. Fisher, Quantum cognition: The possibility of processing with nuclear spins in the brain, *Ann. Phys. (N. Y.)* **362**, 593 (2015).
- [125] M. P. A. Fisher and L. Radzihovsky, Quantum indistinguishability in chemical reactions, *Proc. Natl. Acad. Sci. U.S.A.* **115** (2018).
- [126] L. Muechler, Topological classification of molecules and chemical reactions with a perplectic structure, *Phys. Rev. B* **101**, 045123 (2020).
- [127] C.-A. Palma, Topological Dynamic Matter, *J. Phys. Chem. Lett.* **12**, 454 (2021).
- [128] C. J. Brester, *Kristallsymmetrie und Reststrahlen*, Ph.D. thesis, Utrecht (1923).
- [129] E. Wigner, Über de elastischen Eigenschwingungen symmetrischer Systeme, *Gott. Nachr. Math. Phys. Klass.* **1930**, 133 (1930).
- [130] J.-M. F. Gilles and J. Philippot, Internal symmetry groups of non-rigid molecules, *Int. J. Quantum Chem.* **6**, 225 (1972).
- [131] G. W. Mackey, *Induced representations of groups and quantum mechanics* (W.A. Benjamin and Editore Boringhieri, 1968).
- [132] G. W. Mackey, Induced Representations of Locally Compact Groups I, *Ann. Math.* **55**, 101 (1952).
- [133] A. J. Coleman, Induced and Subdued Representations, in *Gr. Theory its Appl.*, edited by E. M. Loebl (Academic Press, 1968) section: 2.
- [134] T. Inui, Y. Tanabe, and Y. Onodera, *Group Theory and Its Applications in Physics*, edited by M. Cardona, P. Fulde, K. Von Klitzing, H.-J. Queisser, and H. K. V. Lotsch, Springer Series in Solid-State Sciences, Vol. 78 (Springer, Berlin, Heidelberg, 1990).
- [135] R. W. Carter, I. G. MacDonald, and G. B. Segal, *Lectures on Lie Groups and Lie Algebras* (Cambridge University Press, Cambridge, 1995).
- [136] G. B. Folland, *A Course in Abstract Harmonic Analysis* (Chapman and Hall/CRC, 2016).
- [137] B. Bradlyn, L. Elcoro, J. Cano, M. G. Vergniory, Z. Wang, C. Felser, M. I. Aroyo, and B. A. Bernevig, Topological quantum chemistry, *Nature* **547**, 298 (2017).
- [138] N. Mermin, The topological theory of defects in ordered media, *Rev. Mod. Phys.* **51**, 591 (1979).
- [139] K. Liu, J. Nissinen, R.-J. Slager, K. Wu, and J. Zaanen, Generalized liquid crystals: Giant fluctuations and the vestigial chiral order of i, o, and t matter, *Physical Review X* **6**, 041025 (2016).
- [140] S. L. Altmann and P. Herzig, *Point-group theory tables* (Clarendon Press, 1994) ISBN 9780198552260.
- [141] A. J. Ceulemans, *Group Theory Applied to Chemistry*, Theoretical Chemistry and Computational Modelling (Springer Netherlands, Dordrecht, 2013).
- [142] A. Ekert and P. L. Knight, Entangled quantum systems and the Schmidt decomposition, *Am. J. Phys.* **63**, 415

- (1995).
- [143] V. V. Albert, S. Pascasio, and M. H. Devoret, General phase spaces: from discrete variables to rotor and continuum limits, *J. Phys. A Math. Theor.* **50**, 504002 (2017).
  - [144] M. M. Postnikov, Three-dimensional spherical forms, in *Discret. Geom. Topol. Dedic. to 100th Anniv. birth Boris Nikolaevich Delone, Proc. Steklov Inst. Math.*, Vol. 196, edited by E. F. Mishchenko and S. P. Novikov (Nauka, 1992) p. 129.
  - [145] C. Wulker, S. Ruan, and G. S. Chirikjian, Quantizing Euclidean Motions via Double-Coset Decomposition, *Research* **2019**, 1 (2019).
  - [146] D. A. Varshalovich, A. N. Moskalev, and V. K. Khersonskii, *Quantum Theory of Angular Momentum* (World Scientific, 1988).
  - [147] J. M. Leinaas and J. Myrheim, On the theory of identical particles, *Nuovo Cim. B* **37**, 1 (1977).
  - [148] F. Wilczek, Quantum Mechanics of Fractional-Spin Particles, *Phys. Rev. Lett.* **49**, 957 (1982).
  - [149] Y.-S. Wu, General Theory for Quantum Statistics in Two Dimensions, *Phys. Rev. Lett.* **52**, 2103 (1984).
  - [150] D. Arovas, J. R. Schrieffer, and F. Wilczek, Fractional Statistics and the Quantum Hall Effect, *Phys. Rev. Lett.* **53**, 722 (1984).
  - [151] C. Nayak, A. Stern, M. Freedman, and S. Das Sarma, Non-Abelian anyons and topological quantum computation, *Rev. Mod. Phys.* **80**, 1083 (2008).
  - [152] G. A. Goldin, R. Menikoff, and D. H. Sharp, Particle statistics from induced representations of a local current group, *J. Math. Phys.* **21**, 650 (1980).
  - [153] X. G. Wen, Non-Abelian statistics in the fractional quantum Hall states, *Phys. Rev. Lett.* **66**, 802 (1991).
  - [154] G. Moore and N. Read, Nonabelions in the fractional quantum hall effect, *Nucl. Phys. B* **360**, 362 (1991).
  - [155] P. Levay, Berry phases for Landau Hamiltonians on deformed tori, *J. Math. Phys.* **36**, 2792 (1995).
  - [156] C. Nayak and F. Wilczek, 2n-quasihole states realize 2n-1-dimensional spinor braiding statistics in paired quantum Hall states, *Nuclear Physics B* **479**, 529 (1996).
  - [157] T. Seideman, On the dynamics of rotationally broad, spatially aligned wave packets, *J. Chem. Phys.* **115**, 5965 (2001).
  - [158] P. W. Dooley, I. V. Litvinyuk, K. F. Lee, D. M. Rayner, M. Spanner, D. M. Villeneuve, and P. B. Corkum, Direct imaging of rotational wave-packet dynamics of diatomic molecules, *Phys. Rev. A* **68**, 023406 (2003).
  - [159] M. Spanner, *Field-free alignment and strong field control of molecular rotors*, Ph.D. Thesis, University of Waterloo (2004).
  - [160] K. F. Lee, E. A. Shapiro, D. M. Villeneuve, and P. B. Corkum, Coherent creation and annihilation of rotational wave packets in incoherent ensembles, *Phys. Rev. A* **73**, 033403 (2006).
  - [161] A. B. Harris and H. Meyer, Orientational ordering in solid ortho-para H<sub>2</sub> mixtures and analogy with a spin glass, *Can. J. Phys.* **63**, 3 (1985).
  - [162] U. Hochli, K. Knorr, and A. Loidl, Orientational glasses, *Adv. Phys.* **39**, 405 (1990).
  - [163] W. I. F. David, R. M. Ibberson, J. C. Matthewman, K. Prassides, T. J. S. Dennis, J. P. Hare, H. W. Kroto, R. Taylor, and D. R. M. Walton, Crystal structure and bonding of ordered C<sub>60</sub>, *Nature* **353**, 147 (1991).
  - [164] P. A. Heiney, J. E. Fischer, A. R. McGhie, W. J. Romanow, A. M. Denenstien, J. P. McCauley Jr., A. B. Smith, and D. E. Cox, Orientational ordering transition in solid C<sub>60</sub>, *Phys. Rev. Lett.* **66**, 2911 (1991).
  - [165] W. I. F. David, R. M. Ibberson, T. J. S. Dennis, J. P. Hare, and K. Prassides, Structural Phase Transitions in the Fullerene C<sub>60</sub>, *Europhys. Lett.* **18**, 219 (1992).
  - [166] A. F. Devonshire, The rotation of molecules in fields of octahedral symmetry, *Proc. R. Soc. A* **153**, 601 (1936).
  - [167] H. Schmiedt, P. Jensen, and S. Schlemmer, Unifying the rotational and permutation symmetry of nuclear spin states: Schur-Weyl duality in molecular physics, *J. Chem. Phys.* **145**, 074301 (2016).
  - [168] H. Schmiedt, *Molecular Symmetry, Super-Rotation, and Semiclassical Motion*, Springer Series on Atomic, Optical, and Plasma Physics, Vol. 97 (Springer International Publishing, Cham, 2017).
  - [169] S. L. Altmann, *Induced representations in crystals and molecules: point, space, and nonrigid molecule groups* (Academic Press, London ; New York, 1977).
  - [170] W. G. Harter and C. W. Patterson, Induced representations and spontaneous molecular symmetry breaking, in *Group Theoretical Methods in Physics*, Vol. 94, edited by J. Ehlers, K. Hepp, R. Kippenhahn, H. A. Weidenmüller, J. Zittartz, W. Beiglbock, W. Beiglbock, A. Böhm, and E. Takasugi (Springer Berlin Heidelberg, Berlin, Heidelberg, 1979) pp. 77–81.
  - [171] W. G. Harter and C. W. Patterson, Simple Model for Asymptotic Level Clusters in SF<sub>6</sub> Rotational Spectra, *Phys. Rev. Lett.* **38**, 224 (1977).
  - [172] W. G. Harter and C. W. Patterson, Bands, clusters, and crystal field splitting: Understanding SF<sub>6</sub> rotational levels, *Int. J. Quantum Chem.* **12**, 479 (1977).
  - [173] W. G. Harter and C. W. Patterson, Theory of hyperfine and superfine levels in symmetric polyatomic molecules. Trigonal and tetrahedral molecules: Elementary spin- $\frac{1}{2}$  cases in vibronic ground states, *Phys. Rev. A* **19**, 2277 (1979).
  - [174] W. G. Harter, Theory of hyperfine and superfine levels in symmetric polyatomic molecules. II. Elementary cases in octahedral hexafluoride molecules, *Phys. Rev. A* **24**, 192 (1981).
  - [175] W. Harter, Molecular Symmetry and Dynamics, in *Springer Handbook of Atomic, Molecular, and Optical Physics*, edited by G. Drake (Springer New York, New York, NY, 2006) pp. 491–513.
  - [176] J. Zak, Finite Translations in Solid-State Physics, *Phys. Rev. Lett.* **19**, 1385 (1967).
  - [177] D. Jüstel, The Zak transform on strongly proper G-spaces and its applications, *J. London Math. Soc.* **97**, 47 (2018).
  - [178] E. Culf, T. Vidick, and V. V. Albert, *Group coset monogamy games and an application to device-independent continuous-variable QKD* (2022), arXiv:2212.03935.
  - [179] E. Sudarshan, T. D. Imbo, and T. Govindarajan, Configuration space topology and quantum internal symmetries, *Phys. Lett. B* **213**, 471 (1988).
  - [180] P. A. Horvathy, G. Morandi, and E. C. G. Sudarshan, Inequivalent quantizations in multiply connected spaces, *Nuovo Cim. B* **11**, 201 (1989).
  - [181] C. A. Mead and D. G. Truhlar, On the determination of Born–Oppenheimer nuclear motion wave functions including complications due to conical intersections and identical nuclei, *J. Chem. Phys.* **70**, 2284 (1979).



- [182] C. A. Mead, The geometric phase in molecular systems, *Rev. Mod. Phys.* **64**, 51 (1992).
- [183] D. R. Yarkony, Diabolical conical intersections, *Rev. Mod. Phys.* **68**, 985 (1996).
- [184] R. Resta, Manifestations of Berry's phase in molecules and condensed matter, *J. Phys.: Condens. Matter* **12**, R107 (2000).
- [185] J. Moody, A. Shapere, and F. Wilczek, Realizations of Magnetic-Monopole Gauge Fields: Diatoms and Spin Precession, *Phys. Rev. Lett.* **56**, 893 (1986).
- [186] H.-Z. Li, Induced gauge fields in a nongauged quantum system, *Phys. Rev. Lett.* **58**, 539 (1987).
- [187] A. Bohm, B. Kendrick, and M. E. Loewe, The Berry phase in molecular physics, *Int. J. Quantum Chem.* **41**, 53 (1992).
- [188] H. Koizumi and S. Sugano, Geometric phase in two Kramers doublets molecular systems, *J. Chem. Phys.* **102**, 4472 (1995).
- [189] D. Sadovskii and B. Zhilinskii, Monodromy, diabolic points, and angular momentum coupling, *Phys. Lett. A* **256**, 235 (1999).
- [190] F. Faure and B. Zhilinskii, Topological Chern Indices in Molecular Spectra, *Phys. Rev. Lett.* **85**, 960 (2000).
- [191] M. S. Child, T. Weston, and J. Tennyson, Quantum monodromy in the spectrum of H<sub>2</sub>O and other systems: new insight into the level structure of quasi-linear molecules, *Mol. Phys.* **96**, 371 (1999).
- [192] I. N. Kozin and R. M. Roberts, Monodromy in the spectrum of a rigid symmetric top molecule in an electric field, *J. Chem. Phys.* **118**, 10523 (2003).
- [193] K. Efsthathiou, *Metamorphoses of Hamiltonian systems with symmetries* (Springer, New York, 2005).
- [194] M. Modugno, C. T. Prieto, and R. Vitolo, Geometric Aspects of the Quantization of a Rigid Body, in *Differential Equations - Geometry, Symmetries and Integrability*, edited by B. Kruglikov, V. Lychagin, and E. Straume (Springer Berlin Heidelberg, Berlin, Heidelberg, 2009) pp. 275–285.
- [195] M. S. Child, *Semiclassical mechanics with molecular applications*, second edition ed. (Oxford University Press, Oxford ; New York, NY, 2014).
- [196] I. Pavlichenkov, Phase transition in the rotational band of a nonaxial nucleus, *Sov. Phys. JETP-USSR* **55**, 5 (1982).
- [197] I. Pavlichenkov and B. Zhilinskii, Rotation of molecules around specific axes: Axes reorientation under rotational excitation, *Chem. Phys.* **100**, 339 (1985).
- [198] I. Pavlichenkov and B. Zhilinskii, Critical phenomena in rotational spectra, *Ann. Phys.* **184**, 1 (1988).
- [199] B. Zhilinskii, Symmetry, invariants, and topology in molecular models, *Phys. Rep.* **341**, 85 (2001).
- [200] B. Schmidt and B. Friedrich, Topology of surfaces for molecular Stark energy, alignment, and orientation generated by combined permanent and induced electric dipole interactions, *J. Chem. Phys.* **140**, 064317 (2014).
- [201] A. Klein, Y. Shagam, W. Skomorowski, P. S. Zuchowski, M. Pawlak, L. M. C. Janssen, N. Moiseyev, S. Y. T. Van De Meerakker, A. Van Der Avoird, C. P. Koch, and E. Narevicius, Directly probing anisotropy in atom-molecule collisions through quantum scattering resonances, *Nat. Phys.* **13**, 35 (2017).
- [202] M. G. G. Laidlaw and C. M. DeWitt, Feynman Functional Integrals for Systems of Indistinguishable Particles, *Phys. Rev. D* **3**, 1375 (1971).
- [203] J. S. Dowker, Quantum mechanics and field theory on multiply connected and on homogeneous spaces, *J. Phys. A: Gen. Phys.* **5**, 936 (1972).
- [204] L. S. Schulman, *Techniques and applications of path integration*, expanded republ. of the 1996 print ed. (Dover Publications, Mineola, N.Y., 2005).
- [205] P. A. Horvathy, *Prequantisation from the path integral viewpoint* (2024), arXiv:2402.17629.
- [206] J. Milnor, On the existence of a connection with curvature zero, *Comment. Math. Helv.* **32**, 215 (1958).
- [207] J. M. Robbins and M. V. Berry, A geometric phase for m=0 spins, *J. Phys. A: Math. Gen.* **27**, L435 (1994).
- [208] J. Zimba, Anticoherent Spin States via the Majorana Representation, *Electron. J. Theor. Phys.* **3**, 143 (2006).
- [209] J. Crann, R. Pereira, and D. W. Kribs, Spherical designs and anticoherent spin states, *J. Phys. A: Math. Theor.* **43**, 255307 (2010).
- [210] P. Aguilar, C. Chryssomalakos, E. Guzmán-González, L. Hanotel, and E. Serrano-Ensástiga, When geometric phases turn topological, *J. Phys. A: Math. Theor.* **53**, 065301 (2020).
- [211] R. Pereira and C. Paul-Paddock, Anticoherent subspaces, *J. Math. Phys.* **58**, 062107 (2017).
- [212] J. A. Gross, Encoding a qubit in a spin, *Phys. Rev. Lett.* **127**, 010504 (2021).
- [213] C. Chryssomalakos, L. Hanotel, E. Guzmán-González, and E. Serrano-Ensástiga, Toponomic quantum computation, *Mod. Phys. Lett. A* **37**, 2250184 (2022).
- [214] S. Omanakuttan and J. A. Gross, Multispin Clifford codes for angular momentum errors in spin systems, *Phys. Rev. A* **108**, 022424 (2023).
- [215] E. Kubischta and I. Teixeira, Family of Quantum Codes with Exotic Transversal Gates, *Phys. Rev. Lett.* **131**, 240601 (2023).
- [216] E. Kubischta and I. Teixeira, *Free Quantum Codes from Twisted Unitary t-groups* (2024), arXiv:2402.01638.
- [217] L. Vinet, Invariant Berry connections, *Phys. Rev. D* **37**, 2369 (1988).
- [218] S. Giler, P. Kosinski, and L. Szymanowski, The Geometrical Properties of Berry's Phase, *Szymanowski* **04**, 1453 (1989).
- [219] P. Levay, Modified symmetry generators and the geometric phase, *J. Phys. A Math. Gen.* **27**, 2857 (1994).
- [220] S. Giller, C. Gonera, P. Kosinski, and P. Maslanka, Structure of Berry's phase: Some group-theoretical examples, *Phys. Rev. A* **48**, 907 (1993).
- [221] V. V. Albert, *Flat Maurer-Cartan connection iff flat Berry connection* (2024), <https://mathoverflow.net/q/461220>.
- [222] M. C. Tichy, F. Mintert, and A. Buchleitner, Essential entanglement for atomic and molecular physics, *Journal of Physics B: Atomic, Molecular and Optical Physics* **44**, 192001 (2011).
- [223] D. Gross, S. T. Flammia, and J. Eisert, Most Quantum States Are Too Entangled To Be Useful As Computational Resources, *Phys. Rev. Lett.* **102**, 190501 (2009).
- [224] M. J. Bremner, C. Mora, and A. Winter, Are Random Pure States Useful for Quantum Computation?, *Phys. Rev. Lett.* **102**, 190502 (2009).
- [225] S. D. Bartlett, T. Rudolph, and R. W. Spekkens, Reference frames, superselection rules, and quantum information, *Rev. Mod. Phys.* **79**, 555 (2007).
- [226] B. Morris, B. Yadin, M. Fadel, T. Zibold, P. Treutlein, and G. Adesso, Entanglement between identical parti-



- cles is a useful and consistent resource, *Physical Review X* **10**, 041012 (2020).
- [227] B. Bruognolo, J.-W. Li, J. von Delft, and A. Weichselbaum, A beginner's guide to non-abelian ipeps for correlated fermions, *SciPost Physics Lecture Notes*, **025** (2021).
  - [228] A. Guichardet, On rotation and vibration motions of molecules, in *Annales de l'IHP Physique théorique*, Vol. 40 (1984) pp. 329–342.
  - [229] A. Tachibana and T. Iwai, Complete molecular hamiltonian based on the born-oppenheimer adiabatic approximation, *Phys. Rev. A* **33**, 2262 (1986).
  - [230] H. Schmiedt, P. Jensen, and S. Schlemmer, Collective Molecular Superrotation: A Model for Extremely Flexible Molecules Applied to Protonated Methane, *Phys. Rev. Lett.* **117**, 223002 (2016).
  - [231] M. O'Keeffe, E. Chudnovsky, and D. Garanin, Quantum tunneling of the magnetic moment in a free nanoparticle, *J. Magn. Magn. Mater.* **324**, 2871 (2012).
  - [232] C. C. Rusconi and O. Romero-Isart, Magnetic rigid rotor in the quantum regime: Theoretical toolbox, *Phys. Rev. B* **93**, 054427 (2016).
  - [233] C. C. Rusconi, V. Pochhacker, J. I. Cirac, and O. Romero-Isart, Linear stability analysis of a levitated nanomagnet in a static magnetic field: Quantum spin stabilized magnetic levitation, *Phys. Rev. B* **96**, 134419 (2017).
  - [234] Y. Ma, M. S. Kim, and B. A. Stickler, Torque-free manipulation of nanoparticle rotations via embedded spins, *Phys. Rev. B* **104**, 134310 (2021).
  - [235] C. C. Rusconi, M. Perdriat, G. Hétet, O. Romero-Isart, and B. A. Stickler, Spin-Controlled Quantum Interference of Levitated Nanorotors, *Phys. Rev. Lett.* **129**, 093605 (2022).
  - [236] W. Erb, *Uncertainty Principles on Riemannian Manifolds*, Ph.D. thesis, Technische Universität München (2010).
  - [237] J. P. Bizarro, Weyl-wigner formalism for rotation-angle and angular-momentum variables in quantum mechanics, *Phys. Rev. A* **49**, 3255 (1994).
  - [238] N. Mukunda, S. Chaturvedi, and R. Simon, Wigner distributions for non-abelian finite groups of odd order, *Physics Letters A* **321**, 160 (2004).
  - [239] D. Bhaumik, T. Nag, and B. Dutta-Roy, Coherent states for angular momentum, *Journal of Physics A: Mathematical and General* **8**, 1868 (1975).
  - [240] D. Janssen, Coherent states of quantum-mechanical top, *Sov. J. Nucl. Phys.* **25**, 479 (1977).
  - [241] P. Gulshani, Generalized schwinger boson realizations and the oscillator-like coherent states of the rotation groups and the asymmetric top, *Canadian Journal of Physics* **57**, 998 (1979).
  - [242] S. De Bievre, Coherent states over symplectic homogeneous spaces, *Journal of mathematical physics* **30**, 1401 (1989).
  - [243] K. Kowalski and J. Rembielinski, Quantum mechanics on a sphere and coherent states, *Journal of Physics A: Mathematical and General* **33**, 6035 (2000).
  - [244] J.-P. Gazeau and R. Murenzi, Covariant integral quantization of the semi-discrete so (3)-hypercylinder, *Symmetry* **15**, 2044 (2023).
  - [245] E. J. Heller, Frozen gaussians: A very simple semiclassical approximation, *The Journal of Chemical Physics* **75**, 2923 (1981).
  - [246] Wolfram Research Inc., Mathematica, Version 13.0 (2023), place: Champaign, IL.
  - [247] C. N. Jarman and P. F. Bernath, A high-resolution analysis of the A2A'-X2A' transition of CaSH by laser excitation spectroscopy, *J. Chem. Phys.* **98**, 6697 (1993).
  - [248] C. Eckart, Some Studies Concerning Rotating Axes and Polyatomic Molecules, *Phys. Rev.* **47**, 552 (1935).
  - [249] B. R. Judd, *Angular momentum theory for diatomic molecules* (Academic Press, New York, 1975).
  - [250] D. P. Arovas, *Lecture Notes on Group Theory in Physics* (online notes).
  - [251] R. N. Zare, *Angular Momentum: Understanding Spatial Aspects in Chemistry and Physics* (Wiley, 1991).
  - [252] A. W. Harrow, Applications of coherent classical communication and the Schur transform to quantum information theory (2005), arXiv:quant-ph/0512255.
  - [253] J. E. Avron, M. Fraas, G. M. Graf, and P. Grech, Adiabatic Theorems for Generators of Contracting Evolutions, *Commun. Math. Phys.* **314**, 163 (2012).
  - [254] W. Ehrenberg and R. E. Siday, The Refractive Index in Electron Optics and the Principles of Dynamics, *Proc. Phys. Soc. B* **62**, 8 (1949).
  - [255] Y. Aharonov and D. Bohm, Significance of Electromagnetic Potentials in the Quantum Theory, *Phys. Rev.* **115**, 485 (1959).
  - [256] E. Vasselli, Background potentials and superselection sectors, *J. Geom. Phys.* **139**, 139 (2019).
  - [257] A. Alexandradinata, A pedagogical note on geometric phases, private communication.
  - [258] M. Berry, Anticipations of the Geometric Phase, *Phys. Today* **43**, 34 (1990).
  - [259] R. S. Mulliken, Electronic Structures of Polyatomic Molecules and Valence. IV. Electronic States, Quantum Theory of the Double Bond, *Phys. Rev.* **43**, 279 (1933).
  - [260] L. Elcoro, B. Bradlyn, Z. Wang, M. G. Vergniory, J. Cano, C. Felser, B. A. Bernevig, D. Orobengoa, G. De La Flor, and M. I. Aroyo, Double crystallographic groups and their representations on the Bilbao Crystallographic Server, *J. Appl. Crystallogr.* **50**, 1457 (2017).
  - [261] P. M. Sheridan, M. J. Dick, J.-G. Wang, and P. F. Bernath, High-resolution investigation of the excited electronic states of CaSH and SrSH by laser excitation spectroscopy, *Molecular Physics* **105**, 569 (2007).
  - [262] A. Veillard, C. Daniel, and M. M. Rohmer, Cobalt tetracarbonyl hydride and cobalt tricarbonyl hydride revisited: structure and electronic states through ab initio calculations, *J. Phys. Chem.* **94**, 5556 (1990).
  - [263] V. Meyer, D. H. Sutter, and H. Dreizler, The Centrifugally Induced Pure Rotational Spectrum and the Structure of Sulfur Trioxide. A Microwave Fourier Transform Study of a Nonpolar Molecule, *Z. Naturforsch. A* **46**, 710 (1991).
  - [264] A. Maki, T. Masiello, T. A. Blake, J. W. Nibler, and A. Weber, On the determination of C0 (or A0), , and some dark states for symmetric-top molecules from infrared spectra without the need for localized perturbations, *J. Mol. Spec.* **255**, 56 (2009).
  - [265] P. B. Changala, M. L. Weichman, K. F. Lee, M. E. Fermann, and J. Ye, Rovibrational quantum state resolution of the C<sub>60</sub> fullerene, *Science* **363**, 49 (2019).
  - [266] L. R. Liu, P. B. Changala, M. L. Weichman, Q. Liang, J. Toscano, J. Klos, S. Kotochigova, D. J. Nesbitt, and J. Ye, Collision-Induced C<sub>60</sub> Rovibrational Relaxation Probed by State-Resolved Nonlinear Spectroscopy, *PRX*

- Quantum **3**, 030332 (2022).
- [267] L. R. Liu, D. Rosenberg, P. B. Changala, P. J. D. Crowley, D. J. Nesbitt, N. Y. Yao, T. V. Tscherbul, and J. Ye, Ergodicity breaking in rapidly rotating C60 fullerenes, *Science* **381**, 778 (2023).
  - [268] Q. C. Qiu and A. Ceulemans, Icosahedral symmetry adaptation of JM bases, *Mol. Phys.* **100**, 255 (2002).
  - [269] K. Kuchitsu, ed., *Structure of Free Polyatomic Molecules: Basic Data* (Springer Berlin Heidelberg, Berlin, Heidelberg, 1998).
  - [270] K. Balasubramanian, Applications of combinatorics and graph theory to spectroscopy and quantum chemistry, *Chem. Rev.* **85**, 599 (1985).
  - [271] W. G. Harter and T. C. Reimer, Nuclear spin weights and gas phase spectral structure of 12C60 and 13C60 buckminsterfullerene, *Chem. Phys. Lett.* **194**, 230 (1992).
  - [272] W. G. Harter and T. C. Reimer, Erratum: Nuclear spin weights and gas phase spectral structure of 12C60 and 13C60 buckminsterfullerene, *Chem. Phys. Lett.* **198**, 429 (1992).
  - [273] K. Balasubramanian, Comment on nuclear spin weights of 12C60 and 13C60 buckminsterfullerene, *Chem. Phys. Lett.* **200**, 649 (1992).
  - [274] P. R. Bunker and P. Jensen, Spherical top molecules and the molecular symmetry group, *Mol. Phys.* **97**, 255 (1999).
  - [275] H. Georgi, *Lie Algebras In Particle Physics*, 2nd ed. (Westview Press, 2021).
  - [276] J. Hougen, *Methane symmetry operations (version 1.2)* (2001).
  - [277] R. Kirby and M. Scharlemann, Eight Faces of the Poincare Homology Sphere, in *Geometric Topology* (Elsevier, 1979) pp. 113–146.
  - [278] J. C. Baez, *From the Icosahedron to E8* (2017), arXiv:1712.06436.
  - [279] J.-P. Luminet, J. R. Weeks, A. Riazuelo, and R. Lehoucq et al., Dodecahedral space topology as an explanation for weak wide-angle temperature correlations in the cosmic microwave background, *Nature* **425**, 593 (2003).
  - [280] E. Kubischta, Berry connection calculation (2023), private communication.
  - [281] D. Gottesman, A. Kitaev, and J. Preskill, Encoding a qubit in an oscillator, *Phys. Rev. A* **64**, 012310 (2001).
  - [282] N. C. Menicucci, Fault-Tolerant Measurement-Based Quantum Computing with Continuous-Variable Cluster States, *Phys. Rev. Lett.* **112**, 120504 (2014), \_eprint: 1310.7596.
  - [283] D. Marinucci and G. Peccati, *Random Fields on the Sphere* (Cambridge University Press, 2011).
  - [284] Y. Fan, W. Fischler, and E. Kubischta, Quantum Error Correction in the Lowest Landau Level, *Phys. Rev. A* **107**, 032411 (2023), arXiv:2210.16957 [cond-mat, physics:hep-th, physics:quant-ph].
  - [285] E. Knill and R. Laflamme, Theory of quantum error-correcting codes, *Phys. Rev. A* **10.1103/PHYSREVA.55.900** (1997).
  - [286] R. McDowell, C. Patterson, and W. Harter, The modern revolution in infrared spectroscopy, *Los Alamos Science* **3**, 38 (1982).